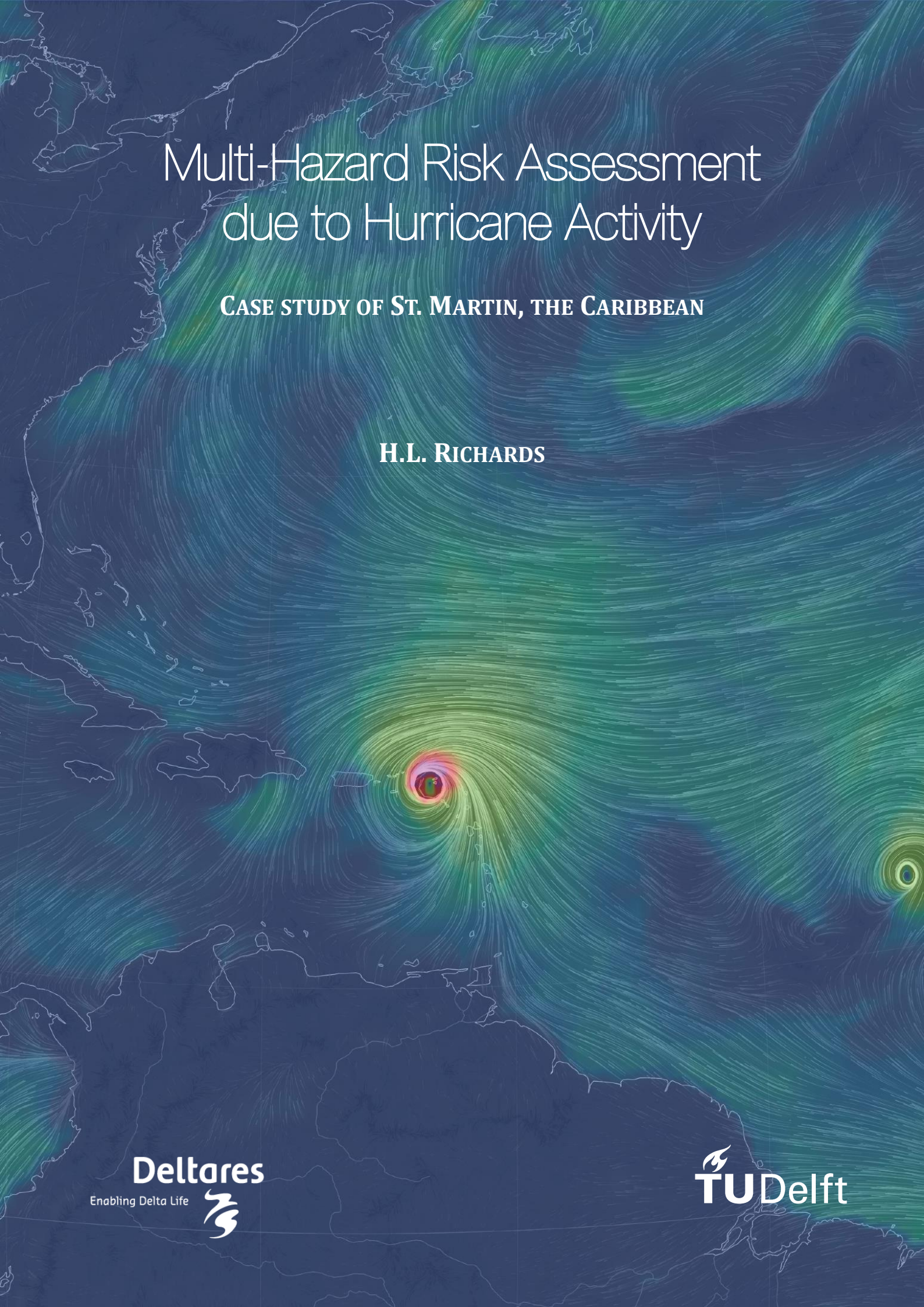

Multi-Hazard Risk Assessment due to Hurricane Activity

Case study of St. Martin, the Caribbean

H.L. Richards

Deltares
Enabling Delta Life

TU Delft

Multi-Hazard Risk Assessment due to Hurricane Activity

Case Study of St. Martin, the Caribbean

by

H.L. Richards

Department of Hydraulic Engineering
Section: Coastal Engineering

in partial fulfillment of the requirements for the degree of

Master of Science
in Civil Engineering

at the Delft University of Technology,
to be defended publicly on 18 July 2019, at 10:15 AM.

Committee Chairman:	Prof.dr.ir Aarninkhof, S.G.J.	TU Delft
Committee members:	Dr. Bricker, J.	TU Delft
	Ir. Pearson, S.	TU Delft
	Dr. Giardino, A.	Deltares
	Ir. Torres Duenas, L.F.	Deltares
	Ir. Wagenaar, D.	Deltares

TU Delft Delft University of Technology

Deltares Enabling Delta Life

References: front and back cover by Beccario (2019), and chapter cover images by Taylor (2018).

Preface

The final component in completing my master's degree in Hydraulic Engineering, at Delft University of Technology, is this research thesis regarding hurricane risk in St. Martin. It was carried out at Deltares (Netherlands) under the *Flood Risk Strategies (SO) Programme*, which provided financial and academic support during the research period. Furthermore, all the course work covered during my study programme at TU Delft provided me with all the necessary tools to complete my research. It prepared me for a future in the world of hydraulic engineering, and specifically coastal engineering, the specialisation I am graduating in. I would like to thank all my teachers and professors at TU Delft for their dedication to the field, and continued contribution to developing the new generations who choose to embark on this same journey. I would also like to take this opportunity to highlight a few important people who made my graduation possible.

Firstly, the TU Delft committee members who supported me from the very beginning of the thesis research. Stefan Aarninkhof, thank you for your time and expertise in the field of coastal engineering. Without your input I would not have been able to keep the bigger picture in mind. Your professionalism and way of communication of concepts inspires me. Jeremy Bricker, thank you for your critical thinking and creativity when it came to conquering hurdles during my research. Without your input I would not have been able to tackle the difficulties that presented themselves along the way within the complexities of my research. Your way of teaching and listening and respect for others inspires me. Stuart Pearson, thank you for your enthusiasm and the energy you provided, on both a personal and academic level. Without your input I would not have been able to maintain a passion and love for my work, and strive for the best possible results. Your dedication and passion for this field of research inspires me.

Secondly, my Deltares committee members who guided me on a daily basis, in discovering the direction of my research and the application in the real world. Alessio Giardino, thank you for believing in my abilities and always challenging me to push the boundaries. Without your input I would not have been able to think outside of the box and produce the work I did. Your creativity and broad range of expert knowledge inspires me. Luisa Torres Duenas, thank you for your daily guidance and encouragement during all the phases of my research. Without your input I would not have been able to organise my work and have a good picture of the end goal. Your focus and work ethic inspire me. Dennis Waggenaar, thank you for all your input and encouragement during the research period. Without your input I would not have been able to make the link between the physical processes I was modelling and the economic aspects of impact. Your insights and curiosity inspire me. A special mention to Kees Nederhoff and Tim Leijnse as well. They were instrumental in helping me to critically evaluate my goals and my approach to reach them. I am forever grateful for their input and help.

Thirdly, I would like to thank Jurjen Wagemaker and Tom Brouwer from Flood Tags. They welcomed me with open arms during my time spent at Flood Tags, collecting and analysing online data for my research. During my time with them I learnt how to retrieve online data and use it in an innovative way for data poor environments. The data I collected with them, was used to validate flooding due to Hurricane Irma which otherwise would not have been possible. This application of the work they are doing shows how the engineering world is developing and how we can use the modern world to our advantage.

To my fellow master thesis students (and now friends), who were also carrying out research at Deltares, you provided countless discussions and encouragement every day during our time together. I am grateful that you made the thesis journey much less lonely.

Lastly, and most importantly, I would like to thank my friends and loved ones for being there for me, celebrating each success and remaining encouraging throughout. I do so appreciate their unconditional love and support.

Hilary Lin Richards
Delft, July 2019

Your paper empire
Awash in nights' aether
Kite in a hurricane

Tomas Vincent Marra

Abstract

Every year hundreds of thousands of people are affected by natural disasters that occur due to various physical phenomenon. They include earthquakes, tsunamis, volcanic eruptions, and hurricanes. In this research we focus on hurricane events and the impact they have on a community. Reactions to extreme hurricane events vary from region to region, as each community is unique in their location, topology and available resources. The ability for a community to bounce back is defined by their disaster resilience which, in turn, depends on their ability to identify vulnerabilities and prepare for the inevitable.

Within this line of research, one of the main challenges is defining local risk due to hurricane events, especially when considering more than one hurricane-induced hazard. Furthermore, the challenge becomes even greater when analysing risk in locations around the world where data availability is scarce. This study aims to clarify and improve the existing methodology to define multi-hazard risk due to hurricanes. This methodology is verified by applying it to the case study of St. Martin, in order to delineate hurricane risk on the island. St. Martin was chosen to investigate, as it is a Small Island Developing State in the Caribbean that recently suffered immeasurable damages during Hurricane Irma (September 2017), and is still struggling to recover.

The two hazards that were considered, in the application of the methodology, were hurricane-induced winds and hurricane-induced coastal flooding. In the case of St. Martin, hurricane-induced winds were found to contribute to 98% of damages due to Hurricane Irma, when compared to the coastal flood damages. These wind damages reached a total of $2.6 billion. Coastal flooding, on the other hand, reached $54.5 million, which were due to both increased storm surge levels and wave-induced flooding, showing that neither one is negligible for a reef island like St. Martin. Furthermore, storm surge variation around the island was found to be minimal due to the scale of the island, and the fact that storm surge was predominantly pressure driven. Validation of the models to simulate hazards and impact on St. Martin proved to be challenging. An unconventional data source was used to validate the flooding model, which included analysis of Twitter data of images posted during Hurricane Irma. This is an example of a solution of how to deal with data scarcity in hazard modelling.

The risk assessment of St. Martin involved simulating synthetic hurricane track scenarios and determining their respective wind and flood damages on the island. Combining the respective damages was done by including a damage threshold to ensure damages did not exceed 100% and was an important addition to current methods. Furthermore, the probability of exceedance for the induced damages were found by analysing the induced coastal water levels around the island. The risk integration resulted in a hurricane risk map of St. Martin indicating Expected Annual Damages for all communities, shown in Figure 1.

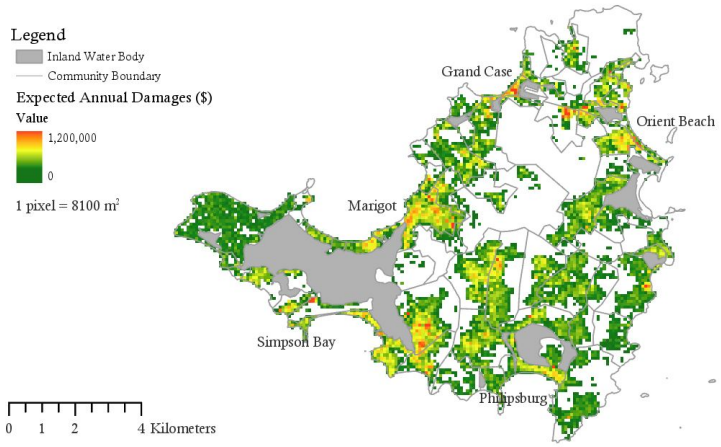

Figure 1: Map showing the hurricane risk (Expected Annual Damages) on the island of St. Martin.

The intention of the improved methodology is to be able to apply it to a hurricane risk prone region, like St. Martin, and to use the outcome to delineate hurricane risk. This indicates hot spots in the region of interest and improvements to disaster resilience can be discussed. The approach of *Build Back Better* is highlighted in this research to show how this risk map can be interpreted and what the results mean. Three branches are discussed, namely building back *stronger* which involves ensuring infrastructure can resist more extreme events in the future. Building back *faster*, which involves reducing disaster impacts by accelerating reconstruction through preparation measures, and finally building back *more inclusively*, which involves ensuring that post-disaster support reaches all affected population groups.

Table of Contents

List of Figures

List of Tables

Symbols & Abbreviations

Abbreviations

Symbol	Description	Units
ALOS	Advanced Land Observing Satellite	–
BBB	Build Back Better	–
DEM	Digital Elevation Model	–
ETM	Empirical Track Modelling	–
FIAT	Flood Impact Assessment Tool	–
GDP	Gross Domestic Product	$
GEBCO	The General Bathymetric Chart of the Oceans	–
GFDRR	Global Facility for Disaster Reduction and Recovery	–
GTSM	Global Tide and Surge model	–
HURDAT	Hurricane Database	–
IBTrACS	International Best Track Archive for Climate Stewardship	–
LIDAR	(Light Detection And Ranging of Laser Imaging Detection And Ranging	–
MERIT	Multi-Error-Removed Improved-Terrain	–
OSM	OpenStreetMap	–
SHOM	Service hydrographique et océanographique de la marine	–
SIDS	Small Island Developing States	–
SRTM	Shuttle Radar Topography Mission	–
TCWiSE	Tropical Cyclone Wind Statistical Estimation Tool	–
TRC	Tropical Cyclone Rainfall Model	–
USD	United States Dollars	–
WES	Wind Enhance Scheme	–
WRF	Weather Research and Forecasting Model	–

Wind Modelling

Symbol	Description	Units
θ	angle defining the hurricane translation direction	°
B	pressure profile exponent(Hollands's parameter)	–
f_c	Coriolis parameter	–
P_c	central pressure	mb

P_n	ambient pressure	mb
P_{drop}	central pressure drop	mb
r	radial distance	km
R'	effective hurricane radius	km
R_{100}	Radius of 100kt wind speeds	km
R_{35}	Radius of 35kt wind speeds	km
R_{50}	Radius of 50kt wind speeds	km
R_{max}	radius of maximum wind speed	km
RMW	Radius of Maximum Winds	km
V_g	10-min averaged gradient wind speed	m/s
V_{tr}	hurricane translation speed	m/s

Probability

Symbol	Description	Units
C_i	cost of loss due to impact of wind/surge	$
d_i	consequence of the scenario	$
$f(d)$	damage function given a damage fraction d	–
$H_{s,max}$	significant wave height during a hurricane	m
i	category count	–
j	location count	–
n	number of objects	–
P_i	probability that a category i hurricane will occur in a given year	–
p_i	probability of the scenario	–
$R^{hurricane}$	hurricane risk	$\$/yr$
R^{surge}	storm surge risk	$\$/yr$
R^{wind}	wind risk	$\$/yr$
s_i	scenario	–
V_{max}	maximum sustained wind speed	m/s

Hydrodynamics

Symbol	Description	Units
η_{setup}	Wave Setup	m
γ	Breaker Coefficient	–
ρ_a	Air density	kg/m^3
τ_s	Shear stress	N/m^2
θ	Incoming Wave Angle	$^\circ$

C_d	Wind Drag Coefficient	–
c_o	wave Group Velocity	m/s
d_{br}	Breaker Depth	m
H_s	Significant Wave Height	m
h_{br}	Breaker Wave Height	m
L	Equivalent Wave Fetch Length	km
$R^{'}$	Effective Hurricane Radius	km
U_10	Wind speed at 10m elevation	m/s

Key Terms

St. Martin: The island of St. Martin is located in the Caribbean and is known under various names, and have various ways of being spelt. This is due to the fact that the island is spilt into two halves, namely, the French side, known as Saint-Martin, and a Dutch side, known as Sint Maarten. This research refers to the entire island and uses the name St. Martin to do so.

Hazard: This refers to the physical phenomenon that has the potential to cause damages and losses to human and natural systems (Giardino et al., 2018).

Risk: Here risk is defined as the product of a hazard and its consequences (Kron, 2005). This means that where there are no people (or values) that can be affected, there is no risk. Similarly, a disaster can only occur when people are harm, or belongings are damaged. Risk is therefore determined by the hazard (including its probability of occurrence), the values (people or objects) at risk, and the vulnerability (lack of resistance to damage).

Exposure: This is local data that represents the presence of people, livelihoods, environmental services and resources (economic, social or cultural) in places that could be adversely affected due to a given event (Gallina et al., 2016).

Vulnerability: This is local information that represents the predisposition of a community, system, or asset to be adversely affected by a certain hazard. This can include economic, social, geographic, demographic, cultural, institutional, governance and environmental factors (Gallina et al., 2016).

Forecasting hurricanes vs Generating hurricanes: Predicting the path of a hurricane currently happening is referred to as forecasting, similar to forecasting weather temperature or precipitation on the daily news, where the time period of interest is in the immediate future. To expand a data set of hurricane information, often hurricane tracks are generated, and their characteristics are drawn randomly based on historical data, this is known as hurricane generation.

Cyclone: A system of winds rotating inwards to an area of low barometric pressure, with an anticlockwise (northern hemisphere) or clockwise (southern hemisphere) circulation (NOAA SciLinks, 2018).

Hurricane: A tropical cyclone in the Northern Atlantic Ocean (NOAA SciLinks, 2018).

Storm surge: A rising of the sea as a result of wind and atmospheric pressure changes associated with a storm (National Hurricane Center, 2018b).

Storm tide: Storm tide is the total observed seawater level during a storm, resulting from the combination of storm surge and the astronomical tide (National Hurricane Center, 2018b).

A Markov chain: This is a sequence of random values whose probabilities at a time interval depend upon the value of the number at the previous time. A simple example is the non-returning random walk (Emanuel et al., 2011).

Synthetic data: This is information that's artificially manufactured and created using an algorithm. It is used as a stand-in for test data sets to validate mathematical models or test cases.

Computational Model (Modelling): This refers to the recreation of a physical process or event by means of numerical relationships and a computer simulation.

1 Introduction

Every year hundreds of thousands of people are affected by natural disasters that occur due to various physical phenomenon. They include earthquakes, tsunamis, volcanic eruptions, and hurricanes, which is the focus of this research. Reactions to extreme hurricane events vary from region to region as each community is unique in their location, topology and available resources. The ability for a community to bounce back is defined by their disaster resilience which, in turn, depends on their ability to identify vulnerabilities and prepare for the inevitable. This study investigates the methodology to define risk in terms of multiple hurricane-induced hazards, specifically winds and coastal flooding. This methodology was applied to the case study of St. Martin in the Caribbean using the recent event of Hurricane Irma to validate the outcomes of each step.

This chapter provides an introduction to the M.Sc. research and briefly describes the background and motivation of hurricane research in Section 1.1. Section 1.2 outlines the problem of identifying hurricane risk for islands like St. Martin, and describes the intention and research domain of the thesis. Section 1.3 states the research objective and intermediate research activities that guided the research towards the final result. Section 1.4 briefly summarises the methodology applied to the case study of St. Martin and finally, in Section 1.5, the layout and intended reading structure is described.

1.1. Background and motivation

Since the beginning of the 20^{th} century more than 629 million people (Doocy et al., 2013) have been affected by tropical cyclones. Depending on their place of origin, these tropical cyclones are known by different names. Those originating from the Northern Atlantic Ocean are known as hurricanes. Their high wind speeds and extreme water levels bring destruction to any area they encounter along their path.

Many Small Island Developing States (SIDS) are among the most heavily affected communities when it comes to hurricane activity. Figure 1.1 shows the relationship between a country's Gross Domestic Profit (GDP) per capita, and their risk to assets due to natural disasters. This was found as part of a global initiative by Global Facility for Disaster Reduction and Recovery (GFDRR), *Building Back Better*, where the aim is to increase disaster resilience through post-disaster reconstruction. In this study a country's socio-economic resilience to a disaster is defined by their ability to cope with a disaster, receive support, and recover and reconstruct (Hallegatte et al., 2018), and is defined by the ratio of asset-losses to well-being losses. Impact on well-being is influenced by two main aspects, firstly by how asset losses affect income and consumption during recovery, and secondly by who is affected. Here we focus on asset-loss determination.

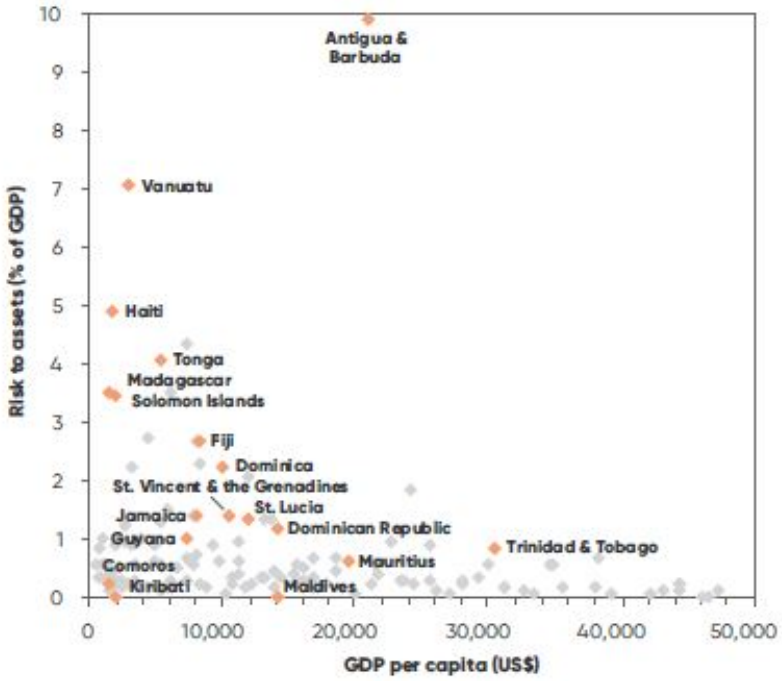

Figure 1.1: Risk to assets for 149 vulnerable countries, highlighting Small Island Developing States (SIDS) in orange (Hallegatte et al., 2018).

For many exposed communities there is a direct relationship between their GDP and how resilient they are to natural hazards, this is directly reflected in the high risk to assets for lower earning SIDS in the figure. In order for these communities to become stronger for when the next hurricane makes landfall, they need to know where to focus their energies. This research focuses specifically on the asset losses in terms of structural damage, and how this can be used to trigger discussion on a country's resilience and how to improve it.

On the 6th of September 2017, Hurricane Irma made landfall in the Caribbean (shown in Figure 1.2) causing devastation to many of the islands and coastlines encountered. Irma was a category 5 hurricane on the Saffir-Simpson Hurricane Wind Scale (Vickery et al., 2000), which means wind speeds exceeded 252 km/h, storm surge exceeded 5.5 m and central pressures fell below 920 mb (CDCC, 2018). One of the many affected Caribbean islands, was the island of St. Martin. Published articles and reports of Hurricane Irma and damage in St. Martin, estimate total damages at between 1.6 to 2.5 billion dollars (Cangialosi, Latto, & Berg, 2017; Copernicus, 2017; NU, 2018; NOS, 2018a; World Bank Group, 2018). Reports further mention that buildings on the French half of the island were destroyed for up to 95% and the Dutch half of the island up to 70%,

including Princess Juliana Airport (Cangialosi et al., 2017; Copernicus, 2017; The Guardian, 2017).

Figure 1.2: A map showing the path Hurricane Irma took across the Caribbean, indicating the location of the island of St. Martin (NPR, 2017).

Very little can be done to reduce hurricane activity on a local scale. Improving disaster resilience in these places therefore, starts with understanding their risk due to hurricane activity. Most research around the topic of hurricane risk, and hurricanes in general, is focused on how to predict their occurrence and intensity, and how to identify risk areas due to a given hazard. Usually this hazard is the hurricane-induced wind speeds, as the intensity of a hurricane is often defined by its maximum wind speed. The most well-known classification is according to the Saffir-Simpson categories (Vickery et al., 2000) which are shown in Table 2.1 in Chapter 2, and define hurricanes from Category 1 to 5 depending on their wind speeds, with Category 5 being the most severe. These categories are used in wind hazard assessments to classify the wind speeds and potential impacts. Generally, the simulation of hurricanes, and their corresponding winds, is done using numerical models in order to represent the hurricane as a wind field map for a particular area. These maps are then used in wind impact analysis for the area.

A popular model for simulating wind fields is the Holland model (Holland, 1980), which represents the recorded wind speeds during a hurricane as a spatial wind field. This spatial wind field can then be used to apply the wind forcing during a hurricane simulation. These simulations can vary from physical wind modelling to complicated hydrodynamic models that simulate the influence of the wind speeds on the local hydrodynamic conditions. The choice of which hurricane-induced hydrodynamic processes to be modelled is dependent on, among others, the local bathymetry and bottom roughness of the location of interest. Different systems have different dominating coastal processes and therefore the choice of which processes to model depend on the local conditions. For reef islands such as St. Martin, typically the waves as well as storm surge are important when determining hurricane-induced coastal flooding. Various coastal models have been developed to model these environments, and include global tide and surge analysis that can be used to simulate hurricane-induced wind forcing and the resulting coastal water levels. These water levels can then be applied as the boundary conditions for a more refined inland flooding simulation.

When considering hurricane-induced inland flooding, the two main forcing components to be considered are the high coastal water levels and extreme rainfall rates. Coastal water levels are comprised of the hurricane-induced storm surge and the local wave conditions inducing wave setup at the coastline. A study by Wu et al. (2018) looks at wave effects on storm surge and inundation and one of the findings is that the presence of waves can increase storm surge levels significantly through wave setup. The extent of wave setup is found to be directly related to the hurricane wind characteristics, and shows how direct wave forcing adds to the total wave setup and therefore also the total storm surge levels. Flooding due to high coastal water levels and extreme rainfall during a hurricane event can occur simultaneously or successively and lead to compound

flooding events. This means that the combination of the two, leads to increased flooding, whereas when considered separately, flooding may not be evident or as extreme.

Asset losses are determined by translating hurricane-induced hazards to impact using vulnerability functions. These functions define the relationship between the hazard extent and the amount of relative damage to a specific asset for the location of interest. These relationships are specific for the type of hazard as well as the type of asset that is exposed. The relationship between wind speed and structural damage is an example of a vulnerability function, where a given wind speed represents a percentage of damage to a specific type of structure. These functions are aggregated based on the maximum hazard intensities and maximum damages. The impact of a hazard is dependent on the exposure of assets, the related vulnerability for the area of interest, and the hazard maps (wind speeds and coastal flooding) indicating intensities.

Performing a risk assessment for hurricane activity for a given area, means simulating multiple hurricane scenarios and the related intensities and impacts. The current general approach for defining risk areas is to determine the risk of the area due to a given hazard. When it comes to hurricanes this is either due to wind or due to flooding. Figure 1.3 shows the conceptual overview regarding risk assessments. The intention of performing a risk analysis is that the outcome may be used within policy making and disaster risk management of the region of interest. Risk reduction measures can be determined once a risk analysis has been performed as this highlights the most at-risk areas within a given region. Risk assessments regarding hurricanes generally consider the hurricane tracks for a specific region to determine the probability that a hurricane will pass by. This analysis is done on a set of hurricane tracks that are either based on historical data or have been synthetically generated to expand a data set. The final output is expressed as expected annual damage or risk. This research is aimed at clarifying the risk analysis of a location of interest regarding hurricane activity. The implementation of risk reduction measures, within risk management, fall beyond the scope of this research.

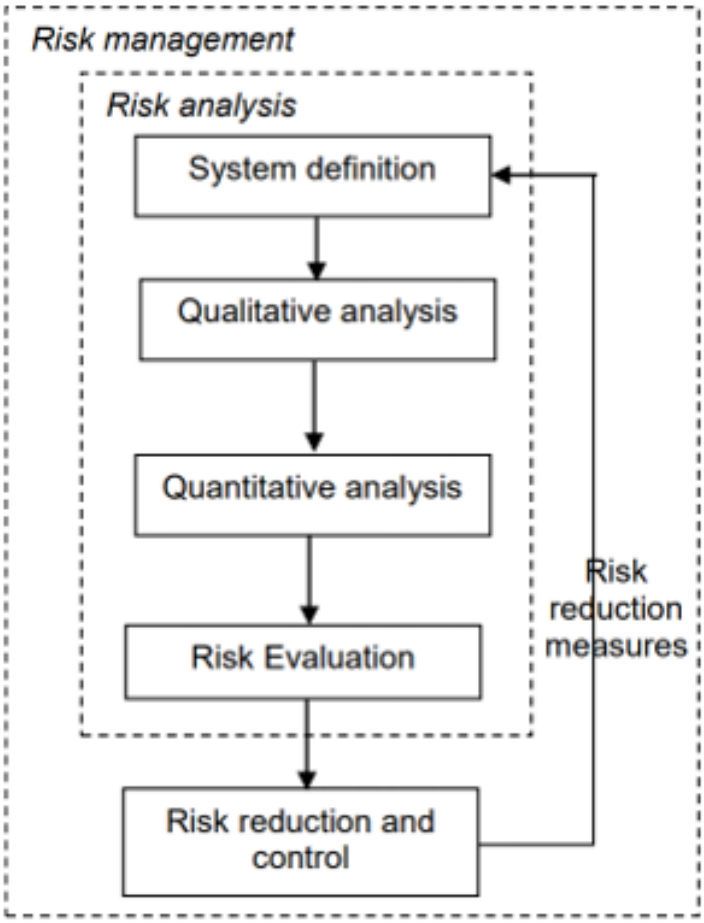

Figure 1.3: Conceptual overview of a general risk assessment within risk management (Jonkman et al., 2017).

1.2. Problem definition

Currently islands, like that of St. Martin, are extremely vulnerable, due to their location, size and topography, to hurricane activity. Their recovery depends on their ability to define high risk areas and focus time and energy on those places to increase resilience for the next hurricane season. After Hurricane Irma hit St. Martin, efforts were made to start rebuilding the island. Touristic areas were the first to be rebuilt, however, areas not relevant to the tourist industry (e.g. residential areas) have still not recovered more than a year later (NOS, 2018a).

Photos of the situation in the Dutch Quarter, one of the poorer areas on the island, are shown in Figure 1.4, which were taken in December 2018. From these images it is clear that parts of the island have still not fully recovered. Efforts have been made to determine the extent of damage on the island however, identifying the damages due to the different hazards (e.g. winds and flooding), and quantifying them, remains a challenge. Furthermore, the hurricane risk for each area of the island has not been determined, and people are unable to sufficiently prepare for upcoming hurricane seasons.

Figure 1.4: Damaged houses in the Dutch Quarter, St. Martin, taken in December 2018, more than 15 months after Hurricane Irma made landfall (de Hamer, 2018).

Traditional engineering solutions such as levees, seawalls or breakwaters are not able to secure safety for locations exposed to hurricane activity, such as these SIDS. These solutions are usually hard structures that prevent high water levels (coastal or inland) from reaching urban or agricultural areas. However, in the case of extreme conditions experienced during a hurricane, these solutions may not be economically feasible or even possible. Other approaches need to be taken into consideration including developing spatial plans, early warning systems or increasing awareness and preparation for the inevitable storms that are to come. In order to do so however, first the risk areas need to be identified which can then be prioritised. In order to define these risk areas, there is a need for expertise in the field of hurricane forcing in order to map hurricane-induced hazards (wind and coastal flooding). Expertise on assessing the impacts of these hazards is also needed.

There are various approaches for identifying hurricane risk. Studies by Hallegatte (2007); Emanuel et al. (2011); Vickery et al. (2009); Emanuel et al. (2006) are examples of studies that look specifically at determining hurricane wind risk by simulating hurricane wind speeds using historical and synthetic events. Studies by de Moel et al. (2015); Gomes et al. (2015); Komi et al. (2017) on the other hand, are examples of studies that look specifically at flood risk, whether it be due to inland flood levels or hurricane-induced coastal levels. These studies determine wind risk or flood risk, however bringing these elements together has received much less attention. An example of a study that does consider multiple hazard risk is the work by Giardino et al. (2018), which looks at damages due to coastal flooding and coastal erosion due to extreme events. All of these studies follow similar general approaches when it comes to risk however there is no clear method when it comes to combining hazards such as flooding and wind for example. There is no guideline for how multiple hazard risk should be combined or portrayed as a whole to the public or authorities and decision makers.

Portraying this risk is further complicated by having limited observations during hurricane events and a lack of exposure data. Studies have been done to determine relationships between hazards and damage, such as the work by Huizinga et al. (2017) to develop global depth-damage vulnerability functions, however results from these studies show the relationships are site specific and cannot simply be applied to other locations. This is also seen in the studies by Tomiczek et al. (2017) and Hatzikyriakou and Lin (2017) for wave impact

vulnerability functions, and studies by M. D. Powell et al. (1995); Murnane and Elsner (2012); Khanduri and Morrow (2003); Prahl et al. (2015) for wind vulnerability functions. These studies show how the amount and value of damage depends on the economy and land value for the specific site or country in question.

In this research, we focus on three main aspects when assessing multiple-hazards and performing hurricane risk assessments. These are the hazard modelling, the impact modelling and the probabilistic assessment. In all three cases data availability plays a large role in the approach and quality of the results. Hazard modelling requires detailed local conditions such as bathymetry data, topography data and historical observations of the hazards being modelled. This information defines the models that are appropriate to model the hazards of interest (winds and coastal flooding). Impact modelling requires detailed exposure data of the assets being considered in the impact assessment as well as the relationship of these assets to damages. These relationships are in the form of vulnerability functions for the various hazard intensities. These functions are site specific and are only as accurate as the input data available. Finally, the probabilistic assessment should be based on an ensemble of hurricane scenarios representing the hurricane climate for the area of interest. This involves simulating the hazard and impacts due to each scenario. The computational efforts of these scenarios further limit the hazard and impact modelling options.

In the case of St. Martin we are faced with a data poor environment in terms of local data for bathymetry, topography, exposure, vulnerability and historical hurricane observations. This means hazard and impact modelling is limited to global data sets and innovation within these aspects is required.

1.3. Objective

The aim of this research is to clarify and improve the methodology of performing a multiple hazard risk assessment due to hurricane activity. The new methodology is applied to the case study of St. Martin in order to validate the methodology and produce a risk assessment for St. Martin. The research will be defined under the following research objective:

Research Objective:

To set up a framework for determining multi-hazard risks due to hurricane activity, as a basis for triggering decision making on disaster resilience, using the island of St. Martin as a case study.

St. Martin is an example of a reef island exposed to hurricane activity, with limited expertise and resources to perform a risk assessment when considering more than one hurricane-induced hazard. The island is located in the Caribbean and finds itself directly along the path of hurricanes that originate from the Northern Atlantic Ocean.

The research domain is limited to the island of St. Martin when it comes to performing a risk assessment for hurricane activity. However, the intention is that the methodology developed here can be applied to similar locations exposed to hurricane activity. The hazard elements that are considered most threatening are the wind speeds and the coastal water levels that the hurricanes induce. These are the phenomena that are considered as hurricane-induced hazards in this research. The research has been structured to answer two main research questions:

Research Questions:

1. What improvements, and clarifications, can be made to the existing methodology for determining multi-hazard risk due to hurricane activity?
2. What are the boundary conditions to delineate hurricane risk in St. Martin based on the application of the proposed methodology?

Seven research activities were also defined and were used to systematically answer the research questions, and reach the final research goal. These activities form the basis of the methodology explained in Section 1.4.

Research Activities:

1. Collect data for hazard modelling and validation.
2. Setup the wind field and flooding model for Hurricane Irma in St. Martin.
3. Determine the wind-speed and water-depth vulnerability functions for St. Martin.
4. Setup the impact model for Hurricane Irma in St. Martin.
5. Generate synthetic hurricane tracks and filter these near St. Martin.
6. Determine the probability distribution of the hurricane tracks near St Martin.
7. Determine the risk associated to hurricane activity using an ensemble of probabilistic events for St. Martin.

1.4. Methodology

The methodology of the research was structured according the the research activities defined in Section 1.3. Each of these activities contributed to answering the research questions on improving the current methodology for determining hurricane risk and its application to St. Martin. Figure 1.5 shows a summary of the research activities grouped into two phases. The first phase consisted of the data collection, hazard model setup and validation and the impact modelling. In this case this was done for St. Martin using Hurricane Irma as the validation case. The second phase was application of the hazard and impact models, set up in Phase 1, to an ensemble of hurricane track scenarios. Synthetic hurricane tracks and their corresponding hazard intensities were generated and modelled using the setup in Phase 1. The results of the hazard intensities and impact due to each hurricane track scenario then formed the basis for the probabilistic analysis and risk assessment for hurricane activity in St. Martin. In this section each research activity is briefly summarised.

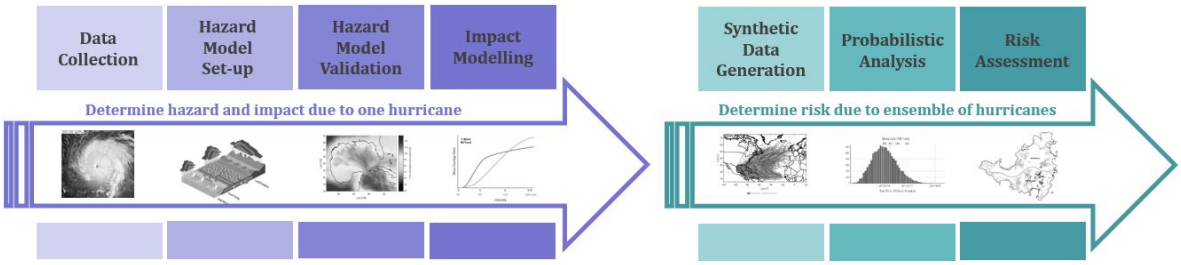

Figure 1.5: The major components for the proposed thesis research.

PHASE 1: Hurricane Irma

1. **Data collection**

   This involved collecting data for the model setup, model validation and impact modelling. The data poor environment of St. Martin meant that most available data sources were open source global data sets. The data needed to simulate hurricane-induced winds was the historical track data from the Northern Atlantic Ocean from the HURDAT (Hurricane Database) database (National Hurricane Center, 2018a). The data needed to simulate hurricane-induced flooding included the global bathymetry and local bathymetry from GEBCO (The General Bathymetric Chart of the Oceans) (British Oceanographic Data Centre, 2018). This data set was extended by digitisation of the navigational charts of Navionics (Navionics, 2019) on a local scale. The global topography data for St. Martin was only available in the form of MERIT (Multi-Error-Removed Improved-Terrain) DEM (University of Tokyo, 2018)

and SRTM (Shuttle Radar Topography Mission) DEM (NASA, 2014). The validation data used for the hazard models was based on the analysis of online images and data regarding the event of Hurricane Irma and flooding in St. Martin. The data needed to simulate hurricane impacts included public local exposure data acquired from Open Street Maps (OpenStreetMap, 2019) and Red Cross exposure data (Red Cross, 2017b). Published flooding and damage maps by Red Cross (Red Cross, 2017a; Pacific Disaster Center, 2017) and Cerema (Cerema & DEAL Guadeloupe, 2017) were also digitised for model validation.

2. **Hazard Model Setup**

   This included setting up the numerical models used to simulate the winds and water levels experienced during a given hurricane. The wind speeds were represented by transforming the spatial wind fields per time step to the maximum 1-minute average wind speed per location. The wind fields were based on the Holland (1980) model and the adaptations by Holland, Belanger, and Fritz (2010) and Nederhoff, Giardino, Van Ormondt, and Vatvani (2019). The hurricane-induced water levels were found by forcing the hydrodynamic system with the wind fields using a Wind Enhance Scheme (WES) (Deltares, 2014) that represented the wind as a shear stress within the hydrodynamic model. This shear stress is included in the shallow Water Equations (SWE) to force the system. The coastal water levels were then simulated using a Delft3D Flexible Mesh (FM) Flow model based on the SWE (Kernkamp et al., 2011). The storm surge levels and wind speeds due to Hurricane Irma were then simulated. Along with storm surge, the coastal water levels also included wave setup. A parametric model by I. Young (1988) was used to estimate offshore wave conditions and wave setup at the coastline was estimated based on these conditions and the concept of depth-limited wave breaking (van Rijn, 1990). The total maximum coastal water was then used as the boundary conditions for the inland flood model. This was a static "bathtub" approach for the island of St. Martin. The output from these models was a maximum wind speed map and a maximum coastal flood map for St. Martin due to Hurricane Irma.

3. **Hazard model validation**

   The flood model was validated using online data including a digitisation of the flood map of the French half of the island and online Twitter data. The Twitter data was collected for the hurricane event of Irma and analysed to determine locations of flooding and flooding depths for each identified location. The points identified from the map and online data were assigned flood depths which were compared to the simulated flooding depths using the static "bathtub" approach. Flood prone areas were also defined based on the modelled flooding and compared the the validation points. The wind speeds were based on the open ocean 10 m elevation wind speeds simulated in the hydrodynamic model and the parametric wave model for offshore wave conditions and wave setup estimation was validated based on a coupled wave and flow model for the conditions of Hurricane Irma.

4. **Impact Modelling** The impact model for St. Martin was set up using FIAT (Flood Impact Assessment Tool) (Slager et al., 2016). This tool uses the local exposure data, hazard extents and vulnerability as input. The exposure data used to determine wind damage that was classified using physical parameters, in this case by building roof material type i.e. tiles, concrete or metal. The exposure data used to determine flood damage was also classified using physical parameters, in this case the use of the building i.e. residential, commercial or industrial. The vulnerability functions were defined for these classes and the corresponding structural damages they induce. The flood depth vulnerability functions used for the case study of St. Martin were based on those derived in a study by Vojinovic et al. (2008) where extreme rainfall events were related to damages for the Dutch side of St. Martin for a given building use type. The wind speed vulnerability functions were based on a case study by Khanduri and Morrow (2003) done for Puerto Rico that related wind speeds to structural damage for a given building frame material. The exposure data and vulnerability data for St. Martin was then used to find the flood and wind damage for Hurricane Irma. These results were compared to published estimates for damages on the island.

This marked the end of Phase 1, and the hazard models and impact models were deemed suitable to be applied to a broader range of hurricane events for St. Martin.

PHASE 2: Risk of hurricane activity

5. **Synthetic Data Generation**

   In order to determine hurricane risk in St. Martin an ensemble of hurricane track scenarios need to be modelled in terms of hazard extent and impact. The historical hurricanes in the region of St. Martin are not enough to perform this analysis and therefore synthetically generated tracks were used. The synthetic hurricane data was generated using the historical hurricane data of the Northern Atlantic. This was done using a track model setup by Hoek (2017) and Nederhoff et al. (2019), called TC-WiSE. The track modelling was based on Empirical Track Modelling (ETM) and the wind field modelling based on the work by Vickery et al. (2000); Holland (1980); Holland et al. (2010); Nederhoff et al. (2019). The synthetic hurricane tracks were generated for the Northern Atlantic Ocean based on historical data and filtered for St. Martin. Each synthetic track was modelled for hazard extent and impact according to the models set up for St. Martin and validated using Hurricane Irma. This resulted in simulation of 1431 hurricanes, their induced winds and coastal flooding, and their damages on St. Martin.

6. **Probabilistic Analysis**

   To determine risk on St. Martin, probabilities have to be assigned to the calculated damages of all the hurricane track scenarios. This was done by looking at the probability distribution of the extreme water levels induced by each track scenario. These water levels were assigned exceedance probabilities based on the empirical fit of the modelled data. The damages corresponding to a given water level were assigned these same probabilities. These damages were defined as the total damages of a given hurricane event, therefore in this case the combination of wind and flood damage. The total damages were determined by adding the wind and flood damage and assigning a threshold value to ensure damages did not exceed 100%.

7. **Risk Assessment**

   The hurricane risk on St. Martin was determined by using the synthetic hurricane tracks as different scenarios with induced damages and corresponding probabilities. The risk integral based on the definition in Section 2.3 by Jonkman, Van Gelder, and Vrijling (2003) was then determined for each point on the island using the empirical relationship between probability and damages. Figure 1.6 shows the conceptual flow of how the total hurricane risk was determined based on these two hazards.

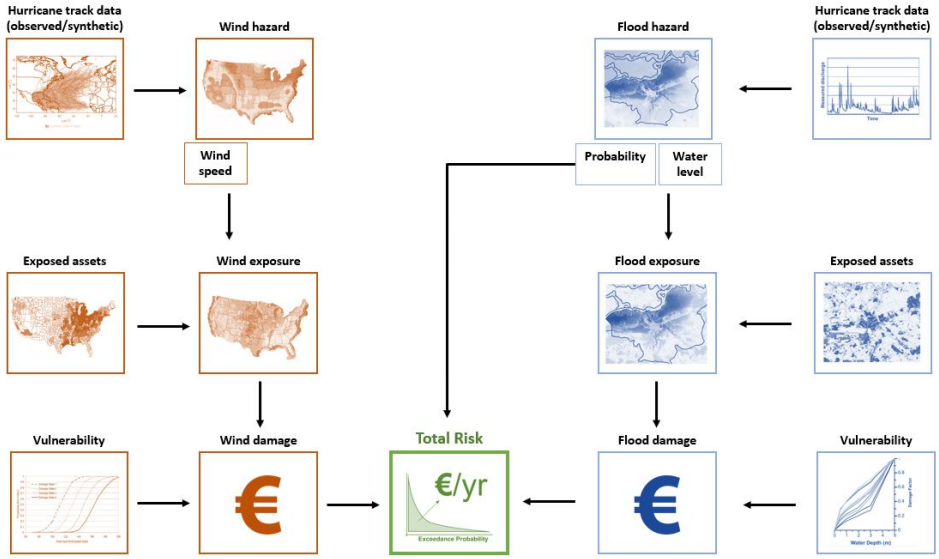

Figure 1.6: Conceptual overview of a general wind and flood risk assessment (de Moel et al., 2015).

The final risk assessment and applied methodology was the reviewed in terms of limitations, discussion and conclusions. The application of the methodology in St. Martin and the implications for disaster resilience were also discussed in relation to Building Back Better (Hallegatte et al., 2018).

1.5. Readers guide

The structure of the report and the research both followed the principle of starting on a global scale, then focusing application and validation on a local scale, and then determining what the global implications are based on the findings. Figure 1.7 shows the outline of the research and how it was structured. This chapter (Chapter 1) looks at hurricanes and hurricane risk from a global perspective and introduces the research by defining the problem, background and research objectives. Chapter 2 sets up the background to the research by reviewing the fundamental literature upon which the research is based. This is focused on hurricane-induced forcing (wind and water levels) and hurricane risk approaches that are currently used.

Chapter 3 describes the methodology of the research which can be divided into data collection for the study area, model setup and model validation. This chapter already starts the refinement process of the research to a local scale where the case study of St. Martin is used. Chapter 4 describes the probabilistic analysis of the chosen scenarios and how synthetic hurricane data generation was used to define these scenarios. This is also done on a local scale for the chosen case study. Chapter 5 combines the results found during the case study and determines the total hurricane risk for St. Martin. An analysis was done on the total risk to determine how the results can be used within the more global scale of disaster resilience.

Chapter 6 discusses the results and proposed methodology for defining multi-hazard risks induced by hurricanes, along with the model setup, validation and probabilistic analysis, and generalises the findings to how they can be applied on a global scale. Finally, Chapter 7 provides the conclusions of the research and what recommendations can be made for this research and future opportunities.

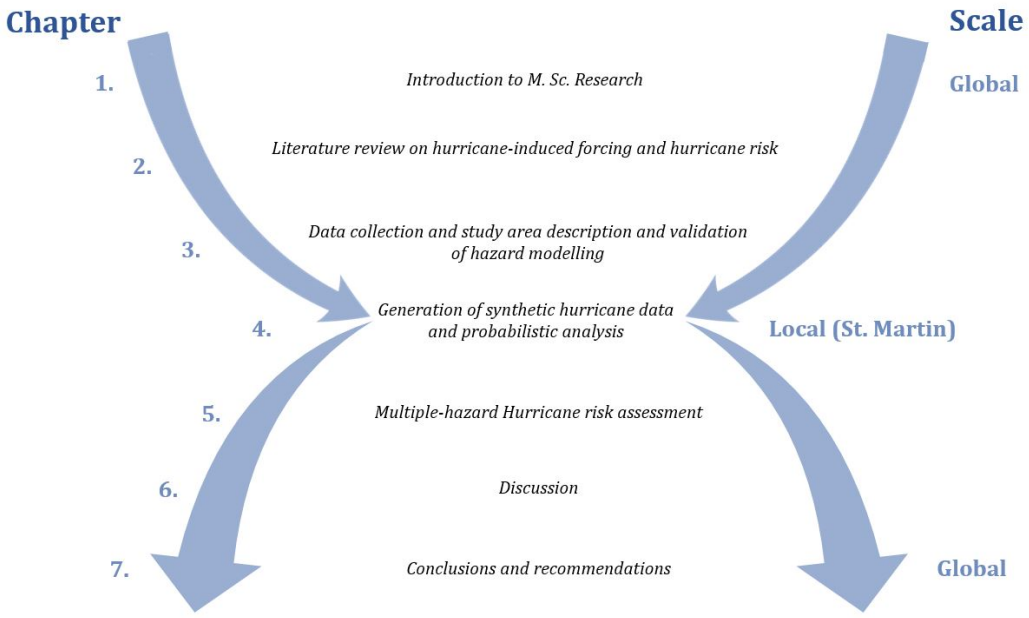

Figure 1.7: Outline of the structure of the research thesis.

2
Background

The following chapter describes the background literature upon which the research was based. Section 2.1 explains hurricane-induced winds in terms of intensity and how they are formed. The most common numerical models used to simulate hurricane winds are discussed as well as how to synthetically generate hurricane tracks for a probabilistic analysis. Section 2.2 explains the most important processes when considering hurricane-induced flooding, specifically looking the coastal water levels and the inland flooding that may arise. The application using numerical models and how to represent hurricane-induced water levels using a shear stress is explored. Furthermore, parametric models to estimate waves and rainfall for hurricanes, when complex modelling is not possible, is discussed. Section 2.3 describes the general approaches taken toward determining risk, namely the *multi-hazard risk* approach and the *multi-risk* approach. Their application and implications for exposure and damages are also explored.

2.1. Hurricane-induced Winds

Hurricanes are formed over oceans, near the equator, when warm air at the ocean's surface rises, causing a pressure depression below. High-pressure areas push air towards the low-pressure area and the "new" air then warms, and rises as well. The rising air eventually cools above and forms clouds. This cycle continues with the oceans' heat driving the whole system. The clouds gather and if the cycle continues long enough, eventually a hurricane is formed. The centre of the system is calm and is known as the eye of the hurricane. The airflow around the eye can increase to very high speeds. These winds, surrounding the eye, define the intensity of the hurricane. Hurricanes are often classified according to their wind speeds, and the most well-known classification is using the Saffir-Simpson Storm Categories, shown in Table 2.1, with a Category 5 storm being the most intense where maximum sustained wind speeds exceed 69.3 m/s.

Table 2.1: Saffir-Simpson Hurricane Categories (Vickery et al., 2000).

Saffir-Simpson category	Min. pressure [mbar]	Max. wind speed (over water) [m/s]	Max. gust speed (over water) [m/s]	Max. gust speed (over land) [m/s]
1	>980	33.1 – 42.0	40.6 – 51.9	36.8 – 48.1
2	979-965	42.0 – 49.6	51.9 – 61.7	48.1 – 58.1
3	964-945	49.6 – 58.1	61.7 – 72.7	58.1 – 69.7
4	944-920	58.1 – 69.3	72.7 – 87.3	69.7 – 85.5
5	<920	>69.3	>87.3	>85.5

Different numerical models have been developed that represent the spatial wind field of a hurricane. These are either parametric in nature or more advanced and solve for the physical processes using a physical model. These advanced models are used to forecast hurricane wind fields and movement. The parametric based model, on the other hand, uses hurricane characteristics as input to generate the corresponding wind fields. The parameters used in these models include the position and heading of the hurricane, and its extent. One of the most applied formulations for the extent and shape of a hurricane is that described by Holland (1980), and adapted models by Holland et al. (2010) and Nederhoff et al. (2019). Examples of studies applying the Holland formulation in hurricane forcing and risk include the work by PCRAFI (2013); Wu et al. (2018); Snaiki and Wu (2017); Valamanesh et al. (2016); Hoek (2017); Hall and Jewson (2007); Langousis and Veneziano (2009) among others.

The Holland (1980) formulation is an analytical model of the radial profiles of sea level pressure and winds in a hurricane. The fundamental equations contain two parameters which are empirically estimated from observations, or determined climatologically for a standard hurricane. The first scaling parameter, A, determines location relative to the origin and the second, B, defines the shape. Parameter B is also known as the Holland B parameter. The model further shows that as the central pressure decreases, the wind profile becomes more peaked with higher winds at the radius of maximum winds (RMW), and a decreased extent of destructive winds (R35). In 2010, a revised version was presented by Holland et al. (2010) where additional wind observations at a certain radius within the hurricane can be incorporated to determine the spatial geometry of the wind field. A study in 2019 by Nederhoff et al. (2019), further elaborates this revision by providing empirical stochastic relationships for the RMW and the R35, which are used in determining the geometry of the spatial wind fields. The application of the Holland model was shown to be superior to two other models, one by Schloemer (1954) and the other being the modified Rankine vortex by Phadke et al. (2003). Schloemer's model is constrained to one shape profile, where B is equal to 1, and tends to underestimate the maximum winds and overestimate the radial extent of destructive winds. The modified Rankine vortex produces large errors in the wind field if RMW is not accurately known where as in the Holland model this is not the case, and the RMW can even be derived.

According to the Holland et al. (2010) wind field model, the tangential wind field around the eye of the hurricane (gradient wind speed) is given by Equation 2.1.

$$V_g(r) = \left(\frac{B}{\rho}\left(\frac{R_{max}}{r}\right)^B (P_n - P_c) e^{\left(-\frac{R_{max}}{r}\right)^B} + \frac{1}{4}\left(V_{tr}\sin\theta - r f_c\right)^2\right)^{0.5} + \frac{1}{2}\left(V_{tr}\sin\theta - r f_c\right) \tag{2.1}$$

Where V_g is the 10-min averaged gradient wind speed, r is the radial distance, B is the pressure profile exponent (Hollands's parameter), ρ is the air density, R_{max} is the radius of maximum wind speed, V_{tr} is the

hurricane translation speed, θ is the angle defining the hurricane translation direction, P_n is the ambient pressure, P_c is the central pressure and f_c is the Coriolis parameter.

The gradient wind component in a hurricane is shown in Figure 2.1, along with the other force components. The pressure gradient force is directed inwards toward the eye of the hurricane and the Coriolis force and centrifugal force are directed away from the eye. The balance of these forces is known as the gradient wind balance. Friction results in the wind near the earth's surface to be angled inward toward the eye of the hurricane.

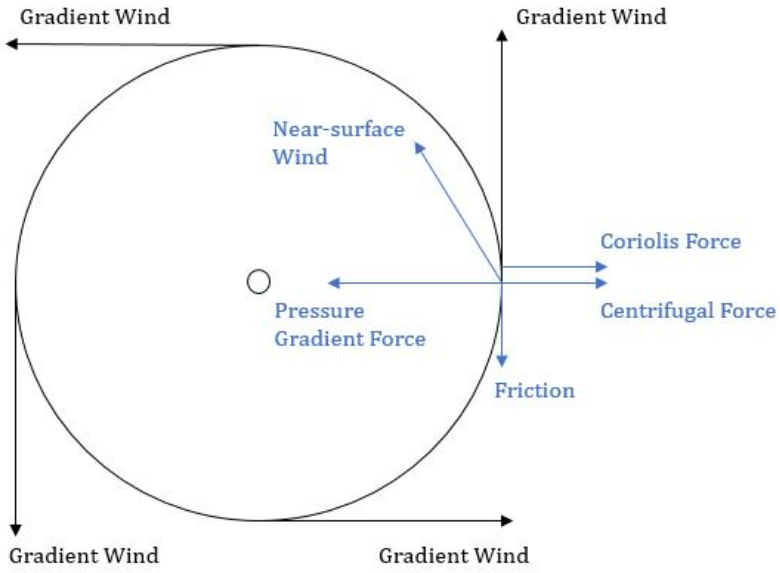

Figure 2.1: Primary circulation of a hurricane showing the different force components (Knowlton, 2015).

The pressure profile exponent, more commonly known as the Holland B parameter, represents the shape of wind decay around the eye of the hurricane and is an empirically determined parameter. In a study on the Northern Atlantic historical hurricanes by Valamanesh et al. (2016), it was found that this parameter decreases with increasing latitude and decreasing RMW. Furthermore, it was found that this parameter has an upper limit of 1.2 to 1.3 for hurricanes with low central pressures, and usually decreases as a hurricane approaches the land.

The second approach to modelling hurricane winds is to use a physical based model. Physical models are used to forecast wind movement and hurricane intensity using atmospheric input. The intensity is often described or predicted by using a coupled atmosphere-ocean model. Here the airflow and temperature effects are coupled with a 1D ocean model, to forecast the formation and movement of the hurricane as is done by Emanuel et al. (2004). These models can be used to describe the spatial wind field movement in two-dimensions, as well as the variation in wind speed over height in the third dimension. This is used to determine wind field variations over local topography by modelling the interaction between the two. Downscaling is an example of technique often used for places with complicated topography, such as mountainous areas, where the spatial variation in wind speeds cannot be ignored. Downscaling involves using low-resolution wind data to statistically infer high-resolution information on a finer grid resolution. Another example is mesoscale modelling, which involves simulating wind flows where surface measurements are scarce.

The physics behind a physical model are beyond the scope of this research and therefore only parametric based models are considered for modelling hurricane-induced winds. Furthermore, the application of the Holland (1980) model and the adaptions by Holland et al. (2010) and Nederhoff et al. (2019) will be used when simulating hurricane-induced winds.

2.1.1. Synthetic Track Generation

The number of hurricane events experienced, and recorded, varies per location and often this data is very limited. Performing a meaningful probabilistic assessment of hurricanes therefore requires much more data. Generating synthetic hurricane tracks is done by predicting the genesis, movement and termination of hurricane tracks using historical data to randomly sample from as done by Vickery et al. (2000); James and Mason (2005); Emanuel et al. (2006); Hoek (2017). In these studies, the properties of the historical events, are used to randomly draw from and generate new tracks. The variation in approach come in the prediction of the movement and translation of the hurricane track. The historical data can be used to sample genesis locations and from there, numerically predict the path the hurricane takes.

The historical track data and locations can also be fitted using copulas and empirical joint distributions to sample other characteristics such as change in direction or speed from, as done by Hoek (2017). The hurricane track is generally modelled using 6-hour time steps in these track generation studies. For each time step the change in direction, speed, and intensity of the hurricane is updated, along with eye location and sea surface temperature. The track is terminated when the wind speed drops below a predefined value or the maximum time of a hurricane is exceeded. In hurricane track generation there are four main factors to consider, namely track position, heading, genesis location and termination.

Track position and heading have been modelled according to different approaches as described in Hall and Jewson (2007). In the approach by Vickery et al. (2000), the entire hurricane track is modelled from generation until landfall, and finally termination. The central pressure is modelled as function of the sea surface temperature (SST) and the hurricane track (position, heading, translation speed) is updated for each time step by randomly sampling these various parameters. This is done also done for 6-hour intervals and using linear interpolation between time steps. A distinction is also made between eastward heading and westward heading hurricanes. An extension of this approach was then proposed by James and Mason (2005) which was based on the Vickery et al. (2000) model but for the Coral Sea near North Eastern Australia. Increments were modelled for latitude and longitude instead of for translation velocity, and scheme which interpolating historical genesis was used.

Another well-known approach is that of Emanuel et al. (2006), where a transition matrix (time and space dependent) is generated to sample from. This matrix relates the track speed and track direction before and after each time step. The matrix is populated using historical genesis data that has been analysed. Generating these tracks using statistics of historical track data to sample from, is known as the Markov method or a Markov chain (Hoek, 2017). This type of chain contains a sequence of random values whose probability depends on the value of the parameter at the previous time step (Emanuel et al., 2006). In this way the hurricane track will not backup on itself.

Synthetic hurricane track generation and wind field modelling is often combined as was done by Hoek (2017) in a study on hurricane tracks for the Gulf of Mexico. The methods described here and those used by Hoek (2017) are chosen as most appropriate when generating synthetic tracks and modelling hurricane-induced winds.

2.2. Hurricane-induced Flooding

Hurricane-induced flooding is determined by two physical processes. Firstly, by the amount of coastal activity causing a rise in coastal water levels (wind waves and storm surge) and the induced coastal flooding. Secondly, by the inland activity of increased water levels due to extreme rainfall inducing inland flooding. The combination of these two phenomena leads to total hurricane-induced flooding. Here both these components will be discussed within the context of hurricane modelling.

Modelling hurricane-induced coastal water levels and flooding requires understanding of the interaction of the hurricane formation, induced-pressures and induced-winds with the ocean. Firstly, hurricane formations induce storm surge that is either wind driven or pressure driven depending on the local ocean depth and bed slope (Donev, 2016). Figure 2.2 shows the difference in storm surge that is wind driven or surge driven. Along with storm surge, the hurricane interacts with the surface of the ocean inducing waves and modelling this requires translating the winds to a shear stress and projecting it onto the hydrodynamic system being

considered. In this section the modelling of these two processes (storm surge and waves) is discussed, along with how to deal with estimating these using simplifications in modelling.

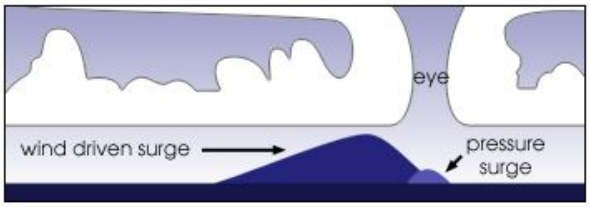

Figure 2.2: Wind-driven and pressure-driven storm surge due to hurricane activity (Donev, 2016).

Different oceanic waves are classified according to their frequency or period as shown in Figure 2.3. Simulation of surge, tides and wind-generated waves (swell and wind sea) are further discussed in this chapter, however, it is important to note that waves of other frequencies can also be relevant to hurricanes.

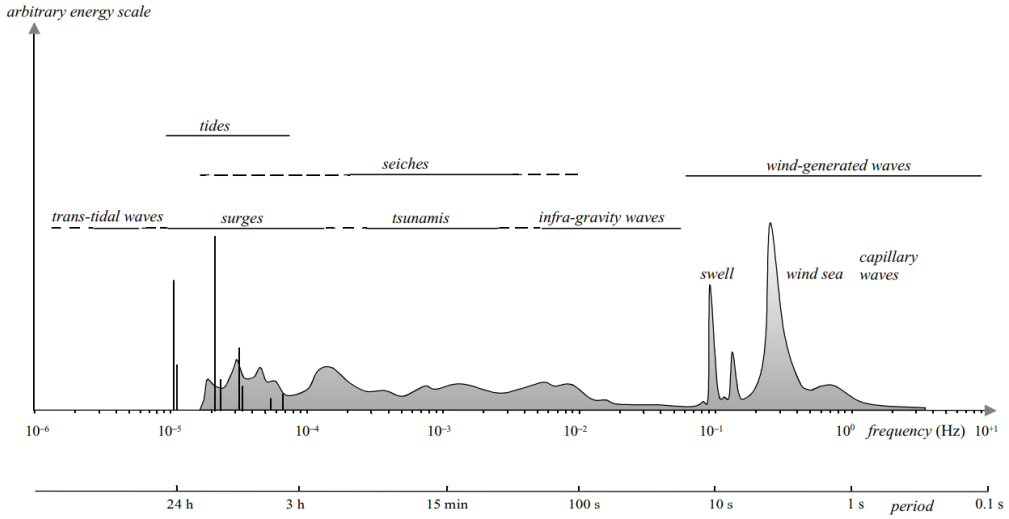

Figure 2.3: Various frequencies and periods of different oceanic variations in vertical motion (Holthuijsen, 2007).

Wind-generated waves are simulated using numerical models that use the shallow water equations as physical basis (Zijlema, 2018). These equations describe the flow below a free surface in a fluid, in this case the ocean. Wind waves are coupled to the shallow water equations as a shear stress. This requires the wind speed and wind drag coefficient as input.

2.2.1. Wind drag in hydrodynamics

The wind drag coefficient can be defined according to various concepts, where the drag is dependent on the wind speed at 10 meter elevation above the water surface. The simplest concept for estimating drag, is assuming a constant drag coefficient. The drag coefficient can also be defined according to Smith and Banke (1975) as linearly varying or piecewise linearly varying, or according to the formulations by Charnock (1955) or Hwang (2005). The (Hwang, 2005) formulation relates the steady state wave conditions to the dynamic roughness and in this formulation the peak period, frequency and wave number are needed. Here the formulation by Smith and Banke (1975) is further explained due to its simplicity compared to the more advanced formulations, while still representing more physics than a constant relationship.

According to Smith and Banke (1975) the drag coefficient is described as linearly varying or piecewise linearly varying. The latter is shown in Figure 2.4 where when only A is defined the relationship is considered constant, when A and B are defined the relationship is linearly varying and when A, B and C are defined the relationship is defined as piecewise linearly varying. When the relationship is defined as in Figure 2.4 it means that for the range of wind speeds between the breakpoints A and B a linearly increase relationship holds, and for wind

speeds between breakpoints B and C a linearly decreasing relationship holds. For all other wind speeds, the drag coefficient is constant.

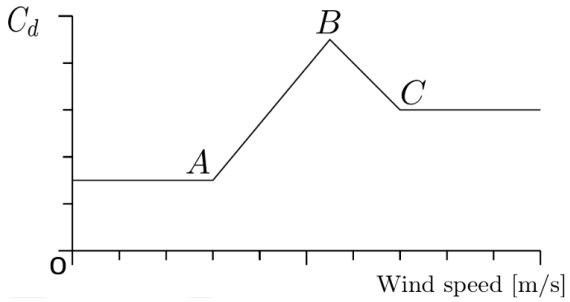

Figure 2.4: The dependency of the wind drag coefficient on the wind speed as described by Smith and Banke (1975) (Deltares, 2019).

There is therefore, a threshold for the drag coefficient that occurs for the wind speed defined at B. Physically this means that as the wind speed increases until wind speed A (moderate winds with wind speeds around 4 m/s to 10 m/s) the drag experienced does not change, from wind speed A and increasing wind speed experiences and increased drag (more resistance) until it reaches a wind speed (B) (strong winds with wind speeds around 10 m/s to 20 m/s) actually starts to experience less resistance, possibly due to the impact of spray (Makin, 2005). This continues until wind speed C, after which the drag is again assumed to be constant (very strong winds, exceeding 20 m/s) (Vickers et al., 2013).

The Charnock (1955) formulation is also widely applied when modelling the wind drag. It is based on the assumption that the wind flow over the water surface is a fully developed turbulent boundary layer, and that the wind speed profile is logarithmic. In this formulation the friction velocity, wind speed (at 10m above the water surface), and friction of the water surface are needed as input. Figure 2.5 shows the Charnock (1955) formulation as well as a new parameterisation by Makin (2005) based on the original formulation and its validation within a hydrodynamic model. It shows how these formulations are represented in the model software Delft-3D, a process-based hydrodynamic model (Lesser et al., 2004), see Section 3.2.2.

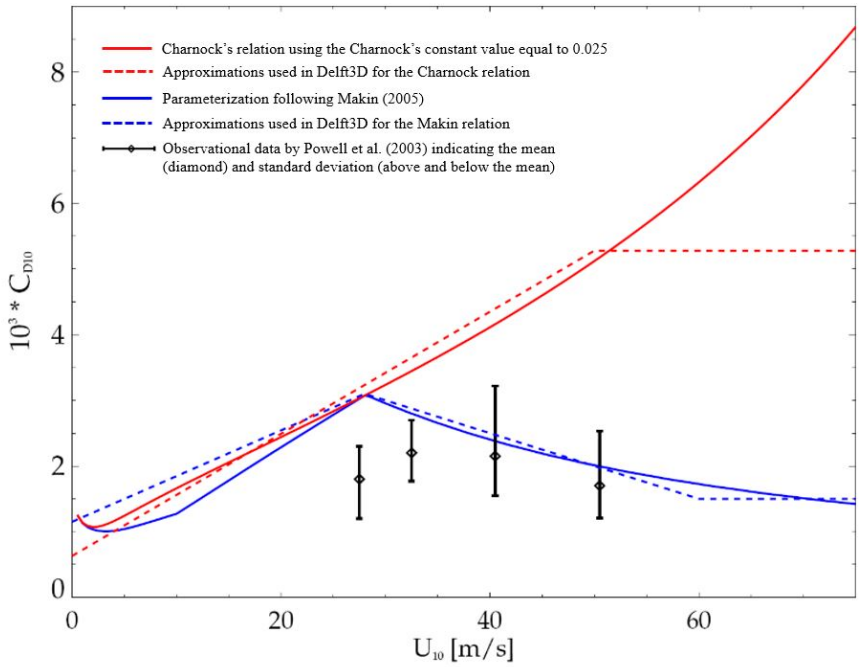

Figure 2.5: Drag coefficient (C_D) as a function of wind speed according to the Charnock (1955) formulation and the new parameterisation following Makin (2005) shown in solid lines. The dashed lines represent the approximations used in model software (Delft3D) (Vatvani et al., 2012) and the bands represent observational data by M. D. Powell et al. (2003).

2.2.2. Parametric wave models

The translation of hurricane-induced winds to a shear stress on the water surface is used when simulating storm surge and wave conditions using more complex numerical models such as Delft 3D. When this modelling is not possible, the spatial distribution of significant wave height can be predicted according to the model of I. Young (1988). This distribution is based on three hurricane characteristics namely, maximum wind speed, translation speed and the radius to maximum winds. The equivalent fetch is determined for the situations where the wave speed is of the same order as the translation speed of the hurricane. Under these circumstances the wind is able to transfer energy to the waves (Valamanesh et al., 2016; I. Young, 1988). The design wave height found is for deep water conditions where there is no influence of water depth on the waves, due to land or sea bed. The design wave height is given by Equation 2.2 with the equivalent fetch length and effective radius given by Equation 2.3 and Equation 2.4 respectively.

$$H_{s,max} = 0.0016 V_{max} \left(\frac{L}{g}\right)^{0.5} \tag{2.2}$$

$$L = R^{'}(-2.17510^{-3} V_{max}^2 + 1.50610^{-2} V_{max} V_{tr} - 0.122 V_{tr}^2 + 0.219 V_{max} + 0.674 V_{tr} + 0.789) \tag{2.3}$$

$$R^{'} = 22500 \log(R_{max} - 70800) \tag{2.4}$$

Where $H_{s,max}$ is the offshore design wave height, V_{max} is the maximum sustained wind speed, L is the equivalent fetch, g is the gravitational acceleration, $R^{'}$ is the effective hurricane radius, V_{tr} is the hurricane translation speed and R_{max} is the radius of maximum winds.

This model assumes that the hurricane track is straight and is only applicable for determining waves for the direction in which the hurricane travels. This is due to the fact that the equivalent fetch is based on the difference between the propagation speed of the hurricane and the group velocity of the waves (Hoek, 2017). Assuming that perpendicularly generated waves have limited growth and that wave-growth is greatest within the hurricane quadrants, the model is appropriate for extreme wave conditions such as those experienced during a hurricane.

2.2.3. Storm surge and tide

The final components considered under coastal water levels are storm surge and tide. Tide is the general rising and falling of the sea due to astronomical influences and storm surge is the overall rise in water level to different physical processes such as hurricane-induced wind-driven surge or pressure-driven surge. Figure 2.6 shows the difference between storm surge and tide.

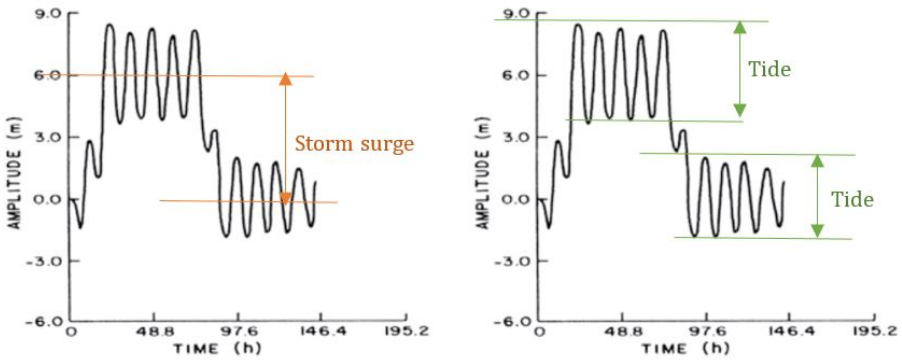

Figure 2.6: A water level time series showing the difference between storm surge (left) and tide (right) (World Meteorological Organization, 2011).

The tide is present irrespective of whether a storm is active or not (Bosboom & Stive, 2013). Storm surge on the other hand is induced when external weather forces cause a pressure difference along the ocean's surface (Wu et al., 2018) and is influenced by factors such as storm intensity, central pressure, storm forward speed,

storm size, angle and shape of the coast and local bathymetry and topography (National Hurricane Center, 2018b). During a hurricane the ocean surface is disturbed due to wind and pressure differences which cause the water to be pushed towards land and "pile up", and the overall coastal water level is raised (Bosboom & Stive, 2013). When modelling storm surge, it is important to realise that the local tidal conditions are not the same as the storm induced surge levels. The tidal oscillations are generally unaffected by the storm surge and only the "mean water level" increases. Global surge and tide models exist to simulate these conditions. An example of one of these models is the Global Tide and Surge model (GTSM) and its output data set, GTSR, developed by Muis et al. (2016). This output data set is often used in research for global reanalysis (Bloemendaal et al., 2018).

The contribution of storm surge to coastal flooding compared to wind-generated waves depends on the local conditions of the coast (Bosboom & Stive, 2013). Long uninterrupted coastlines facilitate the piling up of storm surge much better than short coastlines or islands. For long coasts the storm surge may deem the wind-generated waves negligible and vice versa. Furthermore, the cross-shore profile of the coast can also influence the water levels experienced during a storm and which processes dominate (Inman, 1994). For gently sloping foreshores waves have room to travel and dissipate before they reach the beach. For steep sloped beaches there is less room and the waves that reach the beach have much more energy, meaning these waves cannot be neglected (Inman, 1994). Depending on these local characteristics, the combination of wind-driven surge, pressure-driven surge and tide is defined.

2.2.4. Parametric rainfall models

When determining the inland water levels and flooding, the factors to consider is the local topography, soil type, infiltration rates, inland waterways and their discharges, and how rainfall accumulates during a storm event. Modelling the effect of rainfall on inland flooding therefore requires information on the inland hydrodynamics as well as the rainfall being modelled. Rainfall is usually easy to measure, and most locations have satisfactory rainfall records of water levels during a hurricane. However, for locations without observational data, an assumption can be made on the rain fall rate experienced during the hurricane. This rainfall information can then be implemented into a hydrodynamic model to simulate inland flooding.

There are two options when determining rainfall during a hurricane. The first is an extensive tropical cyclone rainfall model such as TRC (Tropical Cyclone Rainfall Model) (Lu et al., 2018) or WRF (Weather Research and Forecasting Model) (Powers et al., 2017) which generates rainfall along hurricane tracks, incorporating all major rainfall mechanisms (surface frictional convergence, vortex stretching and the interaction with local topography). The second option is to find a relationship between wind speed and rainfall rate. Rainfall patterns can be synthetically simulated by developing an empirical relationship between rainfall rate and wind speed based on observations during a hurricane event. Previous research (Matyas, 2000; Jiang et al., 2006; Langousis & Veneziano, 2009; PCRAFI, 2013; Snaiki & Wu, 2017) relate rainfall rates and wind speeds during hurricane events. In the study by (Jiang et al., 2006), a correlation is found between the spatial distribution of the hurricane wind speeds based on the radius of maximum winds and the spatial distribution of rainfall during a hurricane. Figure 2.7 shows the relationship between rainfall rates and the size of a storm and Figure 2.8 shows how this correlates to the radial relationship of a storm and wind speeds.

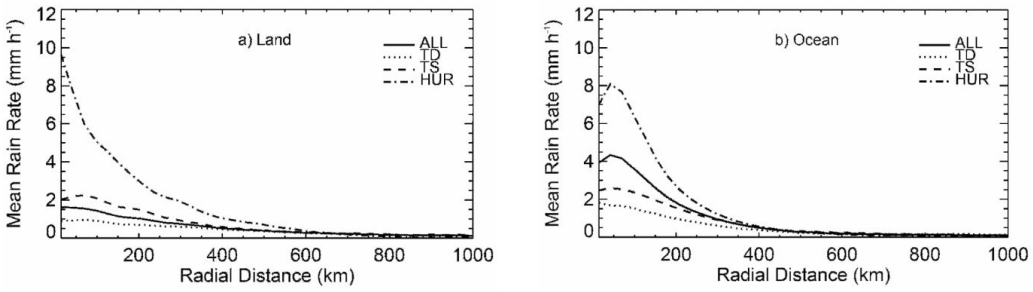

Figure 2.7: Mean rain rates as a function of radial distance for different storm intensities (TD: Tropical Depression, TS: Tropical Storm, HUR: Hurricane) for a) over-land and b) over-ocean (Jiang et al., 2006).

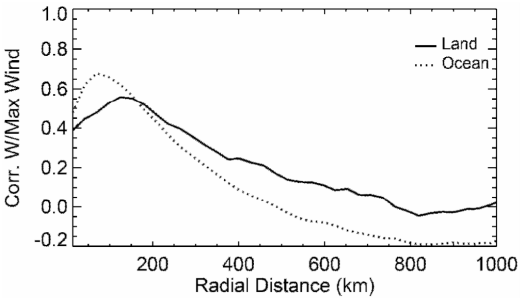

Figure 2.8: Example of the correlations between mean rain rate as a function of radial distance and maximum wind intensity for over-land and over-ocean observations (Jiang et al., 2006).

An established relationship between rainfall and storm size and intensity can therefore be used when estimating rainfall for situation where rainfall observations are limited. A physical-based rainfall model like that of Snaiki and Wu (2017), is an example of this. The typical tropical cyclone wind field parameters, RMW, R35, maximum wind speed and translation speed are used to generate synthetic rainfall distributions. The amount of rainfall is therefore, then dependent on the intensity of the hurricane, its translation speed and the terrain of the location in question. Modelling rainfall can be done by defining the spatial distribution of rainfall based on the spatial wind fields and pressure fields defined for the hurricane to be simulated, and applied as external forcing.

2.3. Hurricane Risk

The final theoretical element to consider is risk and its relationship to hurricane modelling. Once the hazards for a given scenario have been determined, in this case those of hurricane-induced winds and coastal flooding, a relationship between those hazards and their induced damages have to be defined. These relationships are known as vulnerability functions. These functions give insight into induced damages. The other variable involved in a risk assessment is the corresponding probabilities of the scenarios being considered. Once the damages and related probabilities are known the total risk can be determined.

The general definition of risk by Kaplan and Garrick (1981) is given in Equation 2.5. The unit of risk is defined as € per year or $ per year also referred to as the expected value, E(d).

$$E(d) = \sum_{s_i=1}^{n} p_i d_i \tag{2.5}$$

Where s_i is the scenario, p_i is the probability of the scenario and d_i is the consequence of the scenario.

For economic risk, the probability of exceedance of damages can also be represented using a curve, known as the distribution Function of the economic Damages (FD-curve) (Jonkman et al., 2003). The area under this curve is equal to the expected value of damages and the expected risk is given by Equation 2.6.

$$E(d) = \int_{s_i=1}^{s_i=\infty} p_i d_i \tag{2.6}$$

Risk is therefore defined by the scenario that is being considered, its probability of exceedance and the consequence of the scenario occurring. When it comes to hurricanes often risk is considered for the wind speeds or water levels that a hurricane induces, and therefore, the probability relates to the occurrence of a given wind speed or a given water level which is dependent on the relative location of the hurricane to the location of interest. The following section discuss the methodologies related to hurricane activity and how probabilities are assigned to different scenarios. Furthermore, the approach to exposure and damages is also discussed in terms of wind and flooding.

2.3.1. Risk methodologies

Gallina et al. (2016) summarises the current methodologies for hazard risk assessments by describing two main approaches. These two main approaches are the *multi-hazard risk assessment* and the *multi-risk assessment*. The multi-hazard risk assessment approach looks at different hazards, combines them and assesses

total vulnerability. The multi-risk assessment approach looks at hazard specific vulnerability and risk separately and then combines this risk to get a total risk. These steps for these two approaches are shown in Table 2.2.

Table 2.2: Steps of the multi-hazard risk assessment multi-risk assessment approaches for determining risk according to Gallina et al. (2016).

Steps	Multi-hazard risk assessment	Multi-risk assessment
1	Hazard assessment	Hazard assessment
2	Multi-hazard assessment	Exposure assessment of elements at risk
3	Exposure assessment of elements at risk	Vulnerability assessment
4	Vulnerability assessment	Single-risk assessment
5	Multi-hazard risk assessment	Multi-risk assessment.

Multi-risk assessments are comprised of both multi-hazard and multi-vulnerability concepts and are useful for addressing global policy (Gallina et al., 2016), even though they vary in the detail level used in the analysis. Institutions such as the World Bank, the Federal Emergency Management Agency of United States (FEMA) and the Central American Coordination Centre for Disaster Prevention (CEPREDENAC) use this approach to determine hazard risk. Multi-hazard risk on the other hand requires the aggregation of hazard, exposure and vulnerability, often qualitatively by means of questionnaires of categorical scoring. Generally, vulnerability is described independently from the hazard that is considered and analysis often classifies risk as high, medium or low and is not explicitly quantitative (Gallina et al., 2016).

Within these approaches, each step can be dealt with in a different way. Hazard assessments, when it comes to hurricanes, are most often limited to wind assessment or flooding assessment as described in sections 2.1 and 2.2 respectively. Naturally the definition of the hazard can differ, however, the way in which the hazard is assessed can also differ. The detail and accuracy of the assessments are usually the distinguishing factors. For example, when looking at flooding, various factors can be considered, such as flooding due to rainfall or due to wave setup or a combination of both. In this way each aspect of the hazard has multiple dimensions that can either be solved for, assumed or ignored.

When determining risk, the difference between the approaches comes in when defining the scenarios to consider, and how the probability of the scenario occurring is determined. For a multi-hazard risk assessment, a scenario is defined as multiple hazards occurring at a given location. For a multi-risk assessment, a scenario is defined as one hazard occurring and determining the risk to a single hazard first and later a total risk due to multiple hazards. Figure 2.9 shows the difference between these two main approaches to risk.

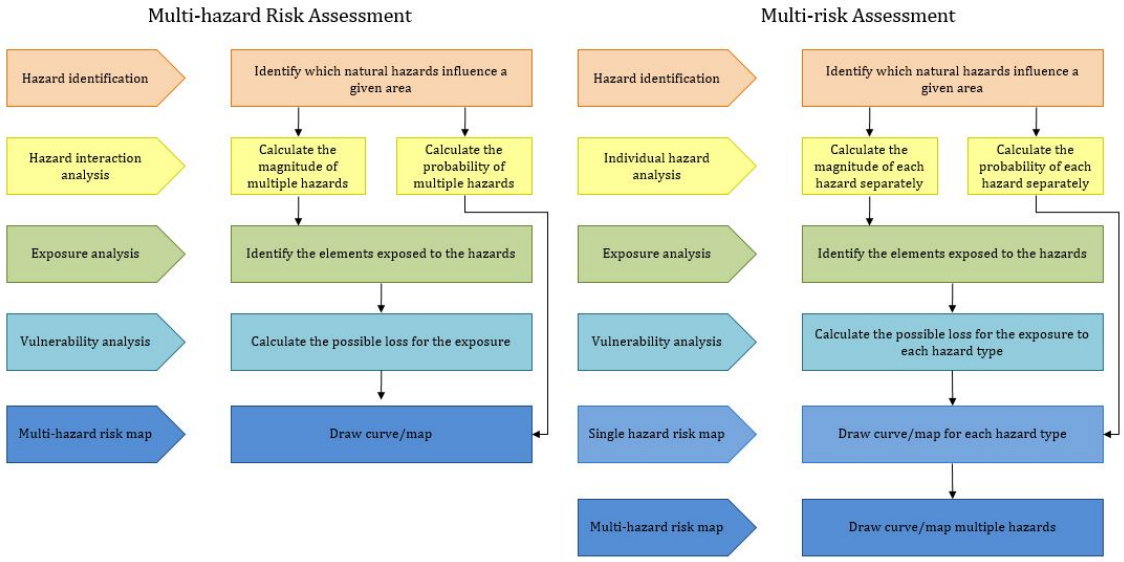

Figure 2.9: Basic framework of a multi-hazard risk assessment and multi-risk assessment (Liu et al., 2016).

Currently hurricane risk is defined by wind risk and considers a scenario as a given occurrence of a wind speed due to a hurricane, and then determining the damage for a given wind speed. It is important to realise that the probability of occurrence of a given wind speed due to a hurricane is different to the probability of occurrence of a hurricane. The former is dependent on the location and intensity of the hurricane and its path, and the latter is dependent on the location of interest and whether the hurricane track makes landfall for example. The same is true for flood risk. The probability of occurrence of a given water level is dependent on the location and intensity of the hurricane and its path. This is different to the probability of a hurricane making landfall and the water levels it induces. Once the scenarios are defined, the probability of a scenario occurring is defined. This again is dependent on the definition of the scenario. Either the probability is determined by looking at the return period of a hurricane for a given location for example, or by looking at the return period of the hazard (wind speed or water level) due to a given hurricane.

In order to determine the probability of a hurricane event occurring there needs to be a probabilistic analysis done on the hurricane data. This is comprised of the synthetically generated data or (if sufficient) the historical hurricane data that is available. The moment of probabilistic analysis varies in past research. In the research by M. Powell et al. (2005), the tracks are filtered for the state of Florida by defining an area around the location of interest within which the hurricanes must pass. From the filtered tracks the annual occurrence of a hurricane track is determined. For each track a wind field model is then run. Emanuel et al. (2006) also take the same approach for the location of Miami, and the frequency of exceedance of hurricane wind speeds are found and then deterministic track intensity modelling is performed. Vickery et al. (2009) however, take a different approach. The tracks are synthetically generated and for each track an intensity is simulated, from there the wind speeds for each hurricane is recorded and the wind speed exceedance maps are determined from a probabilistic analysis done on the recorded wind speeds. This is consistent with defining the scenario as a given wind speed and not as a given hurricane event.

This approach to wind risk is the same when considering other hurricane-induced hazard risk however, the combination of various hazards remains limited to the approaches mentioned previously. The final difference between various risk studies is the way in which the risk is represented. This is of course dependent on all the factors leading up to the final risk calculation such as vulnerability and exposure. Risk can be represented in various ways, using risk indexes such as potential losses or expected value of loss expressed in the local currency.

2.3.2. Exposure and Damages

The definition of exposure varies per study and is usually based on physical objects. It is also often based on the available information about the area of interest. Examples of exposure categories for buildings include residential, commercial or industrial. Exposure can also be defined by land use type using categories such as agriculture, urban and rural areas. The exposure data directly influences how the relationship between vulnerability (or damages) and hazards are constructed, as the relationship is related to the type of exposure data available and the simulated hazard intensities.

The definition of damage varies from physical damages, to economic losses, to social impacts. A difference is further made when considering direct or indirect damages. In all cases however, a relationship is made between the hazard and the damage caused, known as a vulnerability (fragility or damage) function. These vulnerability functions can be time dependent, although most often are not. They vary in terms of detail and complexity with many variables influencing the extent of damage. For example, when considering vulnerability functions for a given building the variables that may influence the behaviour of the building for a given hazard include structure, number of floors, windows, doors, building frame material, construction methods, duration of exposure, type of hazard, and many others. These functions therefore are usually based on the hazard intensity and exposure information available.

Here wind damages and flood damages are explored, however, it is important to note that other vulnerability relationships may exist, for example the damages induced by wave impact and flow velocities. These are not considered in this research, as research for St. Martin, or similar locations, on the topic of wave damages is limited. There are empirical relationships like those developed by Hatzikyriakou and Lin (2017). This however extends beyond the scope of this research as in order to apply these relationships it is necessary to focus on detailed wave and flow modelling and developing empirical relationships for St. Martin. The influence of

waves on total damage is therefore not explored.

Wind damage is typically estimated by determining the structural damage on affected crops or buildings, and wind speeds are defined as the maximum 1-minute sustained wind speed at 10 m elevation above the ground at a given location (PCRAFI, 2013). The relationship between damages and wind speed are determined by defining the damages for a given wind speed, and scaling them to their relative magnitude compared to the maximum possible damage. According to one study done by Emanuel (2005) there is a rough a cubic relationship between wind speed and monetary damages, according to another study done by Nordhaus (2010), this relationship is much higher, more likely up to the 9^{th} power. This too was disputed by Bouwer and Botzen (2011), claiming it to be somewhere between the 6.5 and 8^{th} power. These studies, and the work done by Bertinelli and Strobl (2008), show that the relationship between wind speed and damage is very site-specific. Bertinelli and Strobl (2008) found a relationship of wind to damage to the power of 3.8. The relationships are found empirically by looking at existing damage losses (usually based on insurance data) and comparing them to wind speeds. An example of empirically fitted data to determine a vulnerability function versus wind speed is shown in Figure 2.10. This shows how the site-specific data steers the vulnerability relationship, and therefore, site-specific relationships are preferred when considering wind damage.

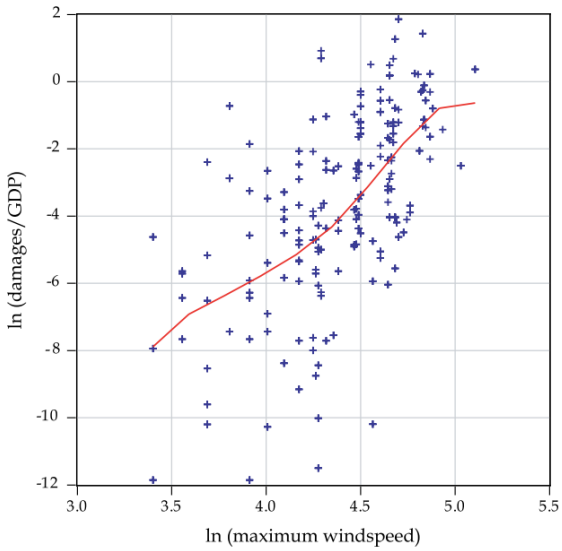

Figure 2.10: Example of U.S. data of damage vs wind speed and the relationship found empirically (Nordhaus, 2010).

Flooding damage is typically determined by estimating the structural damage for a given water level, where these levels are defined as the height of standing water due to fresh water (rainfall) or salt water (surge). Typically the damages for buildings are defined for the content of a building, its structural losses and outside property damage (US Army Corps of Engineers, 1992). The damages are then estimated to their relative damage of the structure, and the water depth versus damage can be determined. Water depth damage functions are currently developed based on land use type for different countries however, most smaller countries have limited or no data within these global studies (Huizinga et al., 2017). In the same way as wind damages are site specific, flooding damages too are very site specific and relationships developed for the location of interest are preferred.

In summary, in order to determine the hurricane risk for a location of interest, it is necessary to follow a given methodology regarding hazard modelling, impact modelling and risk assessment. The approach to hazard and impact modelling is dependent on the local factors of the location of interest, in particular the data availability. The theory discussed in this chapter was applied to the case of St. Martin in order to determine the hurricane risk in the region. Hurricane-induced winds and flooding were modelled in the region for the validation case of Hurricane Irma as well as a series of hurricane track scenarios used in the risk assessment. The outcome of this application forms the basis for the proposed methodology for risk assessment in data scarce regions. This is discussed in the following chapters.

3

Methodology

The following chapter describes the methodology followed during the research regarding hurricane risk in St. Martin. The methodology can be described in two phases. Phase 1 refers to the model setup and validation using Hurricane Irma and Phase 2 refers to the application to synthetic hurricane tracks and the analysis thereof. The structure of this chapter follows the steps involved. Phase 1 is described in Section 3.1, 3.2 and 3.3, and Phase 2 is described in Section 3.4 and 3.5.

Section 3.1 describes the location of interest, St. Martin, regarding the coastal characteristics of the island and the various data sources collected for the hazard and impact modelling of hurricanes. Section 3.2 describes the method of calculating wind speeds and flooding on St. Martin due to a hurricane event and how Hurricane Irma was used as a validation case for this approach. Section 3.3 describes the methodology used to determine the wind and flood damage due to a given hurricane event. The results of the hazard modelling and impact modelling were validated for Hurricane Irma and deemed ready for application using synthetic hurricane tracks. This marked the end of Phase 1. Section 3.4 describes the generation of synthetic track scenarios and how these were modelled to determine hazard extent and damages. Finally, Section 3.5 describes the method used to perform the risk assessment for St. Martin. Here the process of determining the probabilities for impacts due to each hurricane scenario is discussed, as well as the final risk integration.

3.1. Data collection for the Case Study of St. Martin

The data collected for St. Martin was classified into four groups. The first group related to the data collection to define the coastal zone of St. Martin. This included data about the island's beaches, reef zones and building infrastructure in relation to elevations on the island. The second group related to the data needed for the hazard modelling on St. Martin. This included the local information about the bathymetry and topography. The third group related to the data needed for the validation of the hazard models and for the island of St. Martin this data was very limited. The collection of online maps and images were used as validation data for St. Martin. Finally, the last group related to the exposure data used in the impact modelling for St. Martin. This was a combination of data for the building uses on the island, as well as the building structure materials. This section elaborates on these data sources and how they were expanded to improve the modelling possibilities for St. Martin.

3.1.1. Coastal zone of St. Martin

The coastal environment of St. Martin is made up of a variety of features, including sandy bays, steep cliffs, coral reefs and highly urbanised beaches. The typical beach profile of the St. Martin coast is a steep, concave-upward profile that usually lacks an offshore bar, and bar-related surf zone (Boon & Green, 1988). The beach slope is typically in the same order of intermediate and reflective beach slopes, meaning waves are able to propagate onshore without significant attenuation. Figure 3.1 shows various beaches along the coast of St. Martin. The pictures show how the coast is made up of an array of pocket beaches lying between rocky headlands. These bays collect sandy sediments that make up the beaches shown in the images. These sediments are mainly calcium carbonate sands of marine origin, rather than quartz and feldspar-rich detrital sands, as found by Boon and Green (1988). The sandy beaches are connected to the hinterland, which is made up of steep slopes such as those shown in pane 7 in Figure 3.1, as well as more gradual slopes as shown in pane 6.

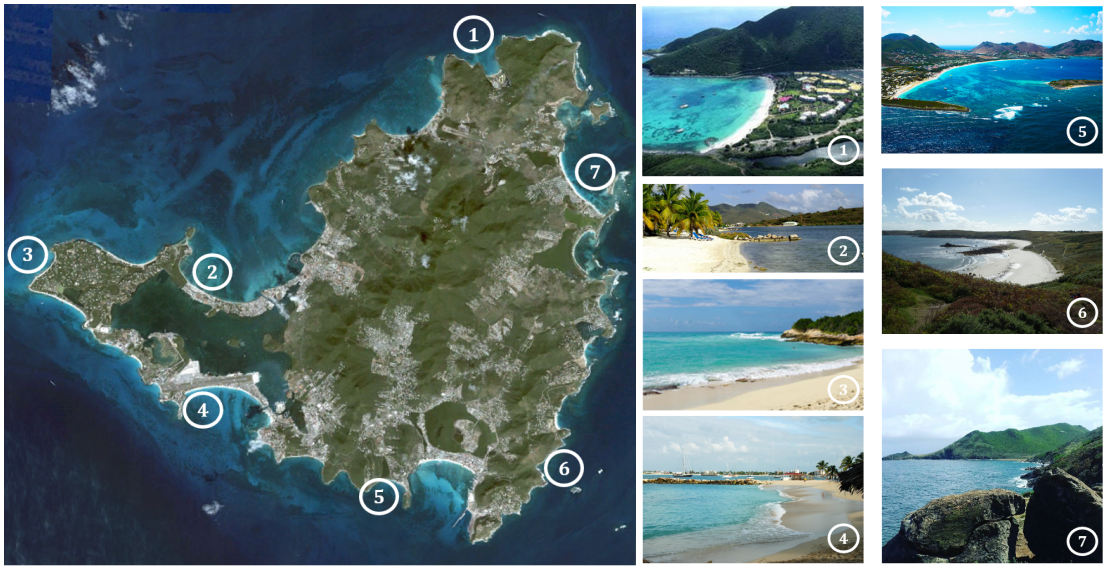

Figure 3.1: Left: Aerial view of the island of St. Martin indicating 7 beaches (Google Earth V 7.3.2.5776, 2005). Right: Beaches along the St. Martin coast namely; 1. Anse Marcel (OnParOu, 2019), 2. Baie Nettlé (Easy Voyage, 2019), 3. Baie aux Prunes (St. Martin Tourist Office, 2019), 4. Simpson Bay (The Crazy Tourist, 2019), 5. Little Bay (A. Young, 2012), 6. Geneve Bay (Hottot, 2017), 7. Orient Bay (Wild Adventures, 2019).

The regular wave climate is made up of relatively low energy waves originating due to the Easterly Trades or distant storms, and the dominant wave direction corresponds to this. For coastlines with a medium to large continental shelf, storm surge plays a dominant role and usually short waves are negligible as they are dampened by the time the reach the shore. In a coral reef environment however, short waves and infra gravity waves are important and the impact of storm surge may be small in comparison to swell and short waves (Giardino et al., 2018). For steep sloping beaches, like those found on St. Martin, there is much less room for waves to dissipate, and therefore the waves that reach the shoreline have much more energy. Often this energy is dissipated on the coral reefs situated just before the shoreline.

Figure 3.2 shows the coral reef system for St. Martin, and shows how beaches, along the southwest part of the island, are fully exposed to deep water waves, where the 100 m depth contour is less than 2 km from the shoreline. Here ocean swell is the most common wave that arrives at the coast. During the windy season, in the winter, this swell reaches above 2.5 m. The eastern coast of the island is rocky, and often fronted by fringing reefs connected to a shallow platform where the 30 m depth contour is found 5 km offshore. The north side of the island fronts the narrow and sheltered Anguilla Channel, between the islands of St. Martin and Anguilla, and therefore the wave conditions are relatively low energy. The tidal range for the island is micro-tidal, roughly 30 cm to 60 cm (The Moorings, 2019).

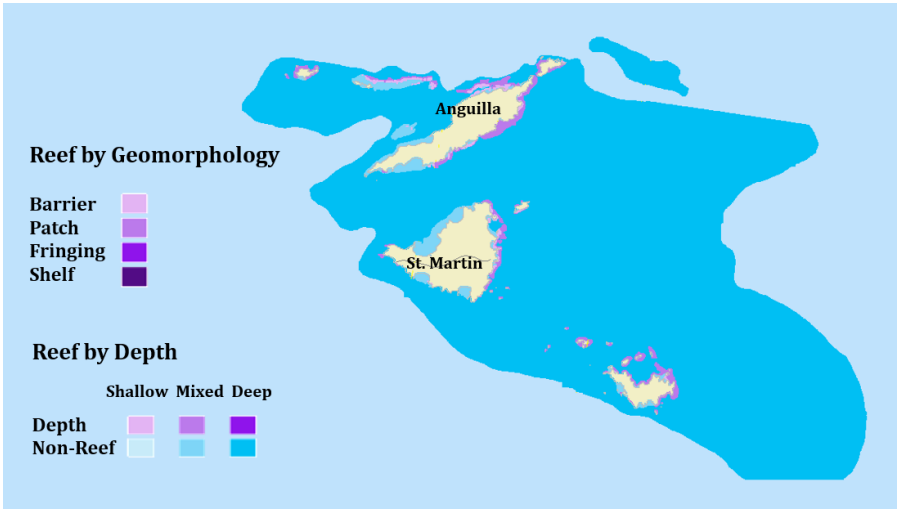

Figure 3.2: Coral reef morphology for the islands of St. Martin and Anguilla in the Caribbean showing reef type and depths (Reef Base, 2019).

The coastal zones on the island also make up the coastal area, along with the coral reef system and beaches. The island is populated with 41,000 people on the Dutch side of the island (Sint Maarten) and 32,000 people on the French side of the island (Saint Martin). The greatest concentration of housing, industry, services and transport infrastructure (main roads and airports) are found in the low-lying coastal zones. In Figure 3.3 the elevation of the island is shown as well as where buildings are located on the island. Very few buildings are found along the higher parts of the island and along the mountain ridge.

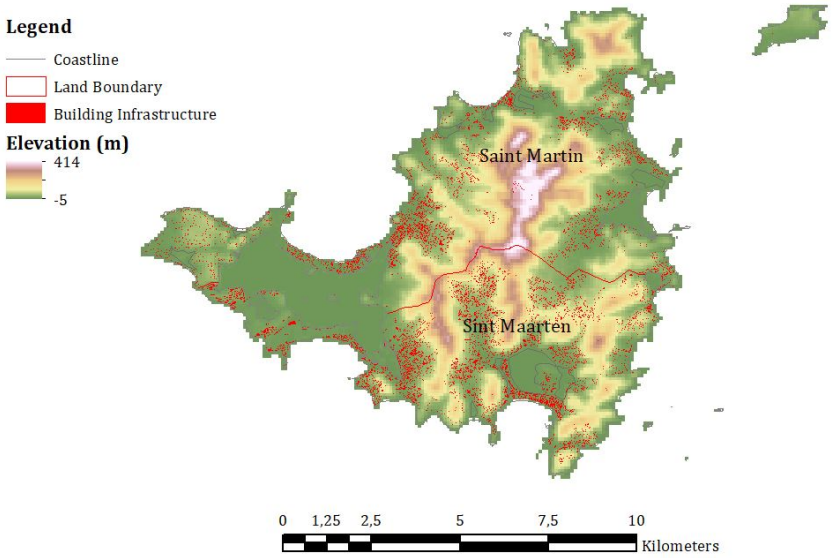

Figure 3.3: Map of St. Martin showing the distribution of building infrastructure (OpenStreetMap, 2019) around the island compared to the elevation heights (University of Tokyo, 2018).

3.1.2. Modelling data

The two data sources described here, include the bathymetry and topography data used in the hazard modelling for St. Martin, as they were fundamental in steering the modelling process. The other inputs into the hazard models are discussed in Section 3.2, and include the hydrodynamic boundary conditions, forcing, computational grid, domain and other physical and numerical parameters.

BATHYMETRY

The bathymetry data collected for modelling hurricane-induced winds and flooding in St. Martin was comprised of two global data sources. The first was from the General Bathymetric Chart of the Oceans (GEBCO), with a 900 m resolution. The second was from Service hydrographique et océanographique de la marine (SHOM), which provided data for a more localised bathymetry of 100 m resolution. Both are shown in Figure 3.4 with the GEBCO bathymetry on the left and the SHOM bathymetry on the right.

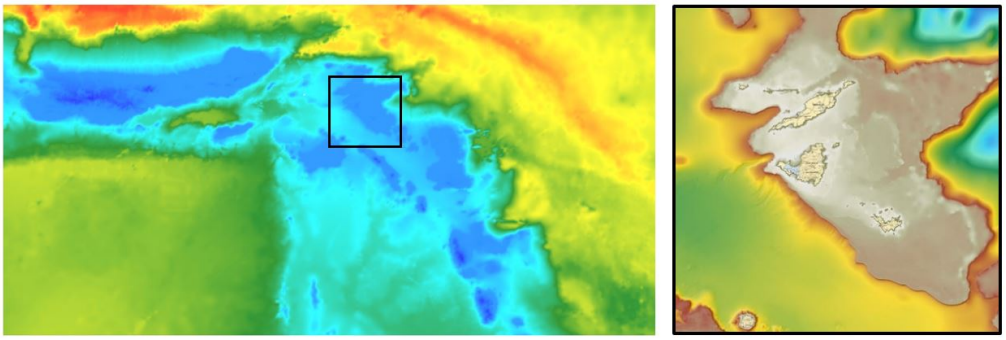

Figure 3.4: Global bathymetry sources available for the Caribbean around St. Martin, Left: GEBCO (British Oceanographic Data Centre, 2018) and Right: SHOM (SHOM, 2018).

The bathymetry around the island was further improved, starting at the 10 m contour depth line. This bathymetry was manually digitised from an online navigation chart, Navionics (2019). Images of the sonar bathymetry details were used to identify point locations with the correct co-ordinates and water depths. Figure 3.5 shows an example of the digitisation. The example is of one bay of St. Martin, Orient Bay. This digitisation was done for the entire coastline of St. Martin. In the figure, the Navionics navigation chart is on the left, and the geo-referenced image is on the right, with points defined along given contour lines. Points along the contour lines; 0.5 m, 1.5 m, 2.5 m, 5 m, 7.5 m 10 m and 20 m were digitised, resulting in 6000 data points with corresponding water depths at the correct co-ordinates. In order to transform these points into a bathymetry, triangular interpolation was used along the computational grid for the inland flooding model. The final bathymetry was therefore comprised of GEBO data (900 m resolution) (British Oceanographic Data Centre, 2018), SHOM (100 m resolution) data (SHOM, 2018) and the digitised Navionics data (0.5 m resolution).

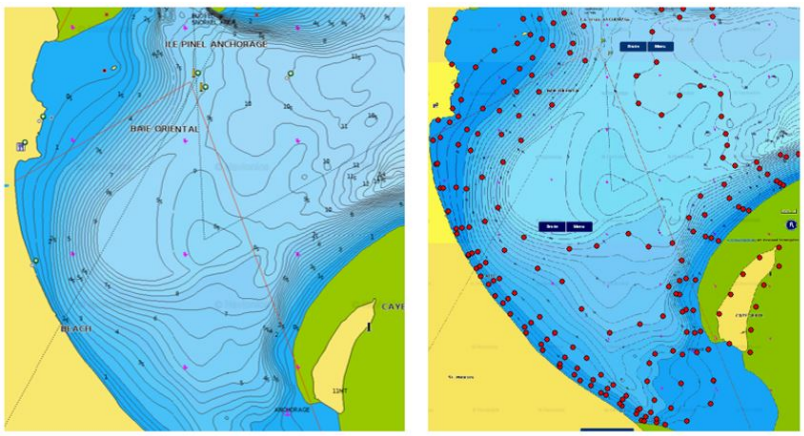

Figure 3.5: Left: Sonar details of depth contours for Orient Bay, St. Martin (Navionics, 2019). Right: Geo-referenced image with point data along different depth contours to extract depth data along the shore.

TOPOGRAPHY

In order to simulate overland flooding, local topography data is needed. For St. Martin the only Digital Elevation Model (DEM) data available was Shuttle Radar Topography Mission (SRTM) DEM (NASA, 2014) and Multi-Error-Removed Improved-Terrain (MERIT) DEM (University of Tokyo, 2018). Other topographic sources were investigated such as LIDAR (Light Detection And Ranging of Laser Imaging Detection And Ranging), TanDEM-X and ALOS (Advanced Land Observing Satellite) DEM's, however there was either no data available for St. Martin, or the data that was available, was not of an improved resolution. The two considered data sets that are described therefore, are SRTM DEM and MERIT DEM.

SRTM DEM is high-resolution topographic data acquired using radars to measure heights from space. The elevation models are arranged into tiles, each covering one degree of latitude and one degree of longitude. A derived three arcsecond (90 m along the equator) data set is available. Each three arcsecond tile has 1,201 rows, each consisting of 1,201 cells. The original SRTM elevations were calculated relative to the WGS84 ellipsoid and then, the EGM96 geoid separation values were added, to convert the heights relative to the geoid. For some locations a one arcsecond (30 m along the equator) data set is also available. The 30 m resolution SRTM data available for St. Martin is shown in the top map of Figure 3.6. This data is of a finer resolution than the 90 m resolution data, however not more accurate.

MERIT DEM is a high accuracy global DEM at 3 arcsecond resolution (90 m at the equator) based on SRTM data, that has been improved by eliminating major error components from existing DEM data sets. MERIT DEM separates absolute bias, stripe noise, speckle noise and tree height bias using multiple satellite data sets and filtering techniques. The bottom map in Figure 3.6 shows an aerial view of the MERIT DEM data set available for St. Martin.

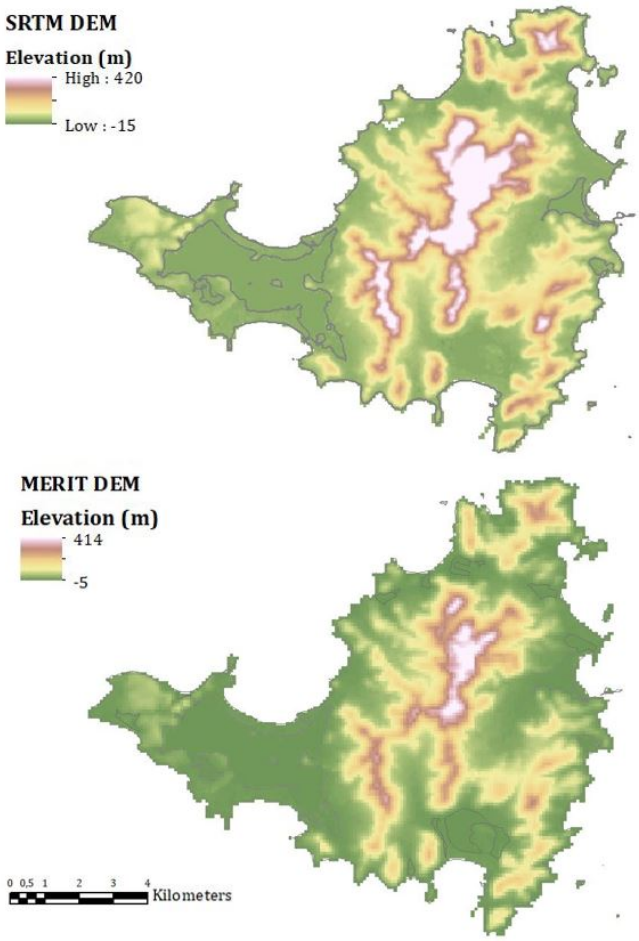

Figure 3.6: Top: An aerial view of St. Martin showing the 30 m resolution SRTM DEM data that is publicly available (NASA, 2014). Bottom: An aerial view of St. Martin showing the 90 m resolution MERIT DEM data that is publicly available (University of Tokyo, 2018).

Various studies have been done to investigate which data set is most accurate when simulating flooding, such as the study by Hawker et al. (2018) and the study by Vousdoukas et al. (2018). In the study by Hawker et al. (2018), the MERIT data is favoured when performing flood risk assessments. In the study, a comparison was made for SRTM DEM and MERIT DEM, both of a 90 m resolution, to LIDAR DEM. The accuracy of the SRTM and MERIT data was compared to LIDAR DEM data for various different locations, where the LIDAR data was taken to be the true elevation height. In the study by Vousdoukas et al. (2018) the underlying uncertainty in DEM data is investigated, specifically looking at SRTM DEM compared to LIDAR DEM. SRTM bias was found to be around 1.2 m vertically and to have a RMSE of around 2 m in the case study. The study concluded that DEM data substantially affects flooding and damage estimates.

In order to determine which data set is the best for this flooding model a comparison should therefore be performed to look at the difference between true elevation and the SRTM or MERIT estimation. For St. Martin there is no LIDAR DEM, or other variant, that would be useful to compare to. As a 30 m resolution SRTM data set is available, the argument could be made to use the better resolution data however, no comparison can be done for the three data sets as there are no reference points to validate with. Therefore, the MERIT 90 m resolution data was chosen to model overland flooding. Figure 3.7 shows a cross-section of the island to highlight the difference between the three data sets.

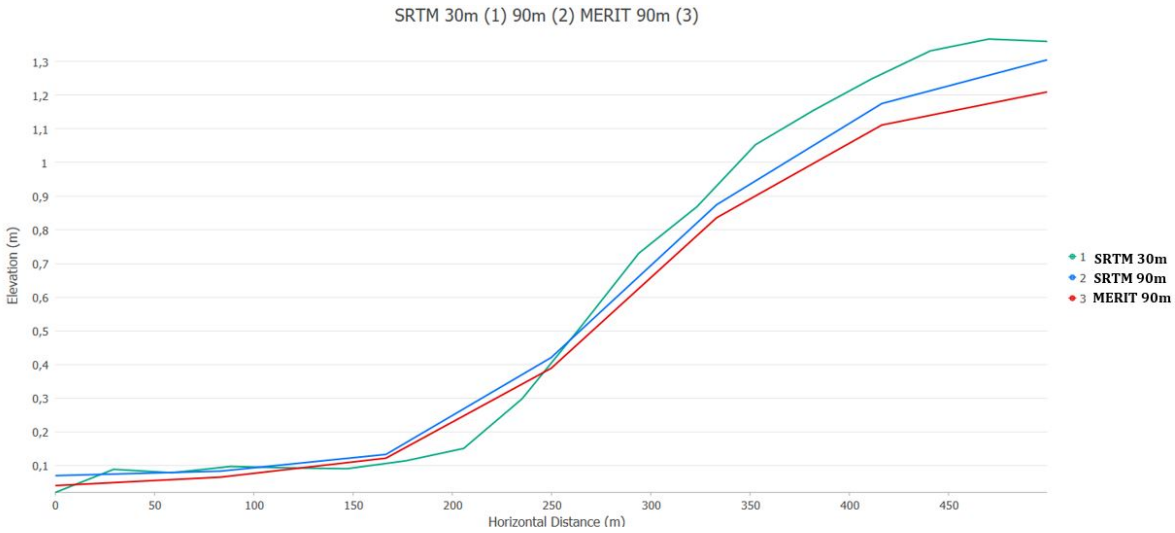

Figure 3.7: A cross section of a beach section on St. Martin showing the three global topography data sets that are publicly available (SRTM 90 m resolution, SRTM 30 m resolution and MERIT 90 m resolution) and their corresponding elevations for a random cross section location.

SRTM is a Digital Surface Model which means it take tree cover into account when estimating the elevation level and therefore, often overestimates elevation. In the figure there is a clear difference between the SRTM data and the MERIT data sets of 90 m resolution, as well as a difference to the finer SRTM 30 m resolution data. As there is no true elevation nothing can be said about which data set is more representative.

3.1.3. Validation data

Validation data used to validate the hazard modelling is discussed in this section. The two hazards being modelled are wind and flooding and therefore the validation data is explained for these two hazards, as well as their damages. The validation data is related to the validation case of Hurricane Irma and the hazard extents experienced during the hurricane. The flooding validation data collected included online sources of images taken during Hurricane Irma, and the wind damage validation data consists of damage maps published after Hurricane Irma.

FLOOD VALIDATION

Validation of flooding models includes taking observational data of the event in question and making a comparison to the modelled values of the same event. Observational data is usually in the form of measurements taken at the location of interest. For coastal and inland flooding this means gauges that measure either coastal water levels at the shore or flood depths inland. Figure 3.8 shows an example of a water level measurement station for St. Martin that was left damaged due to Hurricane Irma. This is the only tidal station off the coast of St. Martin and therefore, no water levels were recorded during the hurricane that are useful to validate a flood simulation. Observational data for St. Martin is very limited, and in the case of Hurricane Irma, not publicly available in terms of measurements. In these locations, where observational data and measurements are scarce, an alternative method has to be used to find validation data to validate a model simulation.

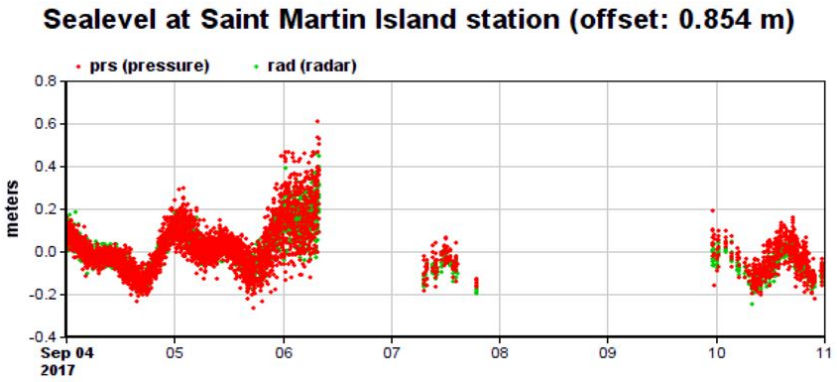

Figure 3.8: Sea level station measurements for St. Martin during Hurricane Irma (Vlaams Instituut voor de Zee, 2019).

One source of validation however, is a map published by the French authorities for the French half of the island (Cerema & DEAL Guadeloupe, 2017) shown in Figure 3.9. This map was used to initially determine flooding on the French half of the island due to Hurricane Irma, in order to assist in the relief management directly after Irma made landfall. The map is only available for the French half of the island, and is based on recorded water levels during the storm. It is unclear whether these records are based on measurements or personal observations after the storm.

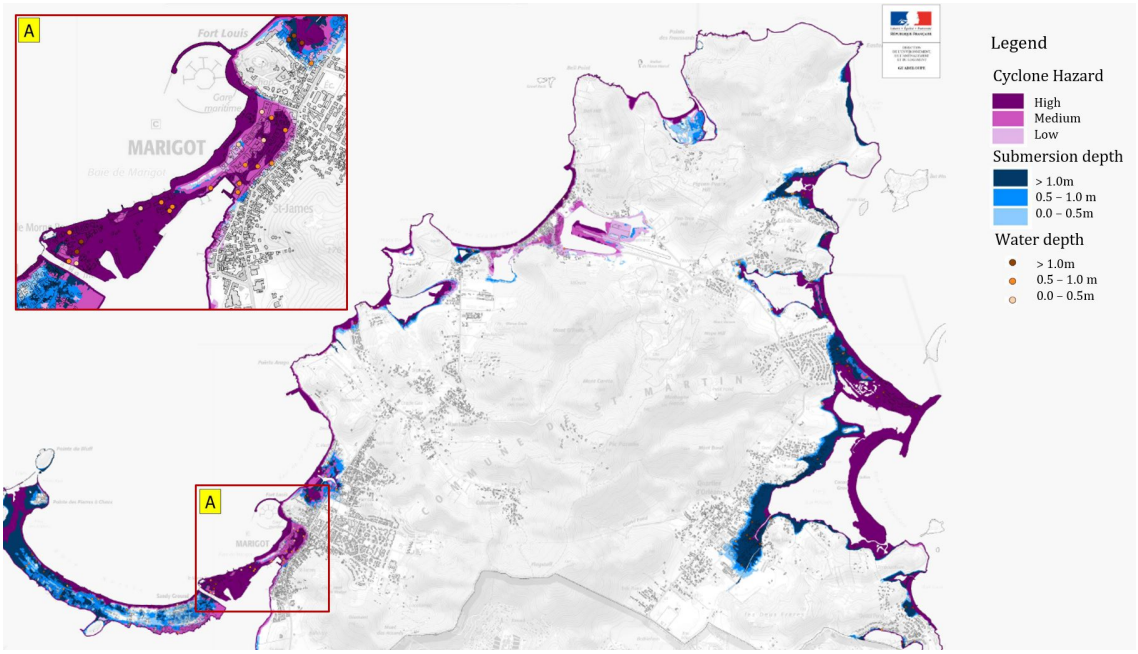

Figure 3.9: Flooding due to Hurricane Irma on the French half of St. Martin indicating an example of the observation locations and water depths in Marigot (Cerema & DEAL Guadeloupe, 2017).

Although this map is important for flood model validation, it leaves the Dutch part of the island without information. To combat this, a new innovation using online data was used. Flood Tags (www.floodtags.com) is a company that monitors online Twitter data (www.twitter.com), for posts by the public regarding flood events. This data is then used to improve real time flood monitoring and early warning alert systems. Flood Tags has been monitoring Twitter data since 2014, and therefore, also has data collected during the Hurricane Irma event related to flooding. All the Twitter data for the month of September was analysed to determine if this data source could be further applied to validate flood models in data scarce environments.

More than 10,000 Twitter posts were found using the initial data filter. This was done by using Open Street Map (OSM) locations defined for St. Martin for the three main languages on the island (English, French and Dutch), and filtering any tweets containing these locations. This data was then further filtered to exclude locations in different countries with the same names as those in St. Martin. This also included location names that may occur in tweets that are unrelated to flooding, such as the area on St. Martin known as "Springs". This location originally flagged tweets referring to Spring, and not specifically flooding or St. Martin. The final data set included approximately 60 Twitter posts that were then observed and analysed manually. Only posts that included an image or exact location name were considered. Using the GPS location of the Twitter post was not possible because the location where the post was made, does not necessarily imply that it was made in the same location (or time) as to when the image was taken.

Figure 3.10 shows an example of one of the Twitter posts that provided information to define validation points for flooding on St. Martin. In the image, a before and after picture is posted of a marina in Marigot, Saint Martin, where flooding can be seen. For this image the water level was estimated to be larger than 1 m. This was done by looking at surrounding structures or objects in the image that could be estimated, such as a lamp post or tree. The water level in the image was then estimated relative to the known object. An example from the image are the beach huts and lamp posts that can be seen in both the before and after image. An estimation was made for the total height visible before and after to arrive at a water depth estimation. Other examples from tweet images, are where the water level could be based off the size of the wheel of a car in the image or the height of the first floor of a hotel lobby that was flooded. In this way each image was analysed and a water depth was estimated.

Figure 3.10: Example of a Twitter post showing a before and after picture of the Marigot marina in Saint Martin (@NNweather, 2017).

Each image and Twitter post was analysed and given a water level classification using the same intervals as the Cerema and DEAL Guadeloupe (2017) flood map. Along with the Twitter data, one of the analysed posts ALSO lead to an online public Photo Map for Hurricane Irma where people could upload an image and indicate on a world map where the image was taken (NAPSG Foundation, 2017). These images were also analysed, and many matched the identified Twitter posts, reaffirming the analysis that had already been done. In total, with the Photo Map and Twitter data, 60 points were identified and classified to use as validation for the flooding model.

In total the flooding validation data therefore consisted of the observational data from the map published by the French Authorities that was digitised, and the points identified by the online Twitter sources. The validation data points were classified for water depths in three intervals, namely 0 m to 0.5 m, 0.5 m to 1.0 m, and larger than 1.0 m.

WIND VALIDATION

The second hazard to be modelled and validates was hurricane-induced winds. When modelling wind speeds over the island often validation points are taken from observations or measurements made during the hurricane event, in the same way that should be done to validate flooding. Figure 3.11 shows examples of wind measurement stations on St. Martin that were left damaged due to Hurricane Irma and therefore unable to provide validation data. In the same way validation of wind speed modelling on the island was limited. For this study the open ocean wind speeds modelled in the hydrodynamic model were used to determine wind impact on the island, and therefore physical modelling of wind speeds on the island and validation thereof fall beyond the scope of this research.

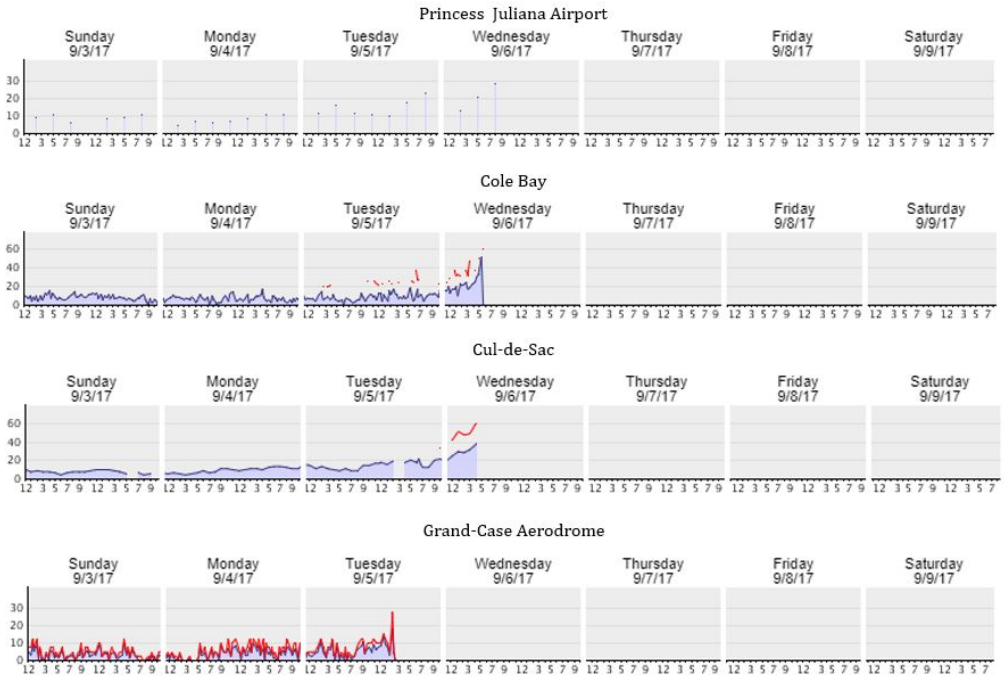

Figure 3.11: Wind station measurements for four locations on St. Martin during Hurricane Irma; 1. Princess Juliana Airport, 2. Cole Bay, 3. Cul-de-Sac, 4. Grand-Case Aerodrome (WindAlert, 2019).

The validation of the wind damages on the other hand could be done because of published maps and articles regarding wind damages after Hurricane Irma. Published articles and reports of Hurricane Irma and damage in St. Martin (Cangialosi et al., 2017; Copernicus, 2017; NU, 2018; NOS, 2018a; World Bank Group, 2018) estimate total damages at between 1.6 to 2.5 billion dollars. Reports further mention that the French half of the island was destroyed for up to 95% and the Dutch half of the island up to 70%, including Juliana airport (Cangialosi et al., 2017; Copernicus, 2017; The Guardian, 2017).

One week after the passing of Hurricane Irma, drones were used to fly around the island and determine roof damages for buildings on the island (Copernicus, 2017) by comparing images of buildings before and after the storm hit. Two damage maps were released for St. Martin. Figure 3.12 shows the damages for the Dutch half of the island as represented by 510 Red Cross (2017). Another map was released by Pacific Disaster Center (2017) which estimated wind impact on the island based on a wind model simulating the actual track data of Hurricane Irma. This map is shown in Figure 3.13. These maps are based on the data collected by Copernicus during the drone investigation, and represent damages to building roofs. The damaged areas between the impact model and these maps were qualitatively compared to validate if the wind impact model indicates the same areas as those indicated in the maps.

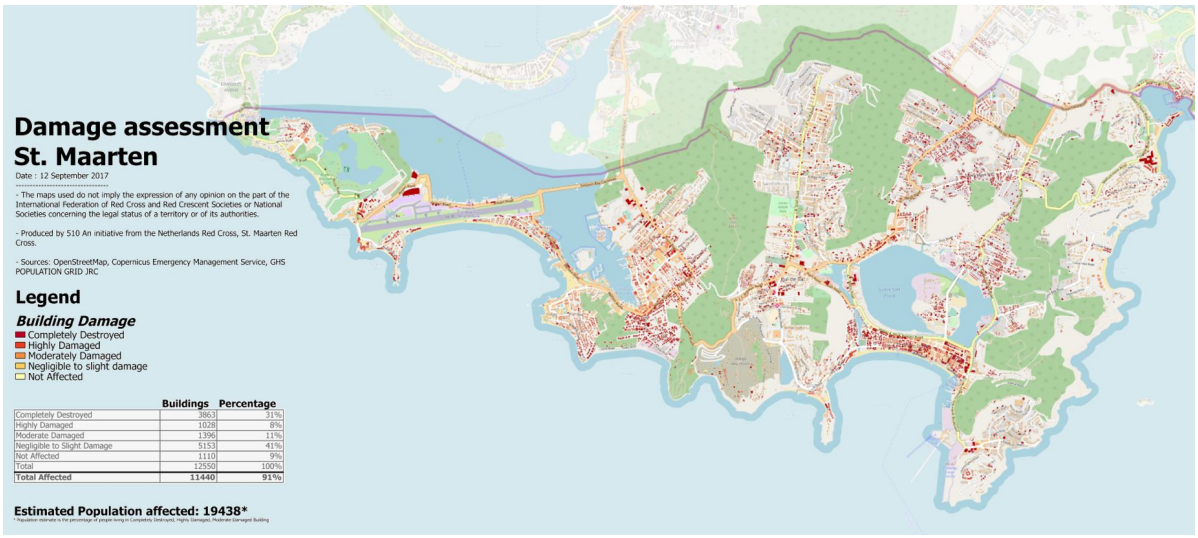

Figure 3.12: Damage per building due to Hurricane Irma on the Dutch half of St. Martin (510 Red Cross, 2017).

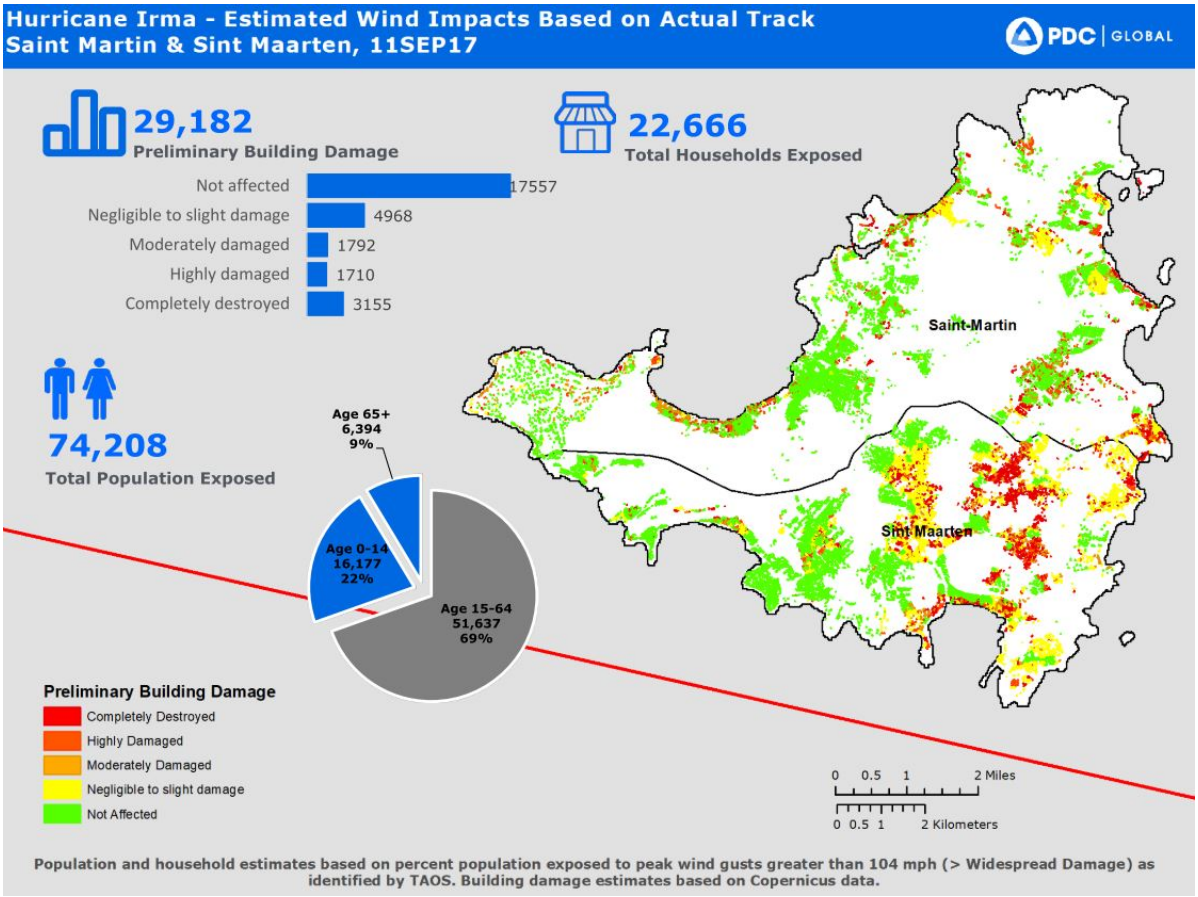

Figure 3.13: Estimated Wind Impact due to Hurricane Irma based on Actual Track data (Pacific Disaster Center, 2017).

3.1.4. Exposure data

The final component of data collection was the input for the impact modelling, namely the exposure data of the island. Two sources of exposure data were available for St. Martin. The first was Open Street Map (OSM) data (OpenStreetMap, 2019) which is a publicly available global data source including streets, administration areas, buildings, land uses, coastlines, water, vegetation and points of interest. The exposure data of OSM defining building type in the classes; residential, commercial and industrial is shown in Figure 3.14 which was used for the flood impact calculation.

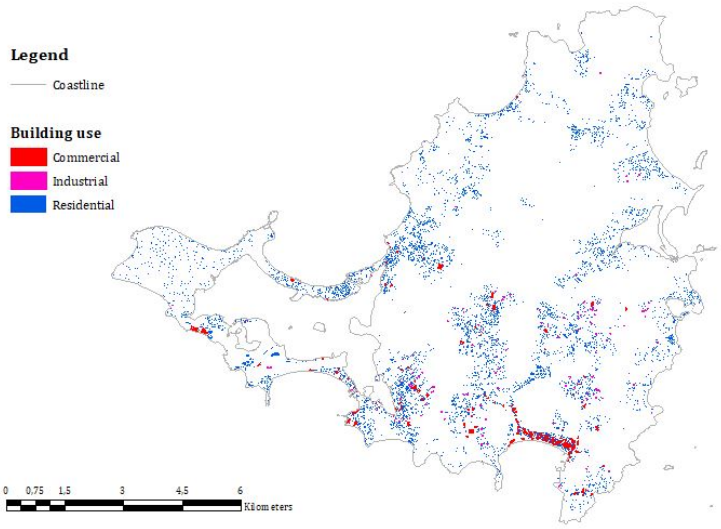

Figure 3.14: Exposure data showing building uses for St. Martin (OpenStreetMap, 2019).

The second source of exposure data for St. Martin regarding building roof materials for buildings on the Dutch half of the island. This data is shown in Figure 3.15, and was used for the wind impact calculation. As this data was only available for the Dutch side of the island, an assumption was made that the ratio of material type was similar on the French side of the island and the final exposure maps are shown in Section 4.3.

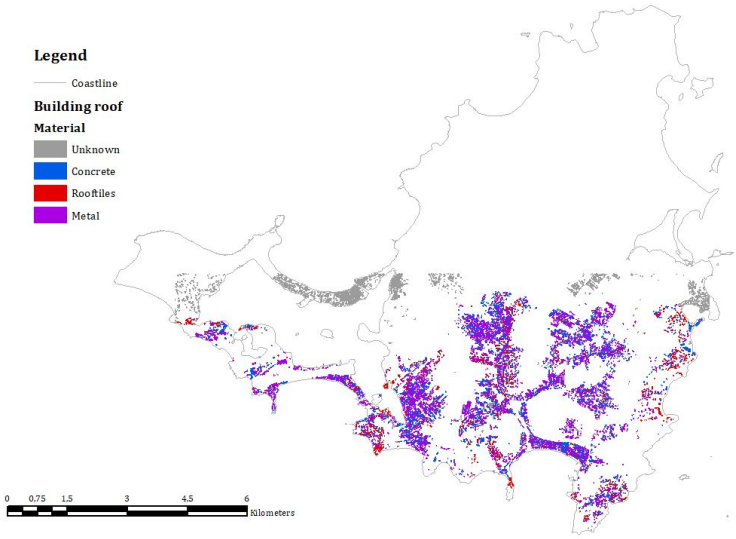

Figure 3.15: Exposure data showing building roof materials for St. Martin (Red Cross, 2017b).

The collection of the hazard modelling data, validation data and impact modelling data meant that the hazard models and impact model could be set up for St. Martin and validated for Hurricane Irma.

3.2. Hazard Model Set-up and Validation

The hazard modelling for hurricane-induced winds and flooding on St. Martin was done using three modelling steps. Firstly, the spatial wind fields around the hurricane centre were determined using a numerical Wind Enhance Scheme (WES) based on the Holland (1980) approach, adapted by (Nederhoff et al., 2019). These spatial wind fields were then used to force the hydrodynamic flow model to simulate storm surge levels around the island of St. Martin. This was done using a 2D depth-averaged flow model on an unstructured computational grid (D-Flow FM) (Kernkamp et al., 2011). These storm surge levels were combined with a parametric estimation for wave setup, and formed the boundary conditions for the final hazard modelling step. The final model step involved estimating flooding on St. Martin using a static "bathtub" approach. Figure 3.16 shows the model train of how the hurricane winds were used to simulate flooding on St. Martin. This section describes each part of the model train and how they were set up for the case of St. Martin.

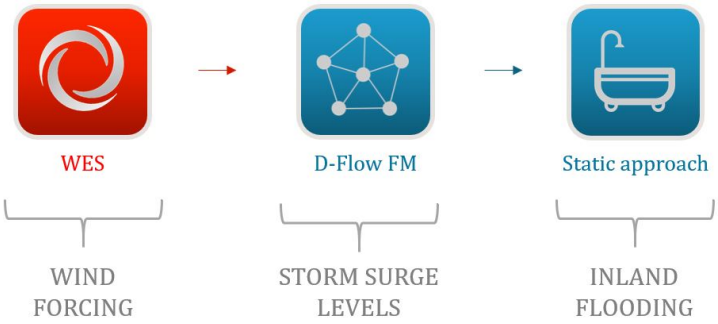

Figure 3.16: Model train used to simulate wind and flooding on St. Martin.

The spatial scales of the hazard models varied. The coastal hydrodynamic model was of the same spatial scale of the Caribbean Sea (approximately 500 000 km^2) and the inland flood model was of the same spatial scale of the island of St. Martin (approximately 100 km^2). The temporal scale of the wind and hydrodynamic model was similar to the duration of a hurricane, around 5 days for the case of Hurricane Irma.

3.2.1. Wind forcing

A Wind Enhance Scheme (WES) based on the Holland (1980) model and the adaption by Nederhoff et al. (2019), has been devised to generate spatial wind fields of tropical cyclones. These wind fields can in turn be used as forcing for storm surge simulations using D-Flow FM (a process based hydrodynamic model further elaborated in 3.2.2). The model computes surface winds and pressures around a specified location of a tropical cyclone centre, given a number of tropical cyclone parameters (i.e. the location of the cyclone centre, the radius of maximum wind (RMW), the maximum wind speed, the central pressure and the current motion of the hurricane). The formulation for the gradient wind speed V_g is given by Equation 3.1.

$$V_g(r) = V_{max}^2 \left(\frac{RMW}{r}\right)^B e^{1-\left(\frac{RMW}{r}\right)^B} + \frac{1}{4}(r f_c)^2)^{0.5} + \frac{1}{2}(r f_c) \tag{3.1}$$

Where V_{max} is the maximum sustained wind, r is the radial distance, B is the pressure profile component (Holland's parameter), and f_c is the Coriolis force component.

According to the Holland (1980) model, there are two parameters that define the wind-field, and are determined empirically. The first is the parameter that determines the relationship between the pressure/wind profile relative to the origin, in WES this is defined as A. The second parameter, known as the Holland B parameter, determines the shape of the pressure/wind profile, in WES defined by B. A is equal to RMW (or R_{max}) to the power of B. These empirical parameters are based on observed hurricane data and depending on what data is available, WES computes what these parameters are. One of the following data combinations is needed in order to use the methods developed in WES:

1. V_{max}, parameter A and parameter B
2. V_{max}, R_{35}, R_{50} and R_{100}
3. V_{max} and P_{drop} and/or RMW

Where P_{drop} is the central pressure drop, R_{35} is the radius of 35kt wind speeds, R_{50} is the radius of 50kt wind speeds and R_{100} is the radius of 100kt wind speeds.

The model introduces asymmetry by applying the translation speed of the hurricane's eye displacement to steer current and by introducing wind speed rotation due to current. The output of the model is suitable as input to simulate storm surge in a hydrodynamic model. The force exerted by the wind is coupled to the flow equations as a shear stress. The magnitude of this stress is determined by the widely used quadratic expression shown in Equation 3.2.

$$\tau_s = \rho_a C_d U_{10}^2 \tag{3.2}$$

Where ρ_a is the density of air, C_d is the wind drag coefficient and U_{10}^2 is the wind speed at 10 m above the free surface. The options for wind drag coefficient are those explained in section 2.1, and for this model the Smith and Banke (1975) piecewise formulation was used for the drag coefficient.

The wind forcing was introduced into the hydrodynamic model by means of a spiderweb grid which contained the spatial wind field of the hurricane per 6-hour time step intervals created using WES. Figure 3.17 shows the 6-hour time step intervals for Hurricane Irma and the corresponding hurricane category for each part of the hurricane track. The initiation point of Hurricane Irma started near the equator off the African coast and travelled towards the Caribbean, with termination near the east coast of the United States. The hurricane track travelled along the border of the Caribbean Sea right to where St. Martin is located. The information for the track data was based on the Atlantic hurricane database (National Oceanic and Atmospheric Administration, 2018).

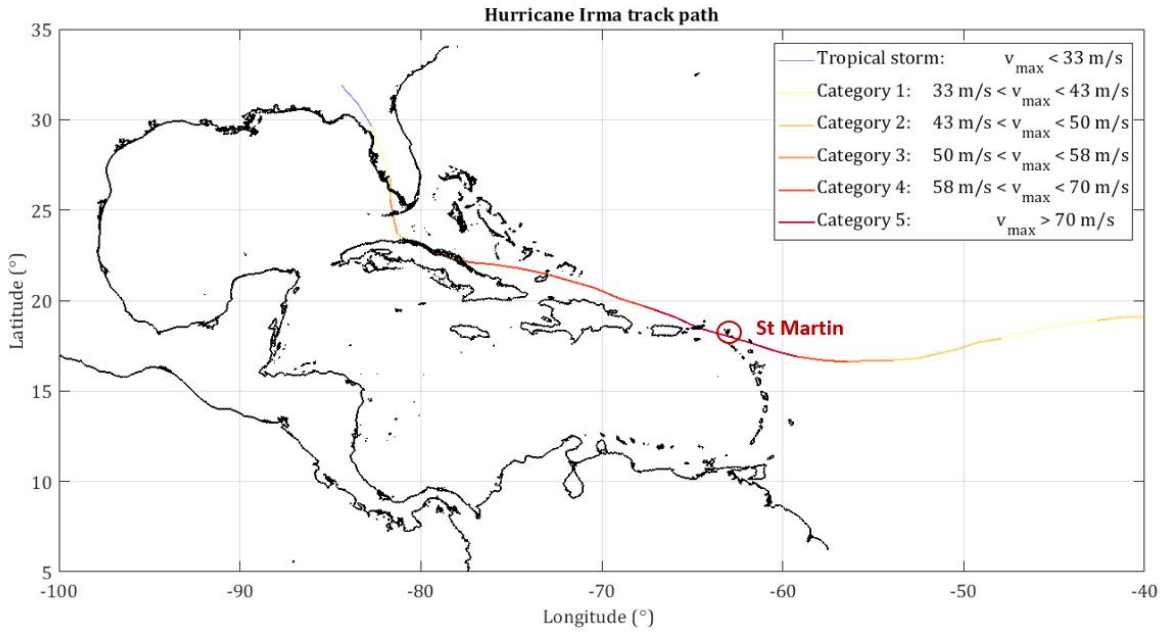

Figure 3.17: Hurricane Irma's track showing the hurricane categories for each time interval, which used as forcing to simulate the coastal levels in St. Martin (indicated on the map) due to Irma.

The output of the flow model included the maximum 1-min average wind speeds for each grid cell during the simulation and these were the wind speeds used in the wind mapping and impact assessment. These winds speeds are calculated for the open ocean and therefore do not take topography into account and do not represent any physical processes regarding wind dynamics.

3.2.2. Coastal storm surge levels

In order to determine the storm surge levels around the island, a coastal model for a portion of the Caribbean Sea was set up. The model is a 2D depth-averaged (2DH) flow model that simulates storm surge levels during a hurricane event (Bloemendaal et al., 2018). D-Flow FM is the model that was used and is a process-based hydrodynamic model that can calculate non-steady flow and transport resulting from tidal and meteorological forcing on an unstructured grid (Kernkamp et al., 2011). The model solves the unsteady shallow water equations (SWE), made up of the horizontal equations of motion, the continuity equation and the transport equations. A 2D depth-averaged approach is appropriate for homogeneous fluids and was applied here in order to simulate storm surge during a hurricane event. D-Flow FM solves the depth-averaged continuity equation, by integrating the continuity equation, for incompressible fluids, over the total depth while taking into account the kinematic boundary conditions at water surface and bed level.

The coastal hydrodynamic flow model consisted of open boundaries that were defined by the tidal conditions in the Caribbean determined from the GTSR data set (Muis et al., 2016) derived using the Global Tide and Surge model (GTSM). Figure 3.18 shows an example of the representative tidal signal used at the Eastern boundary of the coastal flow model. The representative tidal components for the four boundaries of the computational grid are found in Table 3.1.

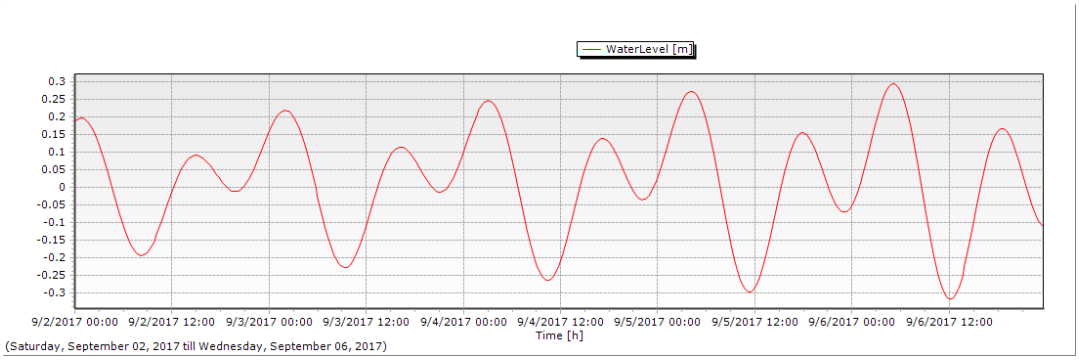

Figure 3.18: Time-series of the tidal signal for the Eastern boundary of the coastal model used to simulate storm surge in St. Martin.

Table 3.1: Tidal components of the four boundaries defined for the coastal flow model based on the Global Tide and Surge for the Caribbean.

	Northern boundary		Southern boundary		Western boundary		Eastern boundary	
Component [-]	Amp. [m]	Phase [deg]	Amp. [m]	Phase [deg]	Amp. [m]	Phase [deg]	Amp. [m]	Phase [deg]
M2	0.07	300.83	0.016	146.95	0.173	11.36	0.153	225.42
S2	0.024	291.12	0.007	11.16	0.027	29.14	0.058	244.45
N2	0.017	275.65	0.007	161.36	0.038	349.42	0.036	209.55
K2	0.007	294.01	0.003	13.63	0.008	27.05	0.015	249.52
K1	0.063	223.4	0.086	237.58	0.085	213.18	0.075	233.27
O1	0.057	218.95	0.058	230.21	0.067	212.31	0.065	224.47
P1	0.021	223.13	0.027	239.83	0.028	214.6	0.025	232.76
Q1	0.012	198.33	0.009	213.28	0.013	194.93	0.013	203.64
MF	0.012	354.01	0.015	355.62	0.013	351.94	0.015	355.67
MM	0.006	351.65	0.007	352.01	0.006	348.71	0.007	352
M4	0.001	338.2	0.002	317.7	0.001	329.72	0.0005	326.14
MS4	0.0004	83.27	0.005	172.85	0.002	138.2	0.0006	113.52
MN4	0.0003	303.9	0.002	28.54	0.0007	352.6	0.0005	358.8

The hydrodynamic model was forced by the spatial wind fields defined by WES. The wind drag coefficient was defined according to the Smith and Banke (1975) piecewise linearly varying formulation (explained in section 2.1) with break points at wind speeds of 0 m/s, 25 m/s and 50 m/s for drag coefficient values of 0.001, 0.003 and 0.0015 respectively. The simulation period for Hurricane Irma was 5 days, starting from when the

hurricane track was within a 500 km range of St. Martin until it left this range again. The time period of the simulation was from 02/09/2017 to 07/09/2017, where landfall of Hurricane Irma in St. Martin occurred at 6 am on 06/09/2017.

The bathymetry used in the model was comprised of GEBCO global data with a 900 m resolution, as well as SHOM data of a more localised bathymetry with a 100 m resolution, and finally, the Navionics digitised bathymetry explained in Section 3.1. Furthermore, observation points were defined along the coastline of St. Martin at 50 m intervals which recorded the surge levels during the simulation.

3.2.3. Wave parameterisation

The choice to only simulate flow for the coastal hydrodynamic model was steered by the total computational time for the simulations, and the number of runs required to perform a total probabilistic analysis of hurricane activity for St. Martin. An acceptable run time was only achievable by excluding the solving of wave conditions in the hydrodynamic model. This mean that waves had to be accounted for in another way. This was done by using a parametric model to estimate wave setup at the coast and add this to the surge levels simulated in the hydrodynamic flow model. To determine the coastal wave setup, the offshore wave height and significant wave height near-shore is needed.

A parametric wave model, developed by I. Young (1988), was chosen to estimate wave heights off shore. I. Young (1988) relates the maximum sustained wind speeds and hurricane characteristics, to the maximum wave conditions offshore. The maximum offshore wave height was estimated using this parametric model by I. Young (1988), with the maximum sustained wind speed, radius of maximum (RMW) winds and translation speed of Hurricane Irma as input. The design wave height found using Equation 3.3 with the equivalent fetch length and effective radius given by Equation 3.4 and Equation 3.5 respectively.

$$H_{so,max} = 0.0016 V_{max} \left(\frac{L}{g}\right)^{0.5} \tag{3.3}$$

$$L = R^{'}(-2.17510^{-3} V_{max}^2 + 1.50610^{-2} V_{max} V_{tr} - 0.122 V_{tr}^2 + 0.219 V_{max} + 0.674 V_{tr} + 0.789) \tag{3.4}$$

$$R^{'} = 22500 \log(R_{max} - 70800) \tag{3.5}$$

Where $H_{so,max}$ is the offshore maximum wave height, V_{max} is the maximum sustained wind speed, L is the equivalent fetch, g is the gravitational acceleration, $R^{'}$ is the effective hurricane radius, V_{tr} is the hurricane translation speed and R_{max} is the radius of maximum winds.

As the wave transformation and development of waves near-shore was not modelled, the significant wave height at the breaker zone had to be estimated. This was done using the concept of depth limited waves and the relationship developed by van Rijn (1990) to determine the breaker depth. Equation 3.6 shows how the breaker depth is estimated based on the significant wave height.

$$d_{br} = \frac{H_s^2 \cdot c_o \cdot \cos\left(\frac{3.14 \cdot \theta}{180}\right)}{(1.8 \cdot 3.13 \cdot \gamma^2)^{0.4}} \tag{3.6}$$

Where d_{br} is the breaker depth, H_s is the significant wave height, c_o is the wave group velocity, θ is the incoming wave angle, and γ is the breaker coefficient assumed here as 0.5.

The significant wave height was found by first estimating the depth at which waves are expected to break, based on offshore significant wave height, and then finding the wave height associated to that depth. To estimate this significant wave height at the breaker zone, the incoming wave angle, wave speed and breaker coefficient were needed. The incoming waves were assumed to be travelling perpendicular to the shore and the breaker coefficient was assumed at 0.5. In reality the wave transformation and wave direction will influence the size of the waves reaching the breaker zone. The wave speed was based on the peak period found using parametric model of I. Young (1988).

Once the significant wave height at the breaker zone is known, an estimation of wave setup at the shore can be made. Equation 3.7 shows the estimation of wave height at the breaker zone and Equation 3.8 shows the estimation of wave setup at the coastline (van Rijn et al., 2017).

$$h_{br} = d_{br} \cdot \gamma \tag{3.7}$$

$$\eta_{setup} = h_{br} \cdot \gamma \cdot 20\% \tag{3.8}$$

Where h_{br} is the breaker wave height, and η_{setup} is the wave setup at the waterline.

Previous coastal flooding assessments find that wave setup can be estimated as a percentage of storm surge levels or significant wave height (Wu et al., 2018; Vatvani et al., 2012) and agree with the assumption here of 20%. The total water levels at the coastline were therefore comprised of the storm surge and wave setup and formed the boundary conditions for the inland flood model.

3.2.4. Inland flooding

When simulating flooding for an island like St. Martin, ideally all major flooding processes are included, namely waves, storm surge and rainfall. In this case only waves and storm surge are accounted for when simulating flooding on St. Martin. The choice for a static approach to calculate flooding for the probabilistic ensemble was based on the computational effort required to resolve the coastal processes contributing to flooding such as wave setup and storm surge.

The second justification of using a simplified flood model is the quality of the available topographic data for St. Martin. This was of a low resolution and therefore, the effort used to resolve the coastal processes were lost, as the model is of a much higher detail level compared to the elevation data. In a study by Poulter and Halpin (2008), the influence of DEM data resolution was investigated when estimating flooding. In this study a static approach was used to estimate flooding and compared various DEM data sources. They concluded that the horizontal resolution of the DEM data was largely influential on the accuracy of the estimated flooding. Another study by Vousdoukas et al. (2018) looks at the underlying uncertainty in DEM data and found overestimation of unfiltered DEM data of the order of 1 to 2 m. This influences the flooding and damage outcomes substantially.

Previous studies, such as by Schneider et al. (2016), Didier et al. (2018) or Vousdoukas et al. (2016), have compared the bathtub approach to more advanced models and found that the bathtub approach overestimates flooding, especially is largely flat areas. It is therefore important that in this study the bathtub approach is used in defining flood prone areas and validated for the flood depth estimation. The accuracy of the flood model and validation data are both only in the order of half a meter. This static approach is a conservative estimation of flooding on St. Martin, and the uncertainties in DEM are deemed to be larger than uncertainties in the flooding method used. The static approach was therefore deemed feasible in terms of the number of runs that need to be made, as well as, the order of accuracy in the results compared to the input data. In this way the bathtub approach aims to give an overview of the areas under risk to identify where funds and resources are focused for disaster resilience for hurricane events like Hurricane Irma.

The main assumption of the static "bathtub" approach is that all areas with an elevation lower than the forcing water levels are flooded. In this way the flow of water is not included as water levels are assumed to be still and therefore assumed to inundate an area based only one one water level. Where the water moves and accumulates is unknown meaning the slope of the topography is not accounted for. The attenuation of waves land inward in this case are not represented in the static approach as the wave setup is assumed to be a static water level along with the maximum surge level. The process of infiltration is also not included in this static model as water levels are not assumed to be varying in time due to processes like the infiltration rate of the ground.

The bathtub approach was applied to the island by dividing the coastline into sections based on the physical features of the island, namely the headlands. The surge level between two headlands was assumed to be constant and the inundation was determined based on the estimated maximum water level during the hurricane event and the local elevation. Inundation was estimated using the difference between the two.

3.2.5. Hazard Model Validation

Model validation involves comparing predicted or simulated results with observations or measurements of the variables being simulated. For the island of St. Martin, historical data is limited for the period of the storm, due to damage during Hurricane Irma, or unavailable to the public, and therefore, traditional methods for model validation are not possible for the flood results used during this research.

The offshore wave conditions, surge levels and wind speeds determined using the hydrodynamic model were validated using a more complex coupled wave and flow model of the conditions due to Hurricane Irma, as well as published results of the observed offshore conditions by CDCC (2018) and Cangialosi et al. (2017). A study by Duvat et al. (2019) also includes advanced modelling of Hurricane Irma on St. Martin and was used in validating the hydrodynamic model for wave heights and wind speeds. Furthermore, validation of the flood model included comparison of flood depths determined using the static "bathtub" approach with the validation data collected for Hurricane Irma. The validation points were used to identify potential flood areas which were compared to the flood results for the static approach.

3.3. Impact Modelling

Once the hazard extents were determined, their corresponding damages or impact could be determined. Impact for each hazard was determined based on the unit-loss method. This means that the impact assessment was based on a property by property assessment (Romali & Sulaiman, 2015). Damage costs were determined for each individual damage type and are expressed in Euro per object and are defined in Equation 3.9.

$$TotalDamage = \sum_{i=1}^{m} s_i \sum_{i=1}^{m} f_{ij}(d_j) n_{ij} \tag{3.9}$$

Where $f(d)$ is the damage function given a damage fraction d, n is the number of objects, s is the potential damage, i is the category and j the location count.

The damages that are calculated belong to the category of direct tangible assets which include capital such as houses, cars, buildings and production losses or income losses. Table 3.2 shows the different categories associated with damages when it comes to impact assessment. In this calculation only tangible assets are considered.

Table 3.2: Classification of damages (Slager et al., 2016).

Category	Tangible	Intangible
Direct	Capital loss (houses, crops, cars, buildings), production loss, income loss	Casualties, injuries, ecosystems, monuments, social disruption, emotional damage
Indirect	Loss of utility outside of affected area, unemployment, migration, cutting of infrastructure lines	Loss of potential for attracting investors, reputation damage

A Flood Impact Assessment Tool (FIAT) by Slager et al. (2016) was used to calculate the impact of each hazard (wind and coastal flooding). It is a tool that combines data needed for impact assessment and runs the model to determine the damage caused. The tool uses exposure data and vulnerability functions as input and based on the provided hazard map, calculates the damage accordingly. Figure 3.19 shows the concept of the tool, which uses the exposure data (object map) as input along with the vulnerability (damage functions and maximum damages) and hazard maps (here wind speed and flood levels). The tool bases its calculation in the grid of the input elements. The exposure data and hazard maps are of the same computational grid and for each grid cell the damages are calculated by associating the given hazard level and exposure type with a maximum damage value. The maximum damages for St. Martin were based on a study by Vojinovic et al. (2008) for flood damages, and based on a study by BCQS (2016) for construction costs in St. Martin.

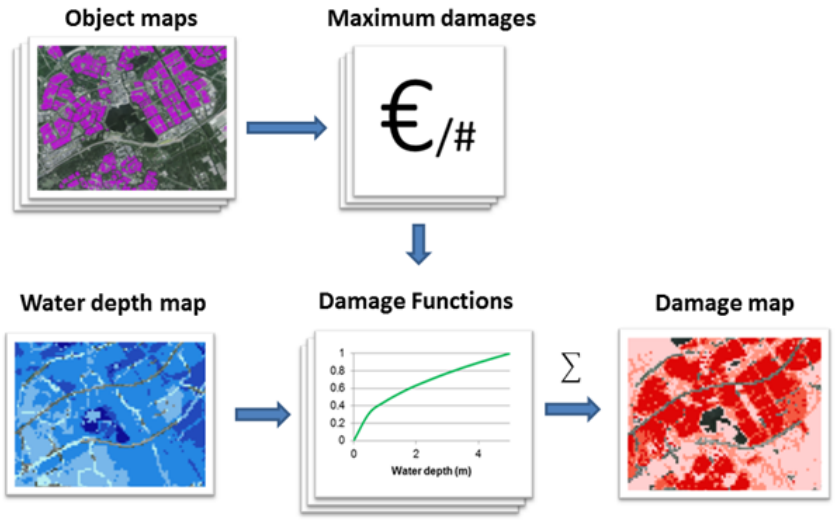

Figure 3.19: Conceptual flow chart of the FIAT setup (Slager et al., 2016).

3.3.1. Vulnerability functions

The final undefined aspects of the FIAT model are the vulnerability (damage) functions. There are two main approaches when it comes to defining a vulnerability function for a given asset. The first is referred to as the expert approach or the synthetic approach. This is where experts come together and define the damages for the given hazard based on previous experience or knowledge. The second approach is data-driven, and is known as the empirical approach, which looks at data from previous hazard events or data collected by insurance companies after an event and the vulnerability function is derived to fit the data. For St. Martin the second approach is possible for the damage data recorded for the Dutch part of the island however, physical wind speed modelling would be needed to simulate hurricane wind speeds during a hurricane, and therefore reaches beyond the scope of this research. Hurricanes on the island of St. Martin are not recorded well and therefore previous knowledge of the circumstances due to a past event is scarce, making the first approach difficult. In order to represent damages as a vulnerability function, assumptions were therefore made based on previous studies that consider similar hazards.

VULNERABILITY FUNCTIONS FOR WIND SPEED

The exposure data defining building roof material was used as the basis to determine which vulnerability function to use, regarding maximum sustained wind speed due to a hurricane event. Wind speed vulnerability functions are often constructed by relating a given wind speed to a percentage of damage for a given structure. The structure can be classified according to various scales of detail such as the building materials, construction, height, number of stories, upstream exposure, distance to the coast and so on. A study by Khanduri and Morrow (2003) related wind speeds to the structural damage based on the frame of the structure namely; wooden frame, masonry low-rise and reinforced concrete low-rise as well as a generic vulnerability function when frame material is unspecified. Khanduri and Morrow (2003) developed generic vulnerability functions of residential and commercial buildings in Puerto Rico based on insurance loss data for Hurricane Hugo in 1989 and Hurricane Georges in 1998. Figure 3.20 shows the data points used in the study by Khanduri and Morrow (2003).

The available exposure data regarding building structures on St. Martin define the buildings according to their roof material namely; concrete, roof tiles and metal. The assumptions therefore made when using the functions developed by Khanduri and Morrow (2003), are: firstly, that the roof material is the same as the building frame material, and secondly, that the structural integrity of the buildings are similar to those in Puerto Rico, another Caribbean island that also experiences hurricane activity. Furthermore, the exposure data is only available for the Dutch part of the island and therefore an assumption was made that the same building materials and construction methods are used for the French part of the island. The vulnerability function for reinforced concrete low-rise is therefore used with the concrete roof exposure date and the generic vulnerability function is used with the roof tile and metal roof exposure data.

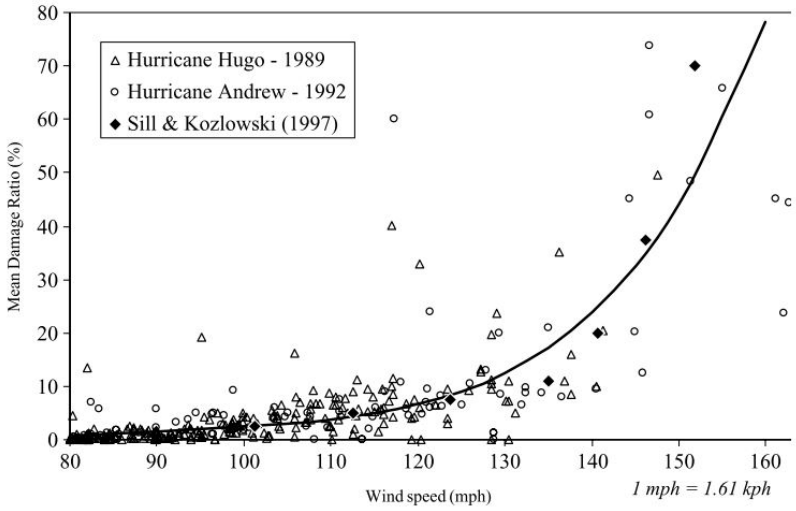

Figure 3.20: Data points for losses during Hurricane Hugo and Hurricane Andrew for given wind speeds (Khanduri & Morrow, 2003). The damage ratio suggested by Sill and Kozlowsk (1997) is also shown.

VULNERABILITY FUNCTIONS FOR FLOOD DEPTH

The exposure data defining occupancy/building use was used as the basis to determine which vulnerability functions to use, regarding maximum experienced inundation level due to a hurricane event. Global depth-damage functions like those produced by Huizinga et al. (2017) for the Joint Research Centre (JRC) are often used when defining the damages for a given inundation level. A study by Vojinovic et al. (2008) for St. Martin was done using the same approach and vulnerability functions were defined for residential, commercial and industrial buildings. The vulnerability functions were derived by simulating flood levels due to extreme rainfall events and determining the damage costs for the simulated water levels.

The study was done for the Dutch side of the island and the classification of occupancy was defined according Table 3.3, which is defined by the same classification as the exposure data available for St. Martin. In order to apply these functions to the whole island of St. Martin, the assumption is made that the buildings on the French side of the island experience similar damages when exposed to the water levels in the study. For each occupancy classification a depth-damage vulnerability curve was developed and used in this research.

Table 3.3: Classification of building occupancy classes according to the study by Vojinovic et al. (2008).

Building Type	Classification
Residential (small)	Area $< 50m^2$
Residential (large)	Area $> 50m^2$
Commercial (low)	Area $< 100m^2$
Commercial (medium)	$100m^2 <$ Area $< 1000m^2$
Commercial (high)	Area $> 1000m^2$
Industrial (low)	Area $< 100m^2$
Industrial (medium)	Area $> 100m^2$

The calculation of wind and flood impact was done for the case study of Hurricane Irma on St. Martin. The wind damages were validated by comparing published damage results explained in Section 3.1. This marked the end of Phase 1 of the research. The hazard models and impact model was set up and validated using Hurricane Irma and was ready to be applied to a broader range of hurricane track scenarios for the risk assessment of St. Martin in Phase 2 of the research.

3.4. Synthetic track generation

Phase 2 of the research involved determining the hurricane risk of St. Martin and involved three steps. The first step, explained in this section, was the synthetic hurricane track generation. The second and third steps are explained in Section 3.5, and describe the probabilistic analysis of the hurricane-induced hazards and the risk assessment of St. Martin.

The first step in determining hurricane risk, is to define an ensemble of hurricane track scenarios that need to be modelled using the hazard and impact models setup in Phase 1. The historical hurricanes in the region of St. Martin are not enough to perform this type of risk analysis, and therefore synthetic hurricane track scenarios can be generated, based on the characteristics of the historical data for a larger domain. In this case the entire Northern Atlantic basin was chosen to develop the synthetic hurricane tracks. Tropical Cyclone Wind Statistical Estimation Tool, TCWiSE, is a tool that generates synthetic hurricane data for a specified ocean basin based on historical data for that basin. The tool was developed and validated in a study by Hoek (2017) together with Deltares and was applied in this research. Figure 3.21 shows the synthetic track generation processed used in TCWiSE.

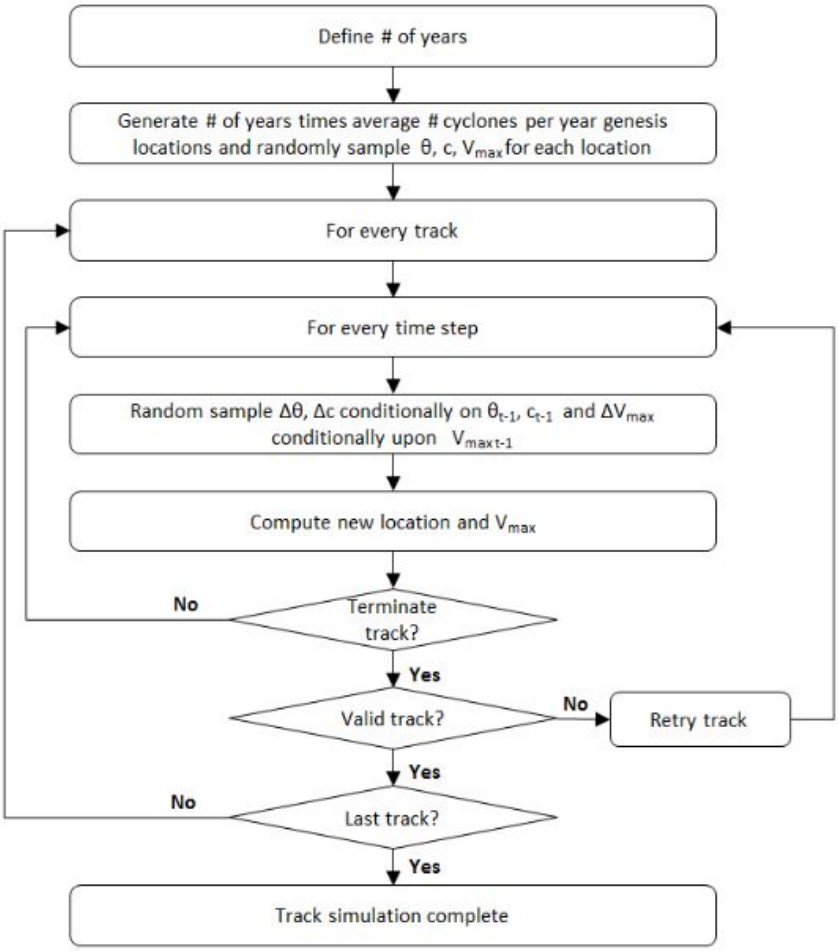

Figure 3.21: Synthetic track generation process of TCWiSE (Hoek, 2017).

Each track was created by modelling the changes in track and intensity, by randomly sampling these changes by means of a Monte Carlo Simulation. This was done in order to determine the hurricane position and intensity for the entire track, using 6-hour interval time steps. The sampling for each variable was taken from probability density functions that were derived based on the historical track data. Relationships for track initiation location, change in track propagation and change in track intensity were used. Termination of a track was defined for a track exceeding a certain duration and intensity.

The data input for TCWiSE was based on the International Best Track Archive for Climate Stewardship (IBTrACS) data set, containing historical hurricane data for past events, based on various sources around the world. For the Northern Atlantic basin this is the HURDAT2-reanalysis data (National Oceanic and Atmospheric Administration, 2018), which belongs to the National Hurricane Center of the National Oceanic and Atmospheric Administration (NOAA). The wind speeds contained in this data set, are the 1-minute averaged wind speeds experienced during the storm. Missing data points often occur in the Caribbean where the hurricanes make landfall however, for 97% of the historical tracks, this is only one consecutive data point, and can therefore be generated using interpolation (Hoek, 2017).

Once all the tracks had been synthetically generated for the Northern Atlantic basin, they were filtered for a given domain, to determine which tracks applied to the location of interest. The generated synthetic tracks were filtered for St. Martin, by defining a domain of 500 km^2 around the island, with the island in the centre, and determining which synthetic hurricane tracks passed through the domain. In total 1431 hurricane tracks were found and formed the probabilistic ensemble to be modelled for hazard and impact on St. Martin.

3.4.1. Hazard and Impact Modelling

Once the 1431 hurricane track scenarios were defined, they could be modelled using the previously validated hazard and impact models set up for St. Martin. In order to use the hazard models for each synthetic track, the spatial wind fields for each time step for each individual track had to be generated. This was done using TC-WiSE (Hoek, 2017) which based on the wind field generation on the approach by Holland (1980) and the adaptations by Holland et al. (2010) and Nederhoff et al. (2019).

In order to construct these spatial wind fields, the radius of maximum winds (RMW) and central pressure were first determined based on the maximum sustained wind speed by using the relationships found by Hoek (2017). Once RMW is determined, R35 is also found, and the wind field can be constructed. Hoek (2017) uses a Gumbel copula to represent the relationship between maximum sustained wind speed and central pressure as shown in Figure 3.22. The relationship between RMW and maximum sustained wind speed was determined using an empirical joint distribution and is shown in Figure 3.23. The same was done for the relationship for R35 conditionally based on RMW and the maximum sustained wind speed and is shown in Figure 3.24.

Using these parameters, the spatial wind field is constructed for each time step within a track scenario. These spatial wind fields are then ready to be passed to WES (see Section 3.2.1), and the same model train described in Section 2.2 can be applied. Each hurricane track is therefore modelled, and the corresponding extreme wind speeds and coastal flooding levels are found for each scenario.

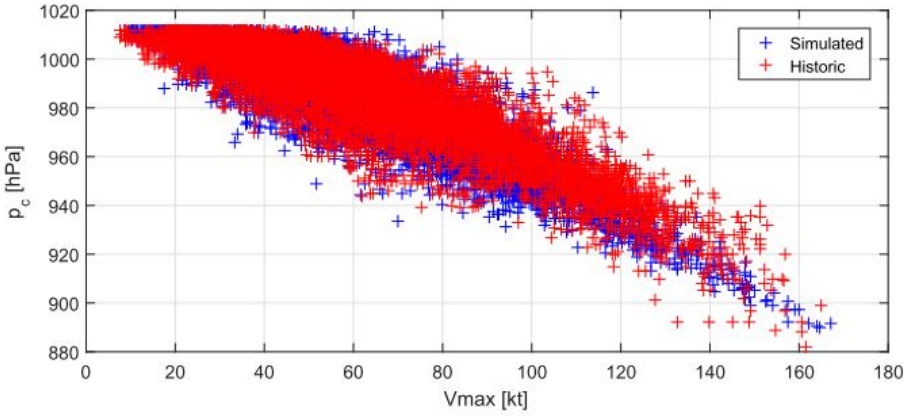

Figure 3.22: Historic observations of central pressure versus maximum sustained wind speed plotted together with the same amount of randomly selected observations of 1000 years of simulated TC events (Hoek, 2017).

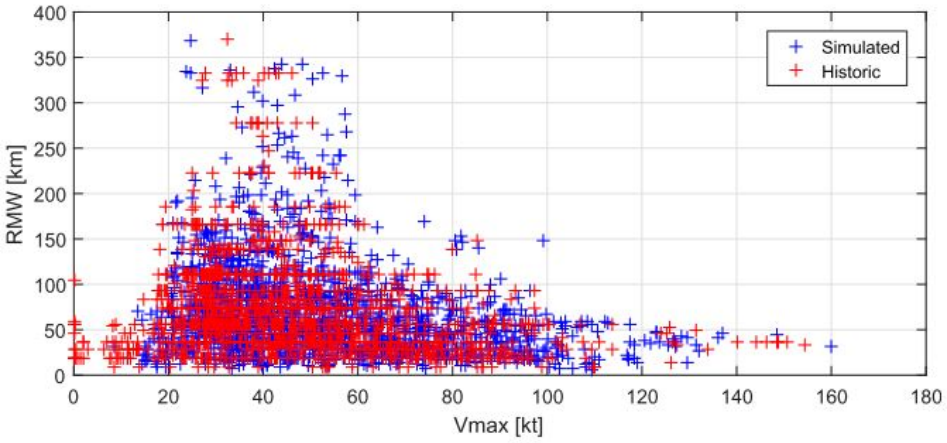

Figure 3.23: Historic observations of radius maximum winds versus maximum sustained wind speed plotted together with the same amount of randomly selected observations of 5000 years of simulated TC events (Hoek, 2017).

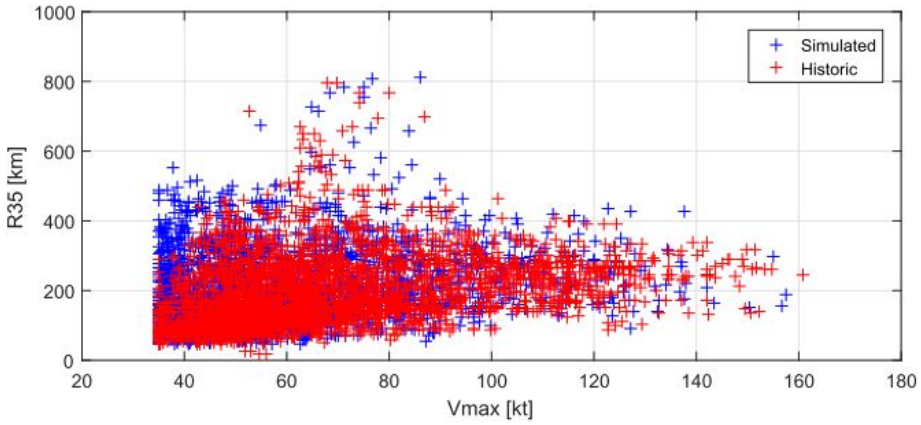

Figure 3.24: Historic observations of 35 kt radius winds versus maximum sustained wind speed plotted together with the same amount of randomly selected simulated observations of 5000 years of simulated TC events (Hoek, 2017).

The wind and flooding hazard extents were then used to simulate damages for each track scenario according to the validated impact model setup in Section 3.3. The exposure data and vulnerability functions were the same as those described in 3.3, and were specific for the island of St. Martin. Damages were determined for each computational grid cell on the island, for each scenario (both wind and flood damage). These damages were represented as hazard maps for each hurricane track scenario and resulted in each computational grid cell containing a value for wind speed, flood level and associated damages for 1431 scenarios.

3.5. Probabilistic Analysis and Risk Assessment

The final step of the research was determining the probabilities associated with the damages calculated for each track scenario, and then performing a risk assessment for St. Martin. These steps coincide with the two components needed for hurricane risk is the induced damages for each considered scenario and the associated probability of occurrence for each scenario. Within this assessment the scenarios were defined as the synthetically generated hurricane tracks that enter the domain around the island of St. Martin. The induced damages were defined as combination of the flood damage and wind damage for each hurricane track.

The total combined damages were determined by adding the flood damage and wind damage together, and assuming a maximum threshold value for each computational grid cell. This maximum threshold was determined by looking at each cell and the percentage of each building structure type and its corresponding maximum damage per cell. This meant that each computational cell had a unique threshold value. The threshold value ensures that damages do not exceed 100%. Therefore if 100% damage has been reached due

to wind damage, the total damage will not increase if there is also a % water damage. The total damages for each hurricane track scenario were recorded for each computational cell resulting in a series of total damages for each cell. The steps involved in determining damage per hurricane scenario is summarised in Figure 3.25, these steps were followed for all hurricane track scenarios.

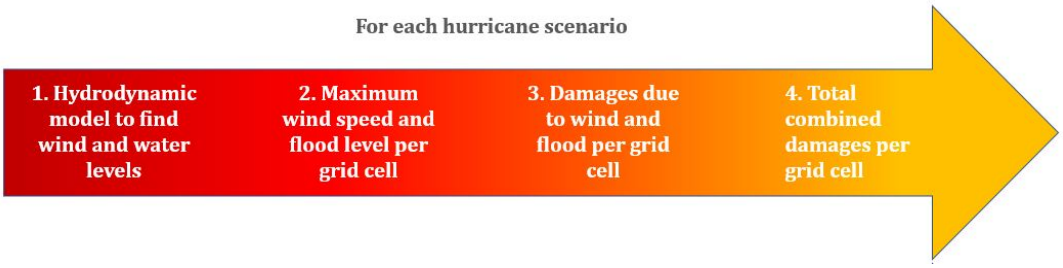

Figure 3.25: Flow chart of how to determine damages per hurricane.

Once total damages have been determined, the risk assessment can be performed. To determine the risk therefore, the corresponding probabilities are needed for the total damages. To determine these probabilities, the hurricane-induced water levels were analysed to determine their respective exceedance probabilities. This was done by looking at the coastal water levels for all 1431 track scenarios. The empirical cumulative density functions were found for the maximum water levels, for each of the 23 flooding basins identified for St. Martin (see Section 4.2). This was done using the modelled data from all the considered hurricane scenarios. This means that for each flooding basin a series of maximum water levels was used to determine the cumulative distribution, and corresponding exceedance probabilities for that basin were found using an empirical fit. These probabilities were then assigned to the damages associated with the given water levels for each basin.

After the exceedance probabilities were assigned to each damage value, for each grid cell, for all the hurricane track scenarios, the risk could be determined. The risk was determined by calculating the risk integral for each computational cell, for the damage - probability data. The risk integral was calculated using the trapezoidal integration method. The final hurricane risk was found for each cell across the island to create a risk map for St. Martin. The steps involved in determining risk per cell, and consequently the whole island, is summarised in Figure 3.26, these steps were followed for each cell covering the island of St. Martin.

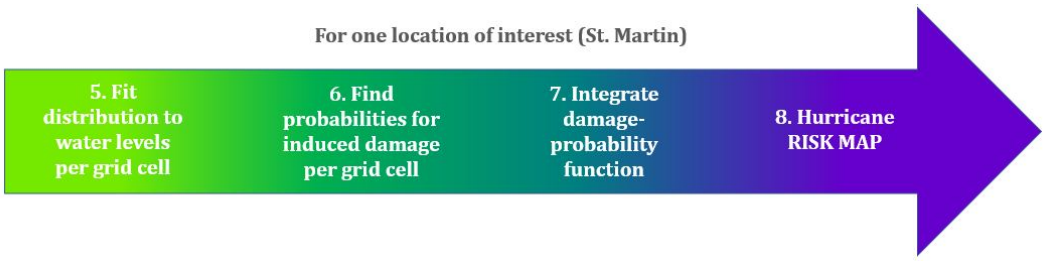

Figure 3.26: Flow Chart of how to determine risk per location of interest.

The maximum water levels were also fitted with standard distributions to determine which represents the data the best for situations when data is limited and the option to produce many scenario results is not possible. The considered distributions were the Extreme Value, Gamma, Generalised Extreme Value, Kernel, Logistic, Normal, Rayleigh, Stable and t-location (Jonkman et al., 2017). For all cases the behaviour of the maximum water levels were similar, and the best fit distribution was determined using the "goodness of fit test" where the normalised root mean square is determined for the modelled water levels and the predicted water levels of the distribution.

4

Case Study - Hurricane Irma

The following chapter describes the results for the methodology used to arrive at impact for a single hurricane event. In this study, Hurricane Irma formed the validation case for determining hurricane induced hazards and corresponding damages on St. Martin. Section 4.1 describes the results of the three main data collection aspects, the final topography and exposure data used in the modelling, and the combination of flood validation data. The results of the process explained in Section 3.2 and 3.3 are also shown in this chapter, and describe the results of Phase 1 of the research. This formed the basis for the modelling performed during the risk analysis for all the hurricane track scenarios considered in this study. Section 4.2 shows the results of the maximum flooding levels on the island due to the hurricane and how these levels were validated, this section further shows the results of the maximum sustained wind speeds. These hazard results, along with the exposure data and vulnerability functions, were used to find the impact of the hurricane. These results are shown in Section 4.3. The hazard and impact results for the validation case of Hurricane Irma are shown in detail in this Chapter, whereas in Chapter 5 only the new probabilistic elements are shown. The hazard and impact results were also produced for all hurricane track scenarios considered in the risk assessment, however are not included in the report.

4.1. Final Data Sources

The first phase of the research resulted in various data sources used in the hazard and impact modelling of St. Martin. In most cases the data described in Section 3.1 was able to be directly implemented into the various models however three data sources required combination and transformation. In this section the final bathymetry, validation and exposure data results are discussed.

4.1.1. Final Bathymetry Data

The final coastal model grid setup included a bathymetry data set combined of three sources, namely GEBCO data, SHOM data and Navionics. These three sources were combined and interpolated onto the coastal model computational grid to arrive at the final bathymetry as shown in 4.1. Here the deepest parts of the ocean are shown in blue and the shallow regions are shown in red.

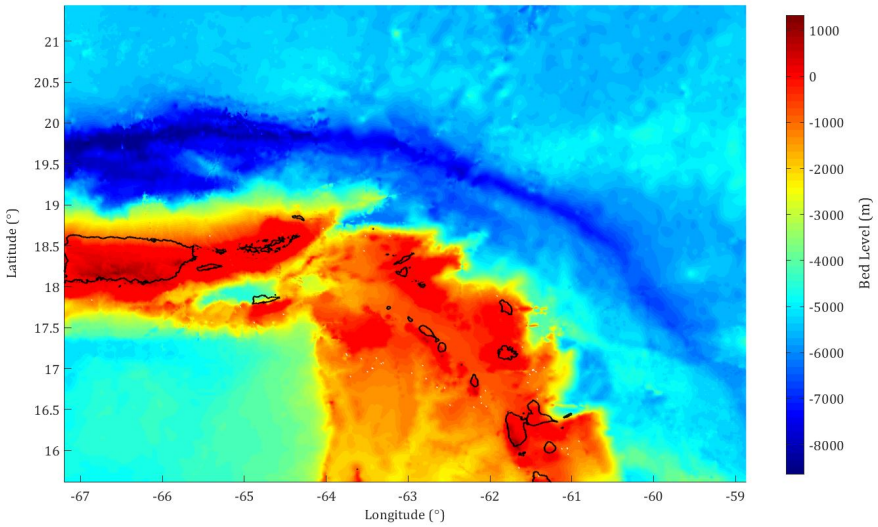

Figure 4.1: Final bathymetry used in the coastal modelling including the three data sources namely, GEBCO (British Oceanographic Data Centre, 2018), SHOM (SHOM, 2018) and Navionics (Navionics, 2019).

4.1.2. Final Flood Validation Data

The validation points defined for flooding due to Hurricane Irma are shown in Figure 4.2 which classifies each point by their associated flood level due to Hurricane Irma.

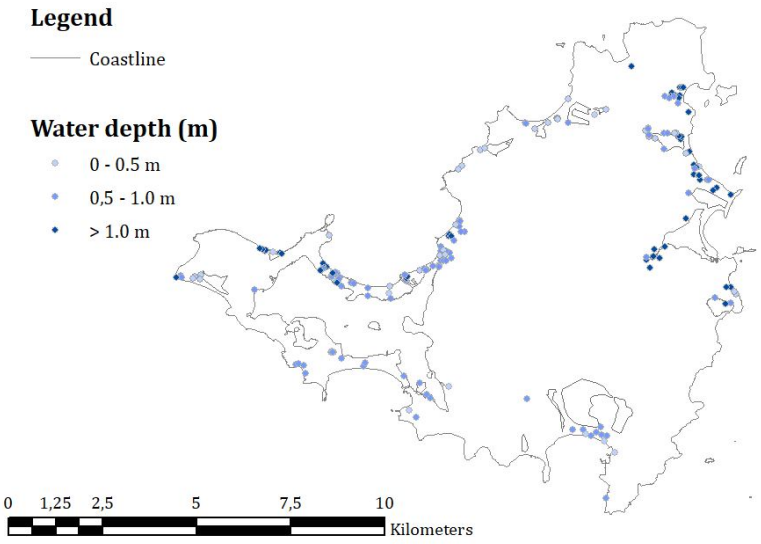

Figure 4.2: Map of St. Martin showing the total flooding validation points based on the data collected using online data sources.

In total 96 validation points were identified to be used in the flooding validation. These validation points, based on the Cerema and DEAL Guadeloupe (2017) inundation map and the 60 validation points based on the online twitter analysis of images taken before and after Hurricane Irma on St. Martin.

4.1.3. Final Exposure data

The exposure data used to determine impact due to hurricane-induced winds and flooding was based on public OSM (OpenStreetMap) data (OpenStreetMap, 2019) regarding buildings on the island and their use, and data provided by the World Bank regarding building roof structure material. To calculate the impact on the island the exposure data was transformed from the original format to a raster file containing grid cells of the same dimensions as the MERIT DEM data used to determine flooding. Figure 4.3 shows an example of OSM exposure data for residential buildings on St. Martin.

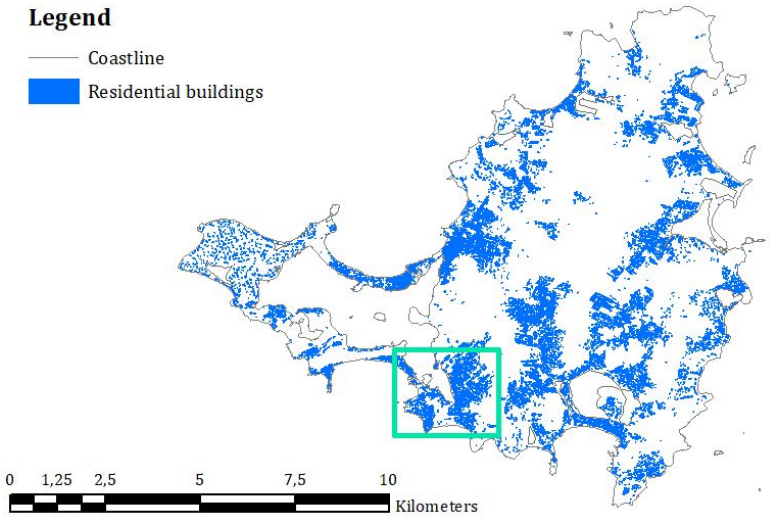

Figure 4.3: Map of St. Martin showing the residential building use types and the area of focus indicated with a green box.

The data in Figure 4.4 consists of polygon shapes of the buildings around the island. These have to be transformed to a cell representing the percentage of residential buildings in that grid cell. Figure 4.4 shows the steps taken do find these percentages.

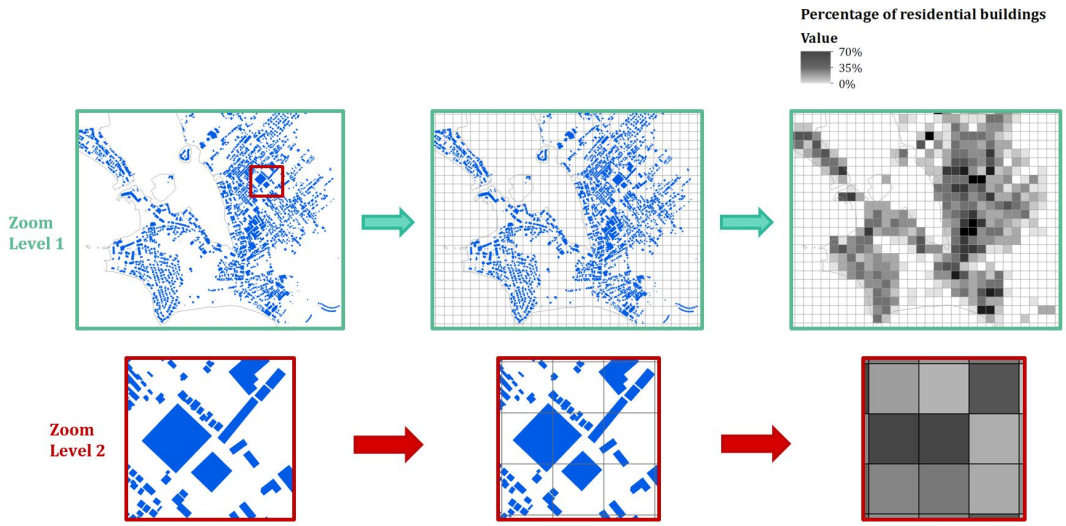

Figure 4.4: Example of the transformation of exposure data for residential building use type. Two zoom levels are shown showing the steps involved from left to right. Firstly, a grid is made and the area of buildings within each cell is determined. Secondly, the ratio of buildings to cell area are represented as a percentage for the entire grid.

First the grid cells were created with the same dimensions as the MERIT DEM data (90 m resolution). Then, for each grid cell, the ratio of the cell area and the area of residential buildings (in this example) within that cell was determined. The result was a grid with cells containing the percentage of a given building type and the result is shown in Figure 4.5. This was also done for the exposure data of the commercial and industrial building use types shown in Figure 4.6 and formed the exposure data for the flood impact model.

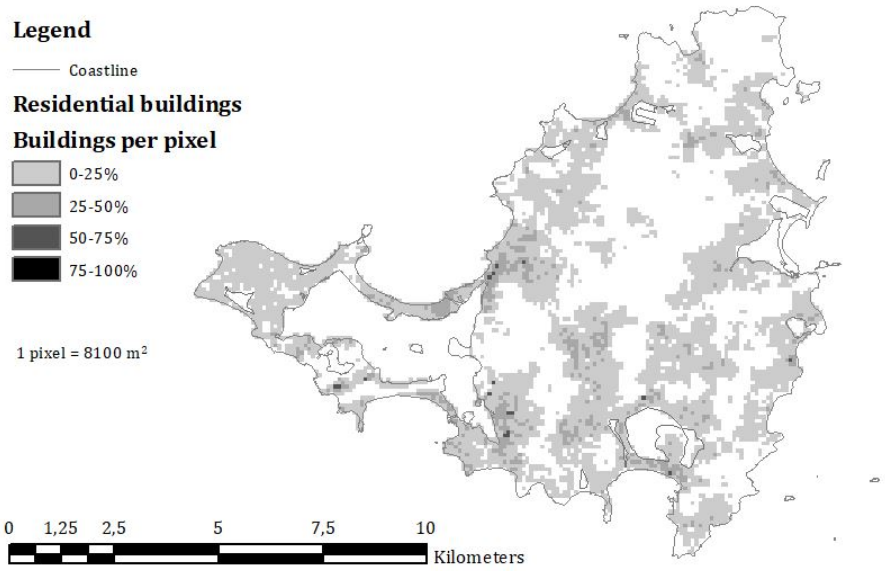

Figure 4.5: Residential building use exposure data for St. Martin.

This processed was also followed to create the exposure data for the commercial and industrial building use types shown in Figure 4.6, and formed the exposure data for the flood impact model. Here it is evident that the data available for building use types was more complete for the Dutch half of the island, than for the French half of the island, where only limited buildings were defined according to their use. Building not defined in the OSM data were given the status of residential use type based on the fact that the majority of the houses on the Dutch half of the island are also residential.

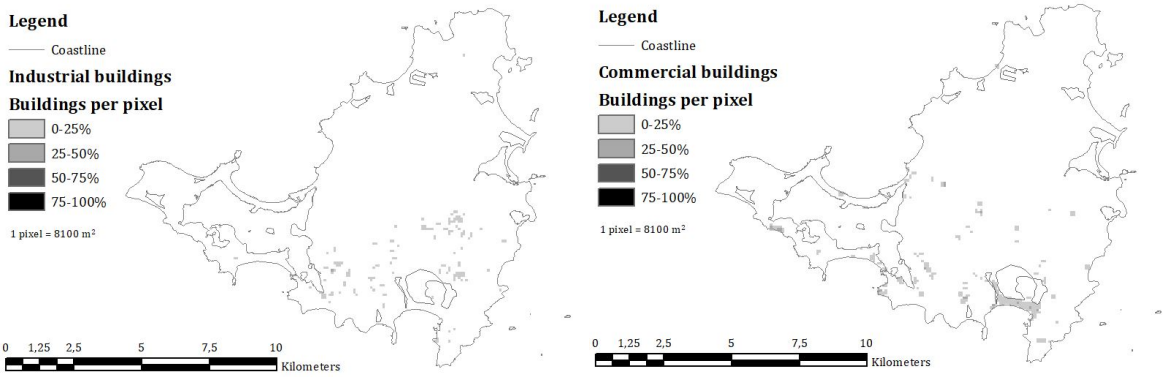

Figure 4.6: Left: Industrial building use exposure data for St. Martin. Right: Commercial building use exposure data for St. Martin.

The exposure data for the wind impact modelling was created in the same way as for the flood impact exposure data. The classifications, used in the wind impact exposure data, were for concrete buildings and for generic buildings as explained in Section 3.3. As the available exposure data was only for the Dutch half of the island, the structure materials for the buildings on French half of the island had to be assumed. They were assumed to be distributed similarly to that on the Dutch half of the island and resulted in the exposure data shown in Figure 4.7 used in the wind impact modelling.

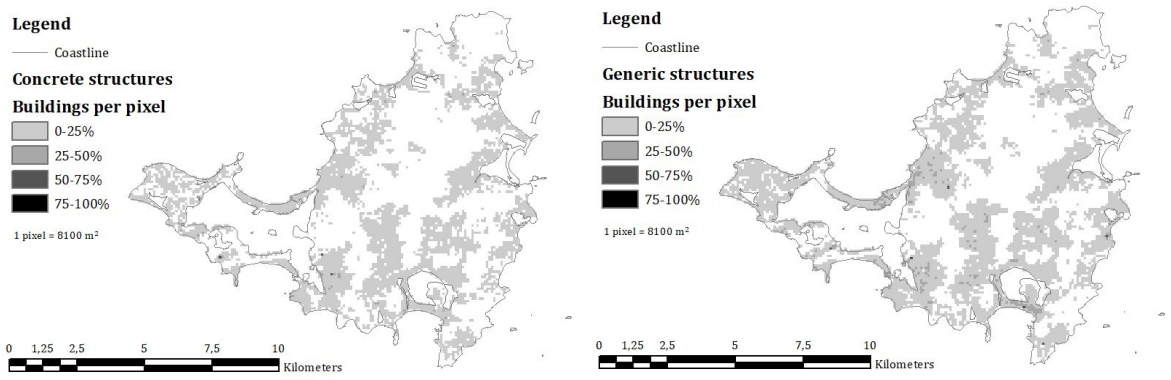

Figure 4.7: Left: Concrete structure building type exposure data for St. Martin. Right: Generic structure building type exposure data for St. Martin.

The exposure data, bathymtery and other data sources form the basis of the hazard and impact models set up for St. Martin. These models were tested as validated for the case of Hurricane Irma and applied in the rest of the research, keeping these data sets the same.

4.2. Hazard Modelling and Validation

A hydrodynamic D-Flow FM model was set up to simulate the storm surge levels at coastline of St. Martin. The coastal model consisted of a computational grid covering part of the Caribbean Sea and the Northern Atlantic Ocean. This computational space was forced with the hurricane characteristics of Hurricane Irma. These characteristics were represented along the path Irma followed, known as her hurricane track. Along this track the hurricane characteristics were represented by means of a spiderweb grid (circular grid used in D-Flow FM to represent cyclones), defining the wind speeds and central pressures along the track, for given time steps. The spatial distribution of the pressures and wind speeds are shown in Figure 4.8 and Figure 4.9 respectively.

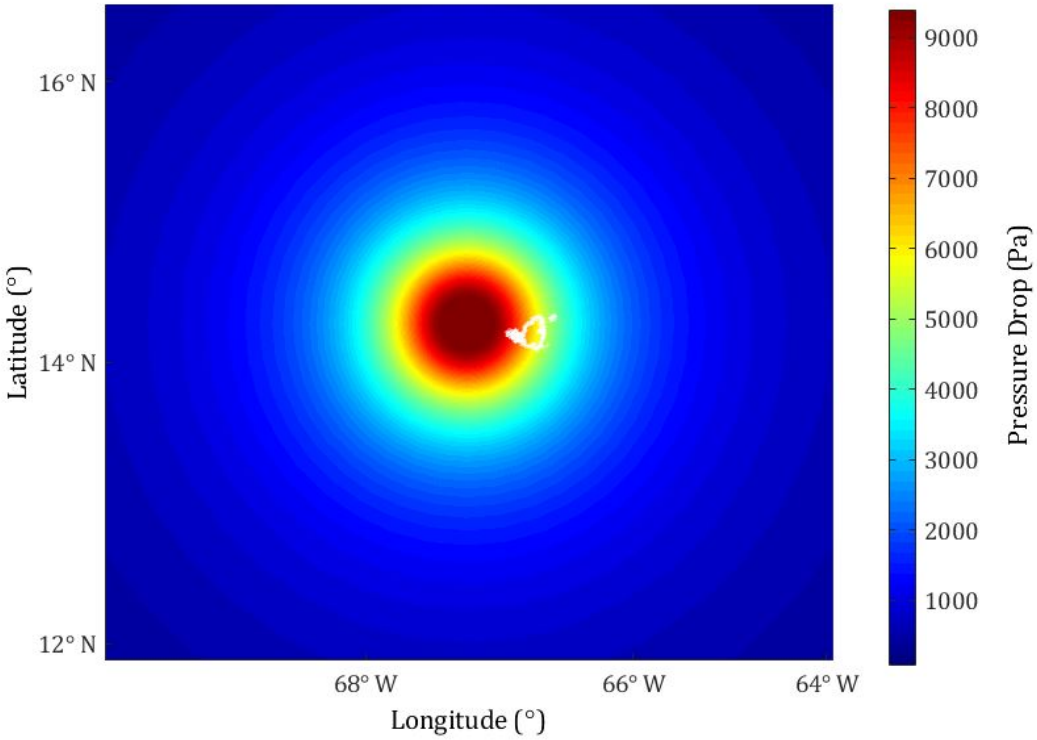

Figure 4.8: Representation of the pressure drop on a spiderweb grid for Hurricane Irma, time stamp 6 September 2017, at 12:00. St. Martin is indicated in white.

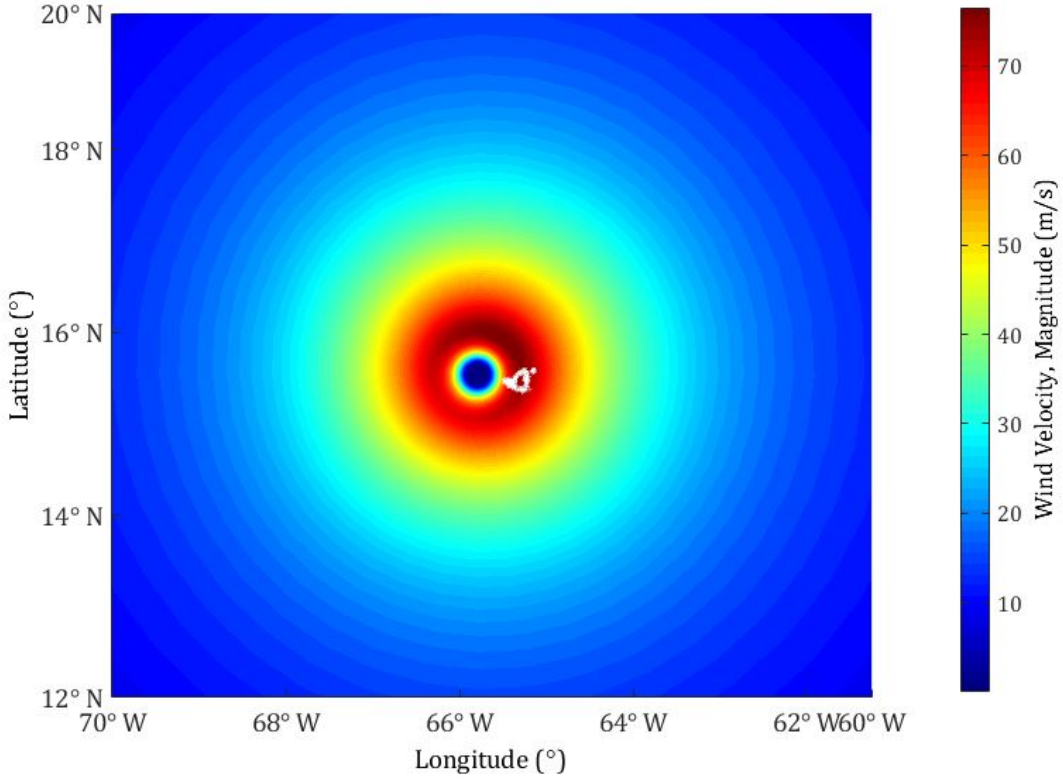

Figure 4.9: Representation of the wind speed magnitude on a spiderweb grid for Hurricane Irma, time stamp 6 September 2017, at 12:00. St. Martin is indicated in white.

These spatial fields were created, based on the approach of Holland (1980) and adaptions by Holland et al. (2010) and Nederhoff et al. (2019). These spatial fields are shown for the time step where Hurricane Irma passes directly over the island of St. Martin. The hurricane track for Irma, with corresponding spiderweb grid inputs per time step, was used to force the system to determine coastal surge levels and maximum wind speeds on St. Martin during Hurricane Irma.

4.2.1. Wind hazard

The winds speeds simulated during Hurricane Irma were based on the historical track data for the period of 2 September 2017 to 7 September 2017 (National Oceanic and Atmospheric Administration, 2018). This included the location of the hurricane track as well as the maximum sustained wind speeds and central pressures for intervals of 6 hours along the track. These characteristics were transformed into spatial wind fields as shown in Section 4.2.

The 1-minute average wind speeds were recorded during the simulation of Hurricane Irma for each computational grid cell for every time step. The maximum wind speeds were recorded for the grid cells on the island of St. Martin to find the extreme wind conditions during the storm. These maximum wind speeds represent the wind speeds at 10 m height above water. This means that no land forms or topography is included when calculating the wind speeds during the simulation. A physical model such as used for weather research and forecasting (WRF) is able to model this however, is beyond the scope of this research.

Wind speeds on St. Martin during Hurricane Irma were estimated to reach 155 knots (79 m/s) based on aircraft observations near Barbuda (Cangialosi et al., 2017). Figure 4.10 shows the maximum recorded wind speeds during the simulation of Hurricane Irma on the island of St. Martin. The maximum wind speeds on St. Martin ranged from around 66 m/s (237 km/h or 130 knots) to 75 m/s (270 km/h or 146 knots). The figure shows little variation in wind speed compared to the topographical data of the island, as the model does not account for the island topography.

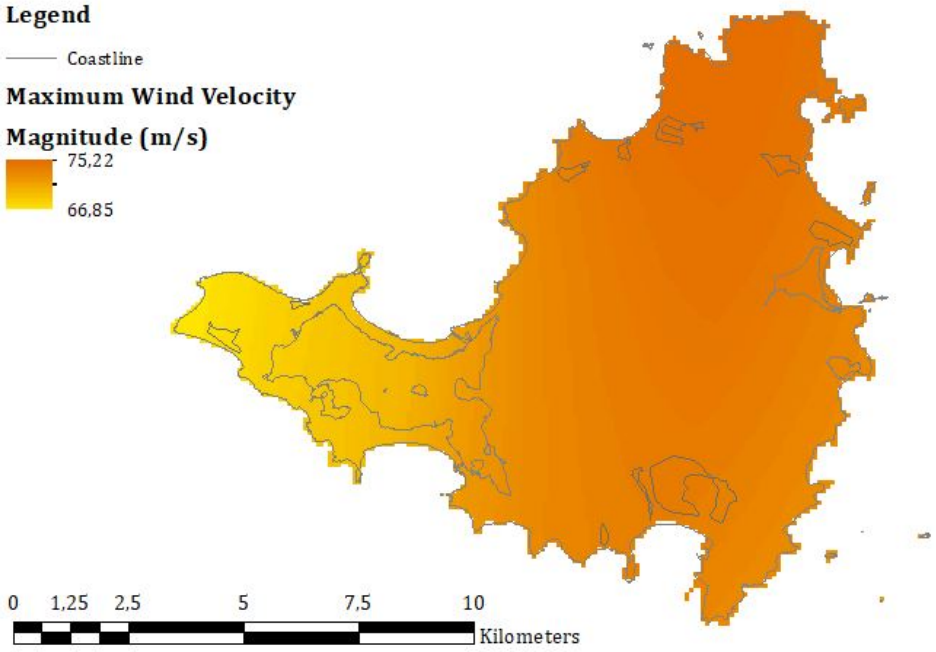

Figure 4.10: Maximum wind speed map during Hurricane Irma on St. Martin.

4.2.2. Flood hazard

The hydrodynamic D-Flow FM model was used to simulate the hurricane-induced surge levels due to Hurricane Irma at the coastline of St. Martin. These surge levels were used to estimate the boundary conditions to estimate inland flooding over the island.

The results from the coastal hydrodynamic model were recorded using observation points along the coast of St. Martin. These observation points recorded the water level during the simulation of Hurricane Irma. In total 618 observation points were identified at the coastline at intervals of around 50 m. Figure 4.11 shows the time series of all the observation points for the total simulation, indicating the time series for the observation point with the maximum peak in surge level (red) and the time series for the observation point with the minimum peak in surge level (blue). These peak levels were used in determining the boundary conditions for the inland flooding model.

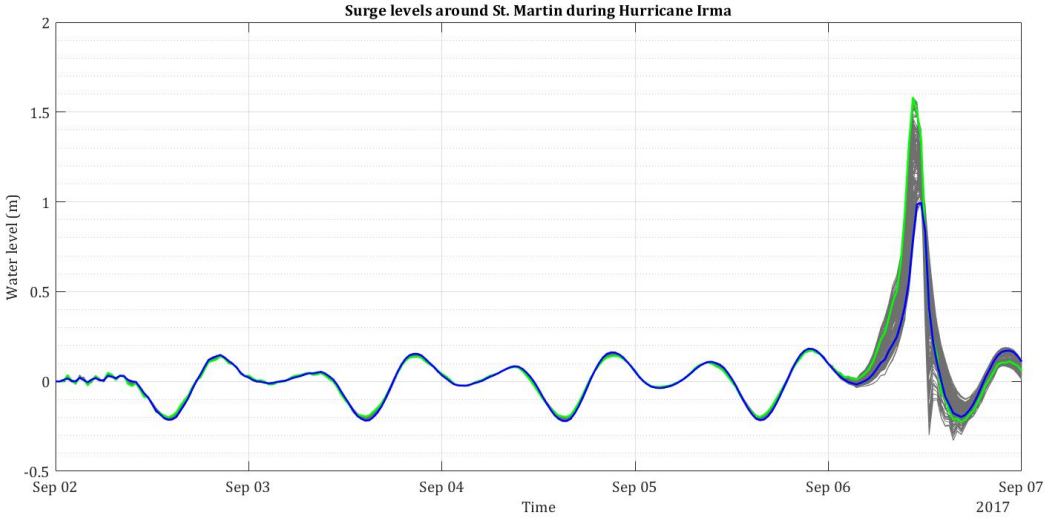

Figure 4.11: Surge level time series at the coast of St. Martin for Hurricane Irma from a Delft 3D Flow model.

The largest peak surge experienced at the coast was around 1.6 m and the smallest peak surge at the coast was around 1.0 m. Measurements for storm surge during Hurricane Irma on St. Martin are not available however, forecasts were estimated at 1.5 m to 3 m surge by NOAA (BBC News, 2017) leading up the the storm. After the storm NOAA released a report estimating surge levels based on observations. For other islands in the Caribbean near St. Martin surge levels between 0.1 m and 2.4 m (NOAA, 2018). These values compare well with the order of magnitude of the peaks of the simulated surge levels.

The maximum surge level was recorded for each observation point during the simulation. This means that at each observation point only one maximum surge level was defined. Figure 4.12 shows a 3D representation of these surge levels around the island where the shape of the island is indicated in grey and the observation points show a vertical bar (shades of blue to green) representing the maximum surge at that observation point.

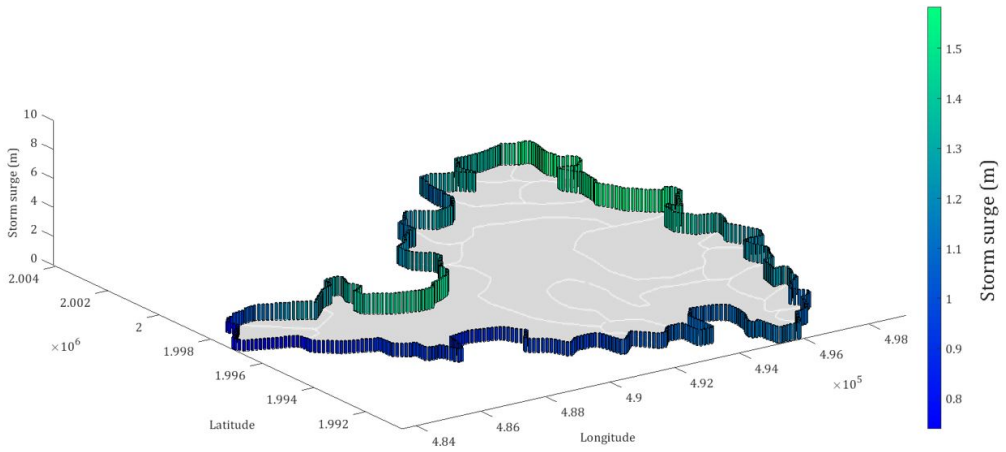

Figure 4.12: 3D plot of the maximum surge levels for each point along the coast of St. Martin during Hurricane Irma (co-ordinates are in UTM).

These maximum surge levels were combined with wave setup, determined using the parametric wave model described in Section 3.2, to find the maximum coastal water levels around the island during Hurricane Irma. A coupled wave and flow model was set up in D-Flow FM for Hurricane Irma to compare the offshore wave conditions to the parametric model. The maximum offshore wave height estimated using the model of I. Young (1988) for Hurricane Irma was around 20 m. The offshore estimation of maximum wave height compares well to the coupled wave and flow model as shown in Figure 4.13.

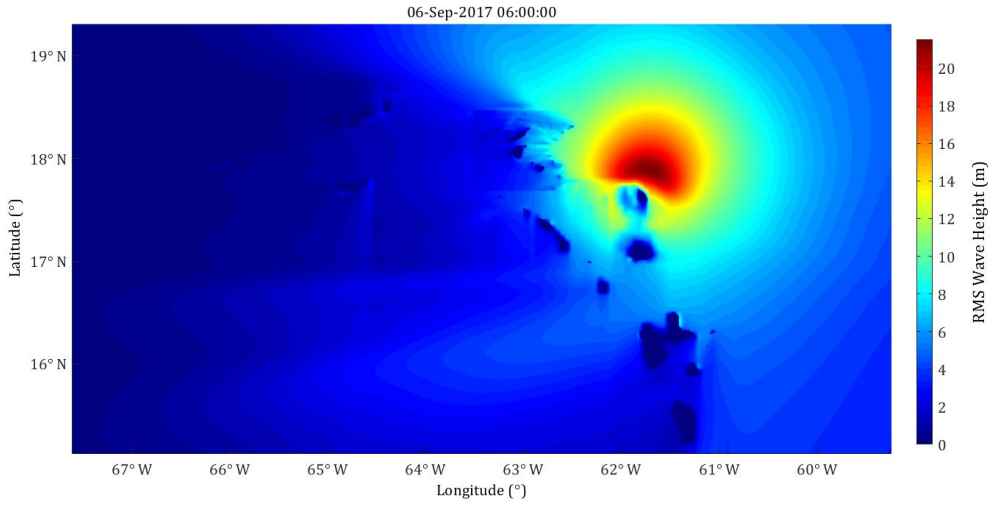

Figure 4.13: Mean wave height modelled by a coupled wave and flow hydrodynamic model for Hurricane Irma at a given time step, 6 September 2017 at 6 am.

Based on this offshore maximum wave height, the parametric model of van Rijn (1990) was used to estimate breaker depth and wave height at the breaking depth of 20 m and 10 m respectively. The wave conditions estimated using the parametric model were validated by comparing estimated wave heights with a detailed study by (Duvat et al., 2019) on Irma induced waves. The wave height map is shown in Section 6.1.1, where wave heights at the breaker zone (20 m depth) vary between 7 m to 10 m. The final wave setup therefore is based on the maximum sustained wind speed and corresponding offshore maximum wave height. This means that for all flood basins the wave setup is the same. In the case of Hurricane Irma wave setup was estimated at roughly 0.9 m. The total water levels (storm surge and wave setup) were used as the boundary conditions for the static bathtub approach to determine inland flooding on the island.

The static approach was set up by defining flooding basins on St. Martin based on the local topography. Each flood basin was defined as the area between two headlands along the coast and extending landward up to an elevation where flooding is not expected (around 30 - 50 m elevation). Figure 4.14 shows the 23 flood basins defined for St. Martin as well as the MERIT DEM and coastline used to define the basins.

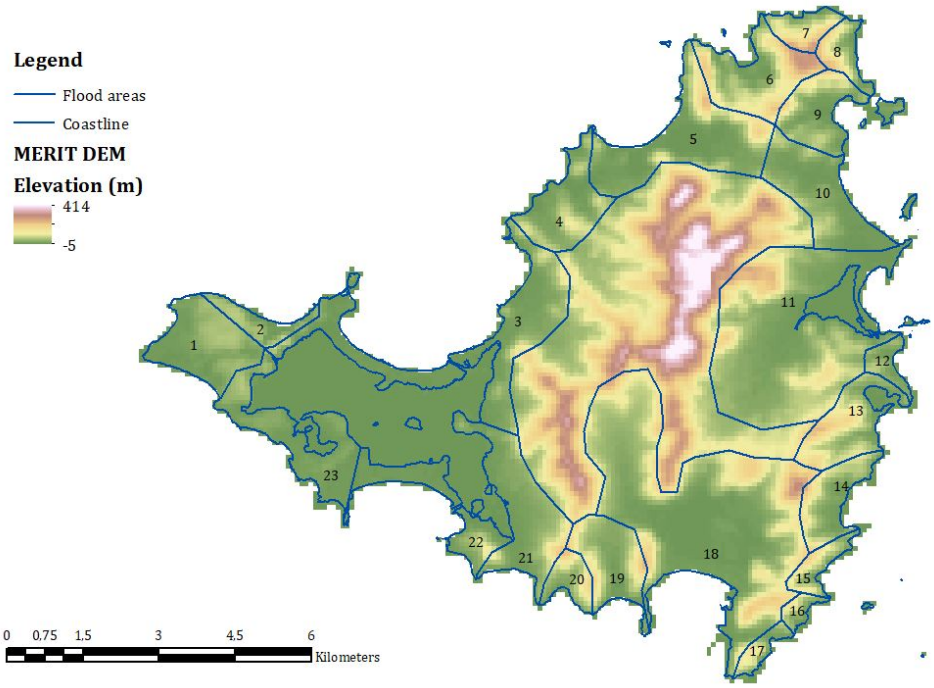

Figure 4.14: Identified flooding basins and observation stations with coastal water level time series.

When determining the flooding in each basin the assumption was made that the variation in maximum surge level between two headlands is negligible, and therefore that for each basin, the flooding level is taken as the maximum level between two headlands. This is a conservative assumption, as in reality the surge levels do vary along the coast and therefore will not all be as high as the maximum used in this approach. Figure 4.15 shows the results of the flooding model for Hurricane Irma on St. Martin.

The static approach was applied to each flooding basin by imposing the maximum water level (surge level and wave setup) to determine the inundation on the island. This was done by assuming that the imposed water level inundated any area, hydraulically connected to the sea, below the imposed level. The flood level ranges were chosen based on the validation data collected to validate the flooding levels and areas. In the figure flooding can be seen along the coastline as well as inland along the inland bodies of water.

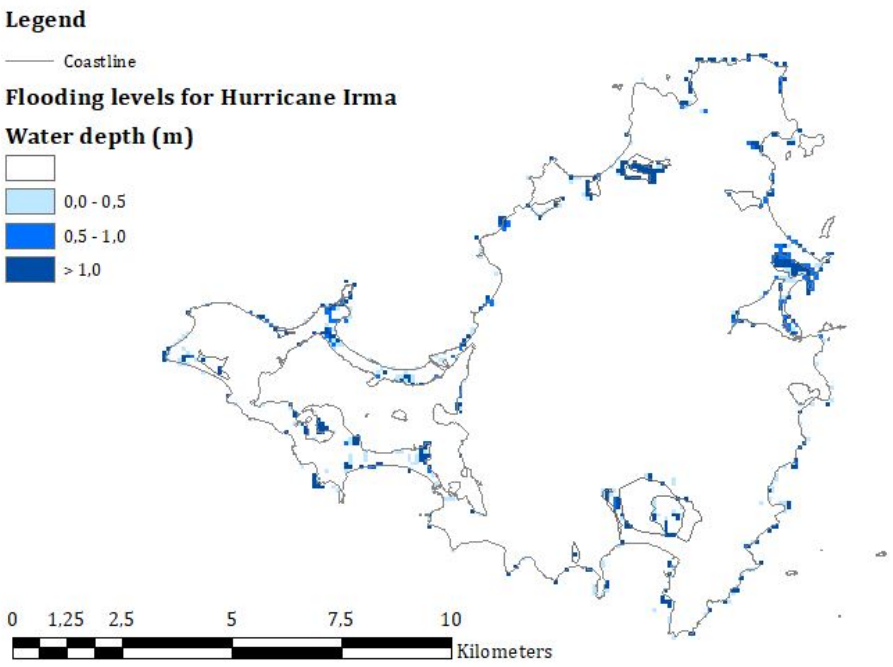

Figure 4.15: Coastal water levels simulated during Hurricane Irma.

4.2.3. Flooding Validation

In order to apply this flooding approach during the probabilistic assessment, validation of the flooding levels and areas was done. Validation was based on data from two sources, the first data source was based on the extracted points with corresponding water levels, based on the efforts by the French Republic Department of Environment, Planning and Housing (Cerema & DEAL Guadeloupe, 2017). The classification of water levels were from 0 m to 0.5 m, 0.5 m to 1.0 m and more than 1 m. Based on these observation points and water levels, potential flooding areas based on their administration boundaries were identified and shown in Figure 4.16.

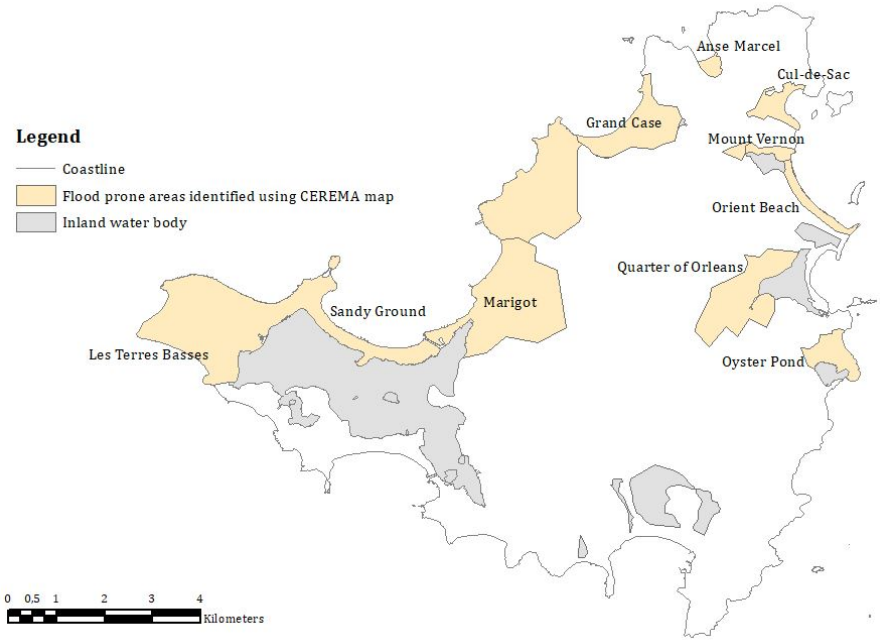

Figure 4.16: Identified flooding areas according to the map published for Hurricane Irma (Cerema & DEAL Guadeloupe, 2017).

The areas identified were Marigot, Sandy Ground, Les Terres Basses, Grand Case, Anse Marel, Cul-de-Sac, Mount Vernon, Orient Beach, Quarter of Orleans and Oyster Pond. All these areas are found on the French side of the island as the observation map was only produced for the French half of the island.

The second validation source was comprised of observation points of water levels during Hurricane Irma derived from online twitter data (www.twitter.com). The data included posts of the event and images indicating water levels during the hurricane. These were analysed to determine locations and water levels as described in Section 3.2.5. Along with the Twitter data, one of the analysed posts lead to an online public photo map for Hurricane Irma where people could upload an image and indicate on a world map where the image was taken (NAPSG Foundation, 2017).

The online validations points were used to identify potential flooding areas, as done before for the observation data published for the French half of the island. The online data was not region specific and therefore information for both the French half of the island as well as the Dutch half of the island was available. Figure 4.17 shows the areas defined based on the identified observation points. These areas are Sandy Ground, Marigot, Grand Case, Mount Vernon, Orient Beach, Philipsburg, Cole Bay, Pelican Key, Simpson Bay and Maho, and are defined by their administration area boundaries.

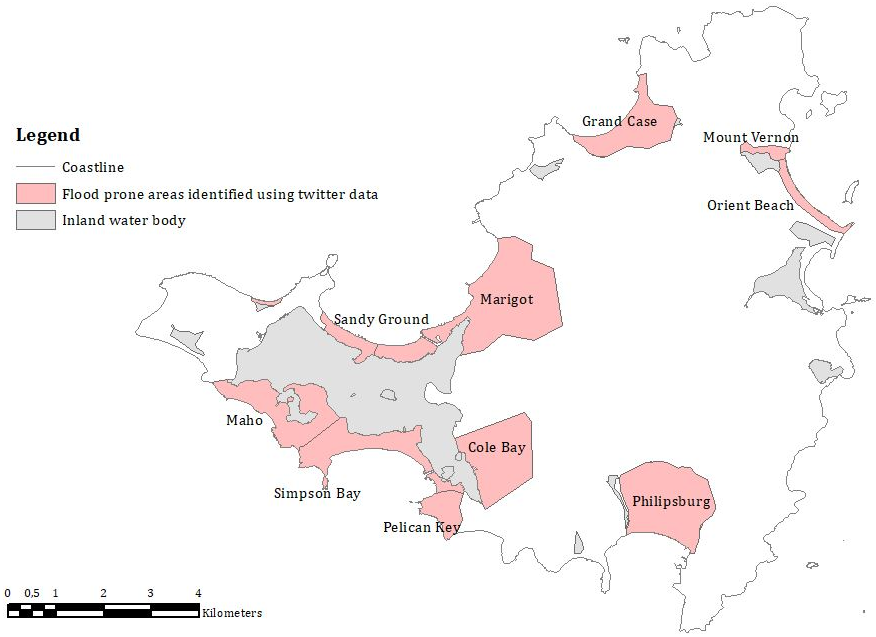

Figure 4.17: Identified flooding areas according to the analysed twitter data posted during Hurricane Irma.

The collected data was used to validate the flooding approach used to simulate flooding in terms of the flooded areas, as well as, the order of magnitude of flooding. Qualitatively the flooding areas compare well between the observation data points and the simulated flooding. Figure 4.18 shows the modelled flooding points and the identified flood areas. The points that do not fall within the flood areas are found along the coastline, where increased water levels do not directly translate to problems for the people or structures (if present), and therefore may have not been observed or reported. Comparing the results of the static inundation to the validation points means comparing water levels within a range of values. The modelled water levels can take on a specific value however the validation point used to verify the flooding does not have a unique value. The validation data has been classified for 0.5 m intervals and therefore, a comparison is done with the modelled water levels and these classes.

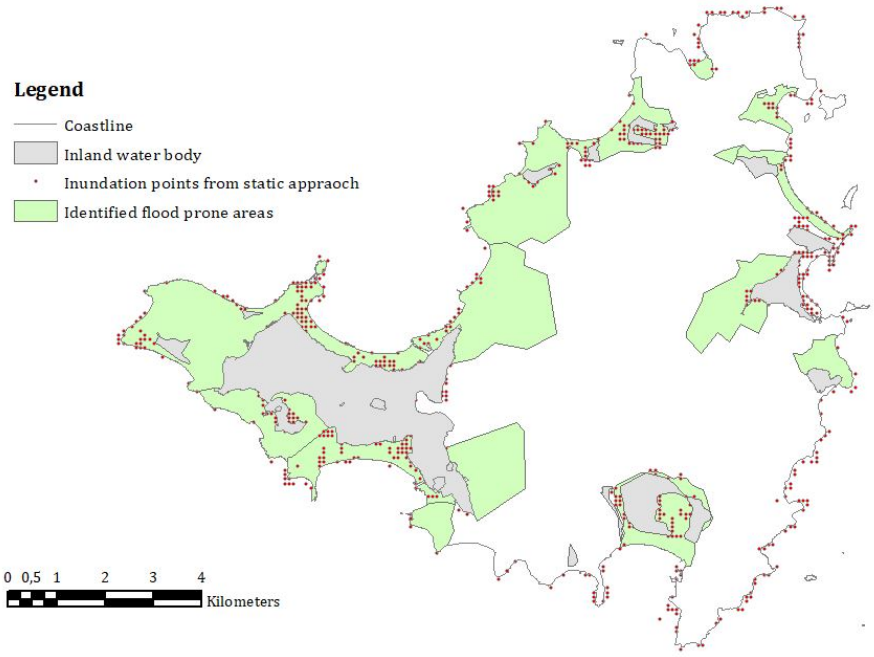

Figure 4.18: Map of the modelled inundation flood points versus the identified flood areas.

Figure 4.19 shows the validation data classes (grey) compared the the modelled water levels. Each point shows the water level modelled versus the validation point (either from the observational data of the French half of the island as a blue circle or from the online Twitter data as a red circle).

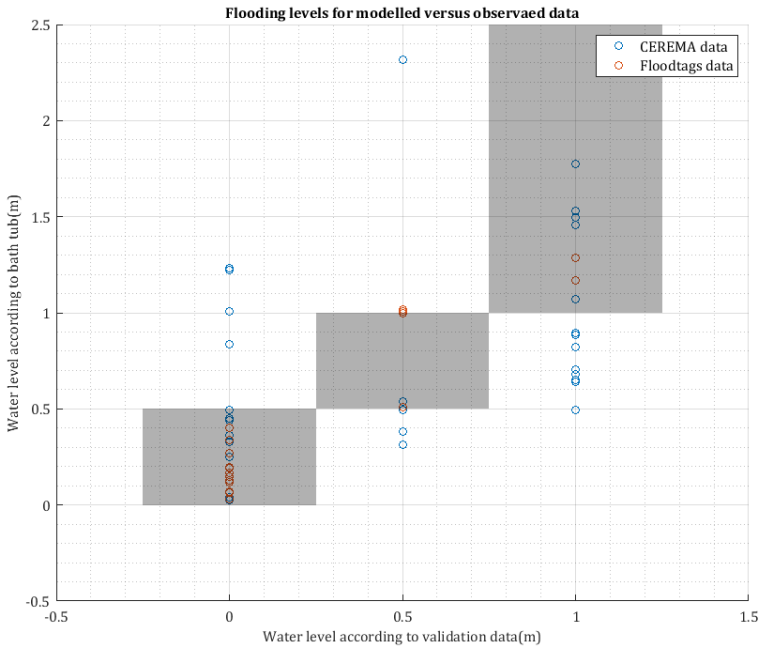

Figure 4.19: Graph showing the modelled data versus the validation data.

The lower water depth interval of 0 m to 0.5 m is modelled well by the static flood approach, producing results within the expected range or in a few cases, an overestimation. The intermediate water depth interval of 0.5 m to 1.0 m has a larger scatter with more modelled water depths falling outside of the expected range. These

points however, still fall within 0.15 m of the expected interval, with one outlier which is over estimated. The largest water depth interval classifies water depths to be larger than 1 m. Here the model either predicts water levels within the expected interval or underestimates water depths by up to 0.5 m for the observational data (Cerema & DEAL Guadeloupe, 2017) of the French half of the island. This comparison shows that the order of magnitude in water depth between the modelled and validation data is comparable. The accuracy of the validation, especially the observational data for the French half of the island is unknown, as well as how these water depths were retrieved. Comparing the model to the derived water depths from the online data shows that the model either estimates the water depth within the expected range or overestimates water depths, as is expected when using a static approach.

4.3. Impact due to Hurricane Irma

To determine the coastal flood impact and wind impact due to a hurricane, relationships between the hazard and exposed assets are needed. Here the impact on a building structure is considered, and therefore the exposure data consists of structure type and use for all buildings on the island. Based on the use of a building, a relationship can be made with the inundation depth and the percentage of expected damage. In the same way a relationship between wind speed and percentage of expected damage is made for the structure types. These relationships are known as vulnerability functions and these were based on previous studies for the island of St. Martin, and surrounding islands in the Caribbean. In this section the final damage functions are shown and the results of applying them to the Irma case are shown. For a more detailed look at the vulnerability functions see Appendix A.

4.3.1. Vulnerability functions for St. Martin

The vulnerability functions for flooding were digitised based on the study by Vojinovic et al. (2008) where these functions were developed for extreme rainfall events. They are shown in Figure 4.20. These vulnerability functions represent damages as $\$/m^2$ for buildings of different uses and sizes. The maximum damage occurs when water depths reach 2 m and remains constant for higher water depths. These damage functions were used for the flood impact modelling and were represented as damage fraction functions.

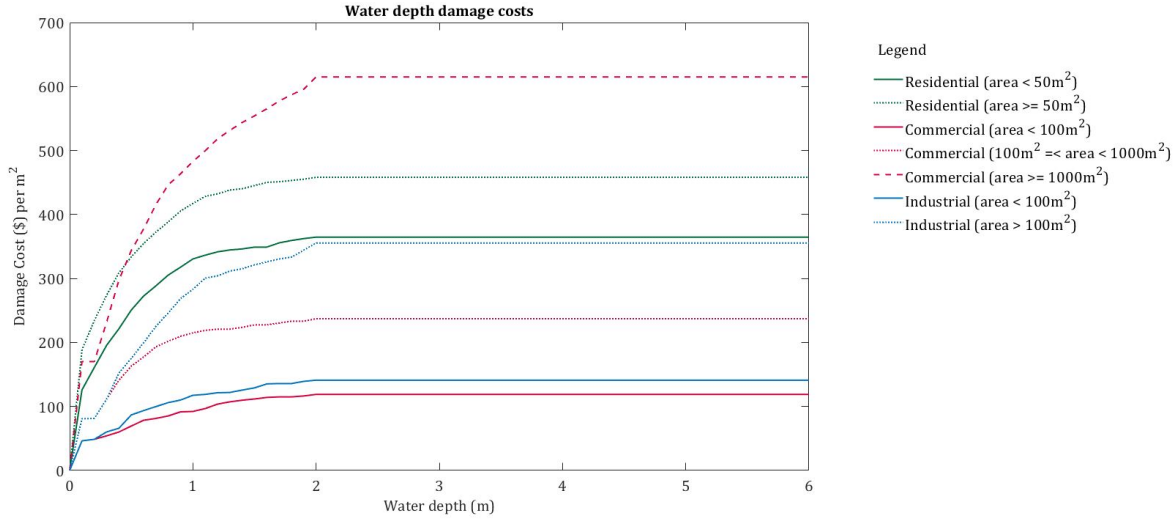

Figure 4.20: Depth-damage vulnerability functions for St. Martin (Vojinovic et al., 2008).

These functions show that for the initial water depths, where levels are increasing from 0 m to 2 m, the shape of the curve is concave down. This means that when levels increase in this interval damages go up at a fast rate, especially between 0 m to 1 m. After this the damages increase with water depth but at a much slower rate. This shape differs drastically from the wind impact vulnerability functions shown in Figure 4.21 and 4.22.

The wind impact vulnerability functions were based on a study by Khanduri and Morrow (2003) for structures in Puerto Rico. The study was used to determine the vulnerability functions for given wind speeds and corresponding damages. The functions shown in Figure 4.21 and 4.22 were chosen for St. Martin, based on the

assumption that buildings in the Caribbean are constructed with that same building standards and codes, equipped for hurricane activity. Furthermore, a generic function was used for the building material types that were not defined in the study by Khanduri and Morrow (2003).

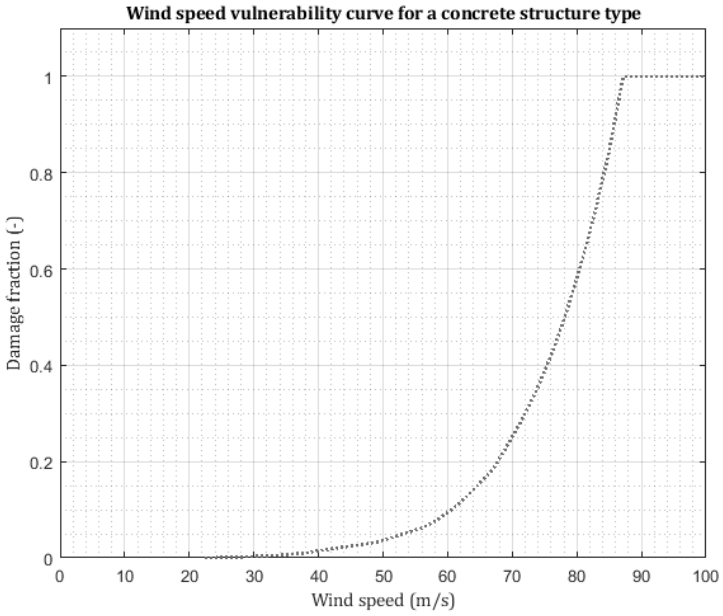

Figure 4.21: Wind-damage vulnerability function for concrete structures (Khanduri & Morrow, 2003).

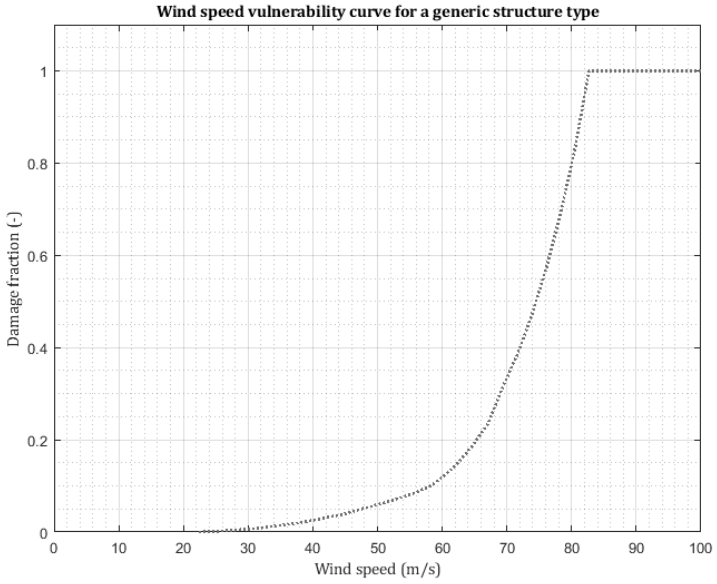

Figure 4.22: Wind-damage vulnerability function for generic structures (Khanduri & Morrow, 2003).

These vulnerability functions have a concave up shape and therefore behave differently to those shown in Figure 4.20. Here we see that only for winds speeds larger than 40 m/s does damage start to occur, and at a slow rate. Once winds speeds increase to more than around 65 m/s to 70 m/s this rate of damage increases significantly. These functions were then extrapolated for wind speeds higher than 70 m/s (150 mph) by fitting the data with a polynomial function. It is clear for these extreme high wind speeds that damages increase quickly to 100%.

4.3.2. Damages due to Hurricane Irma

The final step to determine hazard impact was to combine the various elements to calculate the total damages. This was done for both wind and flood damage using FIAT (Slager et al., 2016) as explained in Section 3.3. Wind damage was determined by using the wind speed map (specific to Hurricane Irma), exposure data (specific to St. Martin) and vulnerability functions (specific to St. Martin) as input and calculating the damages for each computational cell. This resulted in the total damages shown in Figure 4.23. Here the total damages due to Hurricane Irma winds are estimated at 2.6 billion dollars.

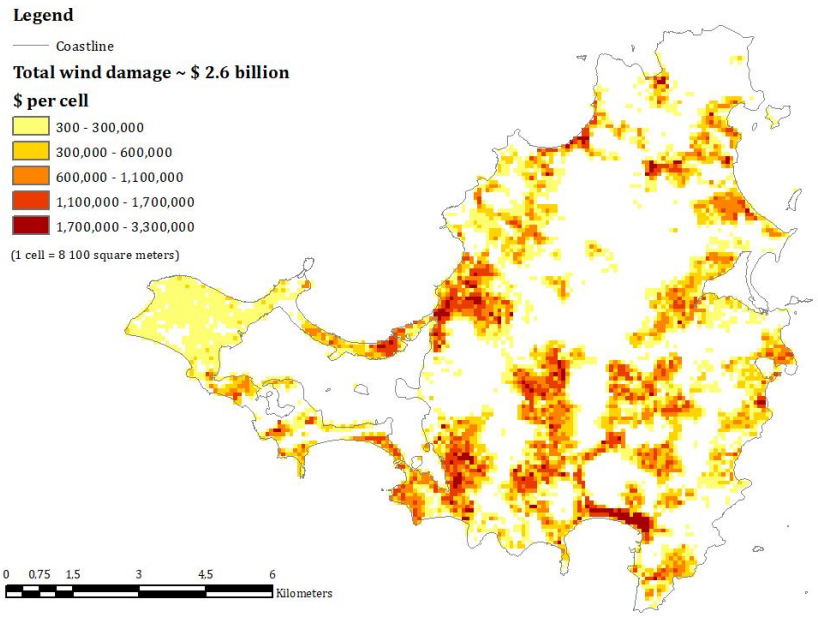

Figure 4.23: Wind Damage due to Hurricane Irma on St. Martin.

The validation of the wind damage for St. Martin was done by making a comparison with published maps and articles regarding wind damages after Hurricane Irma. The estimated wind impact comes close to the estimates of 1.6 to 2.5 billion dollars published after Irma (Cangialosi et al., 2017; Copernicus, 2017; NU, 2018; NOS, 2018a; World Bank Group, 2018). These estimates are done based on the post-disaster investigations that were done to record wind damages on building roofs, and therefore are assumed to correlate to the wind damages and not coastal or flooding damages. An example of a zoomed in comparison to the map released by 510 Red Cross (2017) is shown in Figure 4.24.

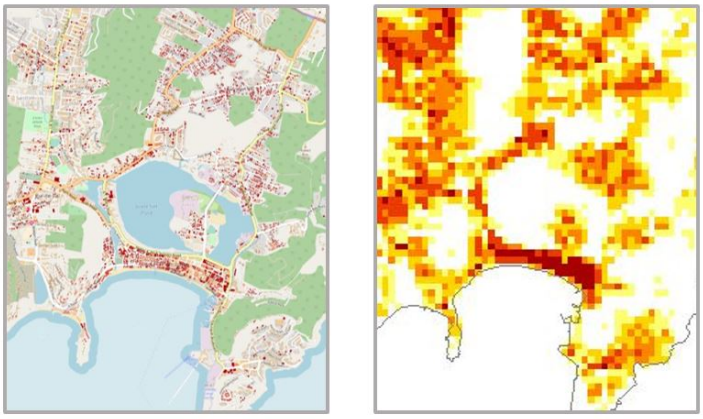

Figure 4.24: Wind Damage due to Hurricane Irma on St. Martin by: Left: 510 Red Cross (2017) and Right: impact modelled applied in this research.

The map by 510 Red Cross (2017) is only applicable to the Dutch part of the island, however compares well. The 510 Red Cross (2017) map is shown on the left and the model on the right. In both images, high damages are indicated in red, the scales are not the same.

Another comparison was made with the map released by (Pacific Disaster Center, 2017) which estimated wind impact on the island based on a wind model simulating the actual track data of Hurricane Irma. Figure 4.25 shows an example of the map compared to the modelled impacts. The largest difference can be seen on the French half of the island when buildings are sheltered by the mountain on the island. This is captured using a physical model and can therefore also be seen in the impact map by (Pacific Disaster Center, 2017).

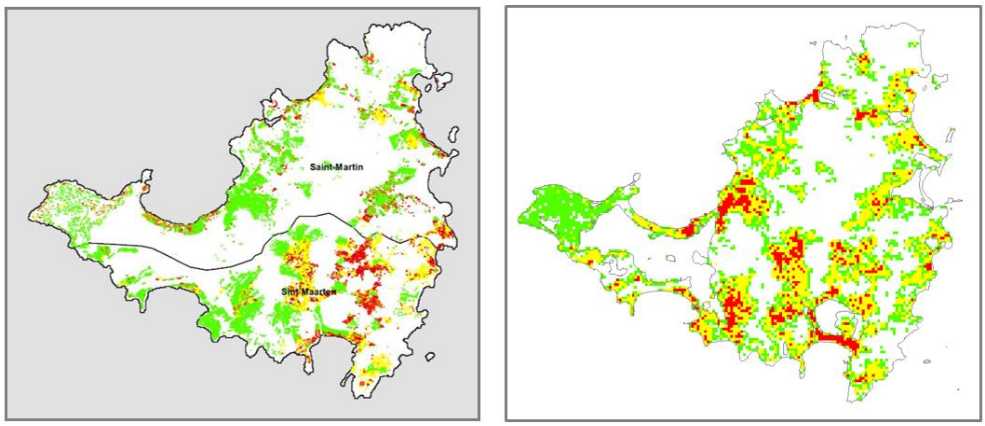

Figure 4.25: Wind Damage due to Hurricane Irma on St. Martin by: Left: (Pacific Disaster Center, 2017) and Right: impact modelled applied in this research.

Flood damage was also determined by using the flood depth map (specific to Hurricane Irma), exposure data (specific to St. Martin) and vulnerability functions (specific to St. Martin) as input and calculating the damages for each computational cell. This resulted in the total damages shown in Figure 4.26. Here the total damages due to Hurricane Irma flooding are estimated at 54.5 million dollars.

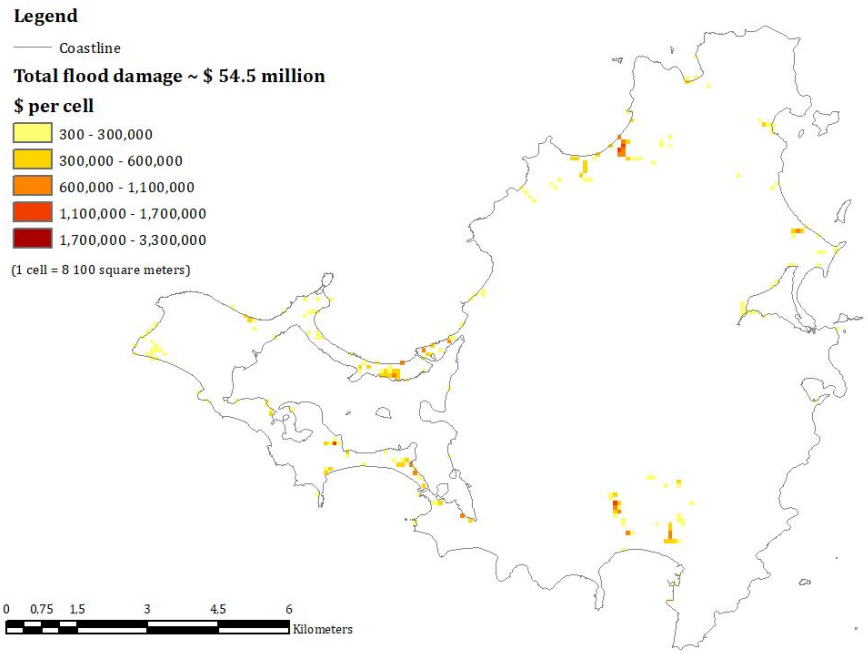

Figure 4.26: Flood Damage due to Hurricane Irma on St. Martin.

The validation of flood damages cannot be done as is the case for wind damages however the estimation of wind damages are deemed acceptable to be applied to the rest of the research during Phase 2, and accounts for 98% of the damage in the case of Hurricane Irma. Coastal flooding accounts for only 2% however, is not negligible when compared to the total costs involved and is also therefore applied to the rest of the research. The identified flooding areas correspond to the flood damages areas and therefore will represent the risk areas well when considering flood and wind hazard. It is important to realise that the coastal flooding and wind speeds are conservative estimations and therefore represent conservative damages as seen in the comparison. The order of damages, and identified areas however are well represented and therefore provide the necessary detail required in a risk assessment.

This section marks the end of Phase 1 of the research. The hazard and impact models have been validated for the test case of Hurricane Irma and are applied to the rest of the hurricane tracks generated in Phase 2 of the research.

5

Multi-Risk Assessment St. Martin

The following chapter describes the results from the multi-risk assessment of St. Martin, which formed Phase 2 of the research. This phase was based on the results and validation of the hazard and impact models set up in Phase 1. The first step in Phase 2 is described in Section 5.1. This was the generation of synthetic hurricane tracks that were each modelled using the hazard and impact models for St. Martin. To simulate each track, the spatial wind and pressure fields were created, and then used as forcing to the system. This section also describes how damages due to wind and flooding were combined to reach total combined damages. The second part to Phase 2 is described in Section 5.2. Here the combination of probability and damages is explained. For the case of St. Martin the probabilistic scenarios used in the risk analysis, were each synthetic track scenario. The exceedance probabilities were found for the coastal water levels of all the scenarios and assigned to their corresponding total damages. This set of damages and exceedance probabilities were then used to calculate risk on the island of St. Martin. Section 5.3 describes the application of the risk assessment and how it can be used to *Build Back Better*.

5.1. Synthetic track generation

There are two steps to generating hurricane tracks that can be used to simulate induced winds and flooding. The first step is to generate the path that the hurricane follows, and the second step is to generate the spatial wind field for each time step of the hurricane track. Both steps were followed in this research using TCWiSE, a tool developed by Hoek (2017) and Nederhoff et al. (2019) to generate synthetic data to be used to run simulations for locations where historical events are limited.

TC-WiSE was validated for hurricane tracks in the Northern Atlantic basin, using the Gulf of Mexico as a validation case, by looking at generation and termination locations for these tracks. Figure 5.1 shows a comparison between the historical genesis densities for each grid cell and the synthetically simulated tracks of TCWiSE. Hot spots for hurricane genesis are found near the west coast of Africa (as was where Hurricane Irma was generated) as well as near the eastern coast of Central America. These genesis locations determine the rest of the track propagation over the ocean. This was how each path was determined for each hurricane track.

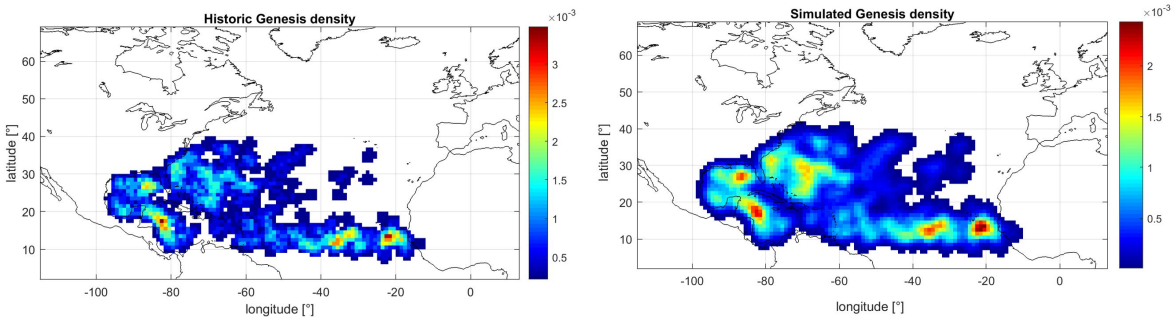

Figure 5.1: Left: Genesis locations for historical data. Right: Genesis locations for synthetic data (Hoek, 2017).

A total of 149 historical hurricane tracks are found in the Northern Atlantic Basin and were used to generate the 5000 years' worth of hurricane tracks used in the probabilistic analysis. Figure 5.2 shows all the historical hurricanes alongside all the synthetically generated tracks using TCWiSE. Each track was constructed by sampling hurricane direction, translation speed and maximum sustained wind based on the genesis location, and then, per time step, sampling the change in direction and change in translation speed to determine the new location of the hurricane eye and its corresponding characteristics.

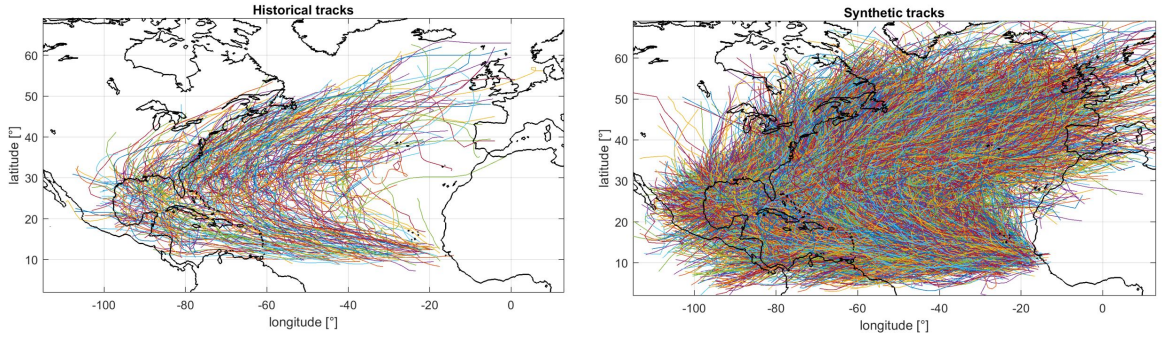

Figure 5.2: Left: Hurricane track paths for historical data. Right: Hurricane track paths for synthetic data (Hoek, 2017).

5.1.1. Hurricane track scenarios for St. Martin

The second step in the synthetic track generation was to filter the hurricane tracks around St. Martin and for each of the chosen tracks, generate the spatial wind fields for each time step. To determine which synthetically generated tracks were of influence to St. Martin, a domain was defined around the island and used to filter all synthetic tracks that passed through the domain at one point during their path. This resulted in 1431

synthetic tracks that formed the scenarios used to assess risk in St. Martin.

The spatial wind fields were then derived for each chosen synthetic track for each 6-hour time step. This was based on the (Holland, 1980) model and the adaptations by Holland et al. (2010) and Nederhoff et al. (2019). The input required included the maximum sustained wind speed, radius of maximum winds and central pressures which we defined when determining the path of each track. Each track was then ready to be passed through the hydrodynamic D-Flow FM model. Figure 5.3 shows all the tracks that were simulated using the Delft 3D hydrodynamic flow model.

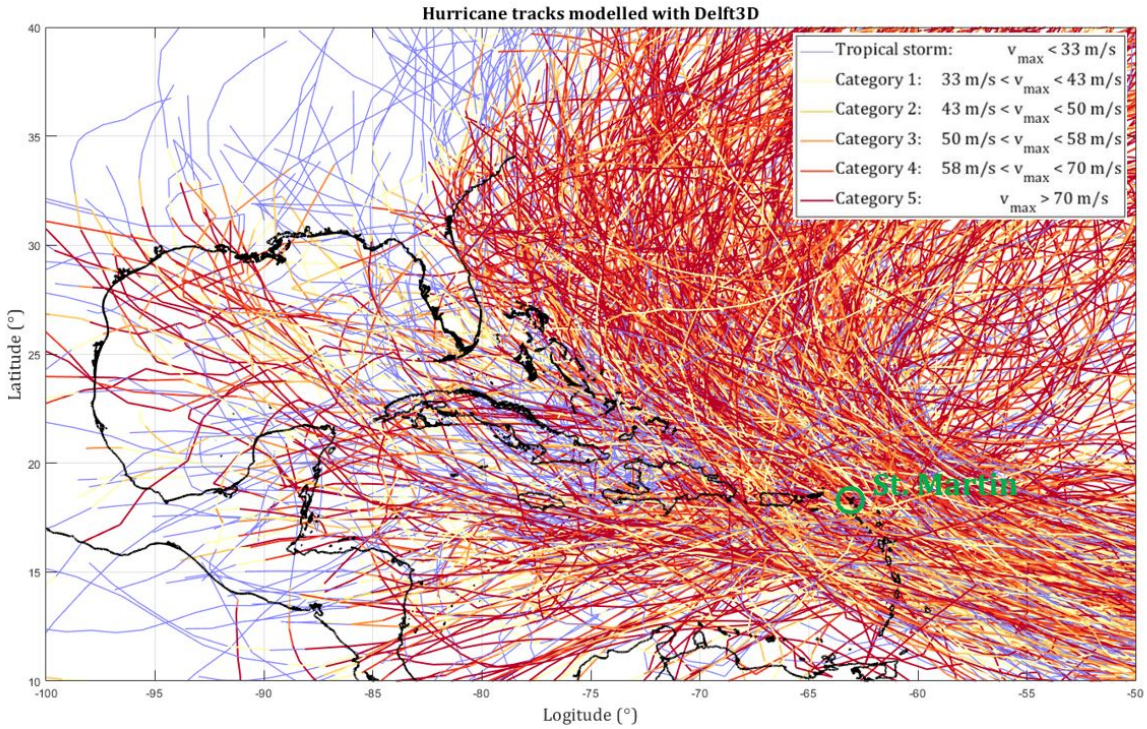

Figure 5.3: Synthetically generated tracks filtered for landfall on St. Martin.

In the figure the Caribbean Sea is visible with the southern tip of Northern America in view, as well as the northern tip of Southern America. The tracks show their intensity as they propagate along their paths, changing between tropical storms and category 1 to 5 hurricanes. These classifications are according to the Saffir-Simpson scale shown in Table 2.1.

5.1.2. Hurricane Track Simulation

Each hurricane track scenario resulted in a unique combination of induced winds and water levels. These hazards were then used to determine the corresponding impact according to the method described in 3.3. For every hurricane track scenario the maximum wind speed and maximum flood level (on St. Martin) per grid cell was recorded and used to create hazard maps for each track scenario. Using the previously defined exposure data and vulnerability functions (which remain unchanged for the different hurricane track scenarios), the impact due to wind and flooding was determined for every track scenario. This resulted in the total wind damage and flood damage per grid cell per hurricane scenario.

In order to move on to the risk assessment of St. Martin, it was important to determine the total combined damages for each hurricane scenario. This was done by combining the wind and flood damages for each track. This was done by adding up the respective damages. A threshold was used to ensure damages did not exceed 100%, and resulted in a total damage per track. This data set formed the basis of the hurricane scenarios used to determine the hurricane risk on St. Martin

5.2. Risk analysis

The risk analysis for St. Martin involved combining the total damages found for each cell for each hurricane track scenario and determining the corresponding exceedance probability, in order to integrate and determine the risk. This process is described in Section 3.5 and the results of the probabilistic analysis and risk assessment are shown here.

In order to perform the risk integral, the probabilities associated to total damages were needed. In this case the exceedance probabilities of the hurricane-induced water levels were chosen to represent each track scenario. These exceedance probabilities therefore represented a given water level, and its corresponding total damage determined in the previous section. In the determination of the coastal water levels, different flooding basins were used for St. Martin. The maximum water level for each basin was used to determine the flooding and therefore each track scenario resulted in water levels for each of the defined flooding basins. In total 23 flooding basins were defined (see Section 4.2). The water levels were analysed for each flooding basin, numbered 1 to 23, in Figures 5.4 and 5.5. For each basin the water levels were fitted empirically to determine the corresponding cumulative density distribution, and probability of exceedance for each basin and water level.

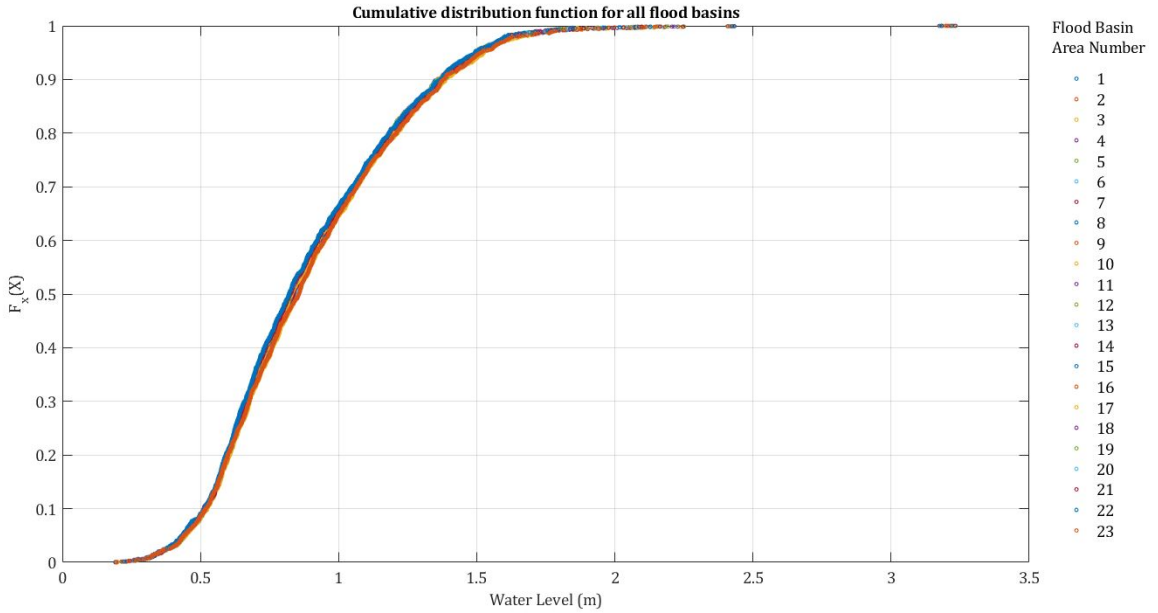

Figure 5.4: Cumulative density distribution for hurricane-induced water levels on the island of St. Martin. These are defined for the 23 identified flooding basins on the island, numbered here from 1 to 23.

Figure 5.4 shows the cumulative density function for each of the 23 flooding basins and how they compare to one another. In the figure it is clear that the distribution of water levels for all of the flooding basins follow a similar curve. This is expected due to the fact that the induced storm surge levels around the island do not vary largely in magnitude due to a given hurricane scenario.

The exceedance probabilities probabilities for each flooding basin were then determined and are shown in Figure 5.5. In this figure again the water levels for the different flooding basins follow similar curves. Variability in the water levels occur at the higher water levels, where probability of exceedance becomes very small, this is in the order of 0.25 m. As the water level increases the probability of exceedance naturally decreases as is expected for extreme hurricane events. When the water levels experienced due to Hurricane Irma are compared to these empirical distributions for each flooding basin, a probability of exceedance of $\frac{1}{500}$.

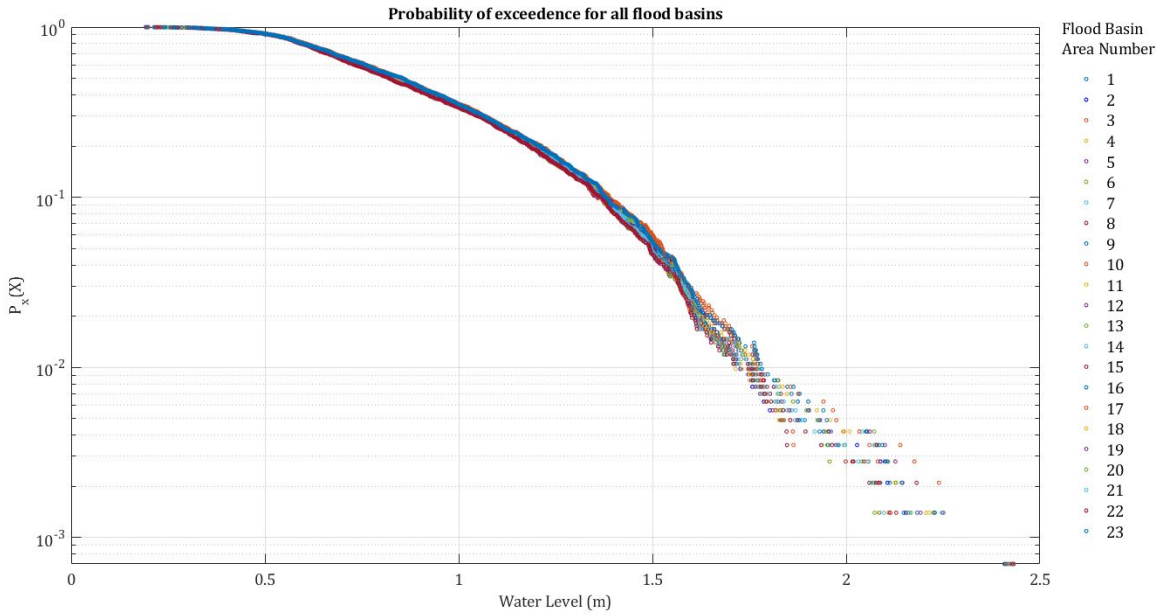

Figure 5.5: Probability of exceedance for hurricane-induced water levels on the island of St. Martin. These are defined for the 23 identified flooding basins on the island, numbered here from 1 to 23.

5.2.1. Hurricane Risk

The exceedance probabilities determined for the water levels were associated to their respective total damages. Using these damages and probabilities, the risk integral, according to the definition by Jonkman et al. (2003), could be calculated for each point on the island. The result is represented as the risk map shown in Figure 5.6 for St. Martin. The risk integral was determined for each pixel by finding the empirical fit of the exceedance probabilities and total damages, and integrating the curve. In this case the integration was calculated using trapezoidal integration.

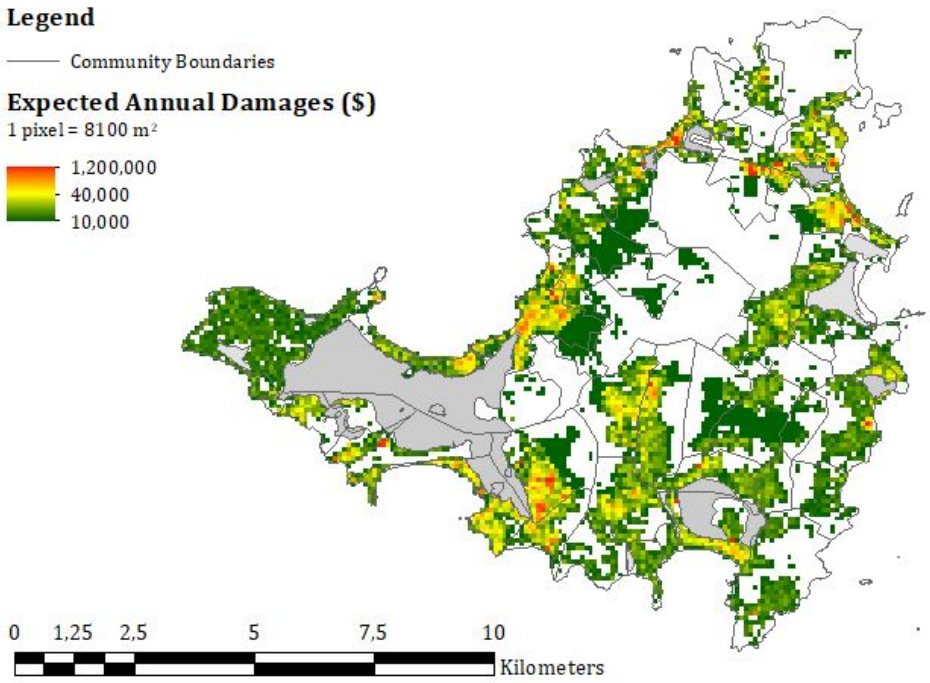

Figure 5.6: Map showing the hurricane risk (Expected Annual Damages) on the island of St. Martin.

The map indicates expected losses in terms of structural damage due to hurricane-induced winds and hurricane-induced coastal flooding. It is important to realise that the assumption was made that these two hazards are linearly related and therefore does not represent possible compounding or a magnifying nature between the two types of induced damages. This approach is however, better than considering the risk of each hazard separately as it considers the correlation between water level and wind speed. Considering the hazards separately would imply that the hurricane-induced winds were independent from the hurricane-induced flooding, and damage probabilities for each case would differ.

The risk map is displayed showing community (administration) boundaries so that people living in St. Martin are able to look at the map and determine their situation based on where they are living. Higher risk areas are shown in red and yellow and less risk areas are indicated in green. The map shows the Expected Annual Damage (EAD) value per year per pixel. This means that the colour a pixel is indicated by determines the expected losses for buildings within that pixel due to hurricane activity. Furthermore, these separations by community are useful for communication and governance within St. Martin. The map can be used, for example, to determine where disaster risk management is most needed on the island. The next section explains how to interpret the map in relation to disaster resilience and *Building Back Better*.

5.3. Building Back Better

Building Back Better involves three aspects according to Hallegatte et al. (2018). Each of these aspects should be considered when looking at St. Martin and determining how to increase disaster resilience for future hurricane events. Combining these three approaches after a disaster event could reduce disaster-related well-being losses up to almost 60% in small island states (Hallegatte et al., 2018), like St. Martin, who have high levels of vulnerability. The three aspects are explained below by looking specifically at the case of Hurricane Irma in St. Martin.

1. **Build back stronger**

   This involves reducing losses by ensuring that reconstructed infrastructure can resist more intense events in the future. In St. Martin this means looking at building codes and standards and comparing these to where wind and flood damages were experienced during Hurricane Irma. If building codes and standards are not strict enough these can be improved, and if they are, enforcement of these standards needs to be monitored. Improvement of infrastructure in terms of wind can mean strengthening of joints or strapping on roofs or using more resistant materials. In terms of flooding, buildings can be raised or reconstructed at higher elevations for example. According to Hallegatte et al. (2018) this can reduce overall well-being losses by up to 40%.

2. **Build back faster**

   This involves reducing disaster impact by accelerating reconstruction through preparation measures. This includes reconstruction plans, pre-approved contracts and financial arrangements. After Hurricane Irma, St. Martin struggled with this aspect of *Building Back Better*. Numerous sources (NOS, 2018b; NU, 2018; de Hamer, 2018; NOS, 2018a) reported that buildings had not been reconstructed more than one year after the event. This meant that buildings were not ready by the next hurricane season. Funds collected for disaster management have still not been fully redistributed. According to Hallegatte et al. (2018) well-being losses can be improved by up to 14 % when focusing on building back faster.

3. **Build back more inclusively**

   This involves ensuring that post-disaster support reaches all affected population groups. A documentary of Sint Maarten was made in the beginning of 2019 specifically looking at victims of Hurricane Irma, and their recovery after the disaster (NOS, 2019). Many people reported having to still live in broken down houses due to the fact that they were not able to rebuild themselves, and that financial support was not available due to their residential status on the island. Many low-income households exist on St. Martin, including informal settlements that are more vulnerable and exposed. Including these communities in reconstruction plans and financial aid can help reduced well-being losses up to 27% according to Hallegatte et al. (2018).

In this section we will look at the results of the risk assessment and determine how this type of assessment can be applied to disaster resilience in St. Martin. Different locations on the island are highlighted and discussed.

5.3.1. Application to St. Martin

In order to use the risk assessment, to improve disaster resilience, it has to be interpreted for the location of interest. In this case four locations are highlighted for St. Martin and discussed in terms of *Building Back Better*. Figure 5.7 shows the risk map of St. Martin and the areas chosen to examine. The capitals of the French half of the island (Marigot) and the Dutch Half of the island (Philipsburg) were chosen to highlight, as well as the airports on each half of the island, in Simpson Bay and Grand Case.

Figure 5.7: Risk map of St. Martin indicating the locations on the island used to elaborate on Building Back Better.

Philipsburg

Philipsburg is the capital of the Dutch half of the island and is an important tourist area. Figure 5.8 shows the area of Philipsburg, including the strip of land between the beach front and a salt pond, that includes a small island where people live. Along the beach front strip the risk due to hurricane activity is high. Many commercial buildings are located along this strip and they attract many tourists that visit the island. In this area wind and flood risk are important and therefore improving resilience would mean focusing on building back stronger. The options of building back faster and more inclusively can also be applied, however building back stronger is important due to the fact that businesses are likely to want to continue because of their prime location.

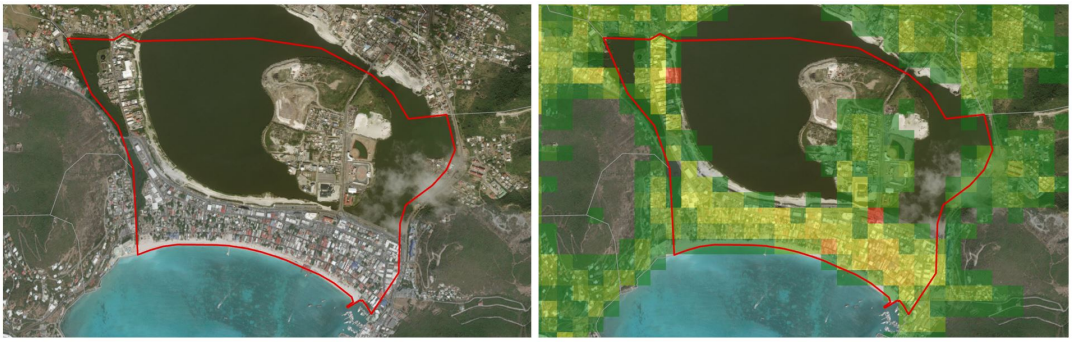

Figure 5.8: Aerial view of Philipsburg, Sint Maarten (right) and the hurricane risk for the area (left).

Figure 5.9 shows an aerial view of Philipsburg in pane 1 and the beach front of Philipsburg in pane 2. In pane 3 another factor to consider is shown, namely the dump site located on the island in the salt pond. As seen in Figure 5.8, risk exists on the island and therefore people located near the dump site are not only vulnerable to the toxic waste but also due to the hurricane risk on the small island. Spatial planning should consider these factors when deciding where to reconstruct after a hurricane event.

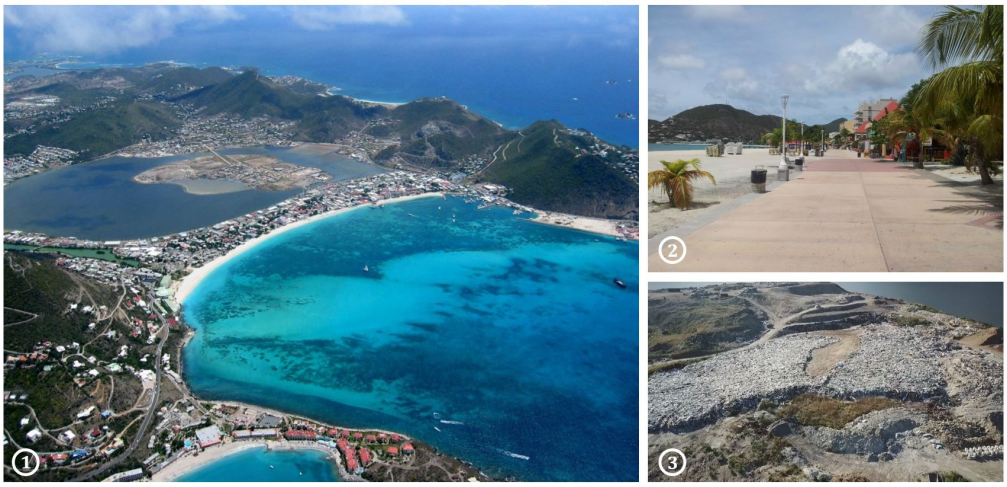

Figure 5.9: Pane 1: Aerial view of Philipsburg, Sint Maarten (Knipselkrant Curacao, 2017), Pane 2: Philipsburg Boulevard (Vermeulen, 2013), and Pane 3: Dump location on Pond Island (NOS, 2019).

Marigot

Marigot is the capital of the French half of the island and is an important tourist area, like Philipsburg for the Dutch half of the island. Furthermore, Marigot has an important ferry terminal located along the coastline, behind the sheltered marina, as shown in Figure 5.10. This marina is an example of one of the many flooded areas during Hurricane Irma that also experienced wind damage.

Figure 5.10: Aerial view of the ferry terminal in Marigot, Saint Martin (Multiverse, 2019).

.

The area where the marina is located, as well as the area behind the marina, is high risk when it comes to hurricane activity. Figure 5.11 shows the risk for Marigot, ranging from closer to the coastline, to quite far inland. Here too, the build back stronger approach can be considered as the ferry terminal and surrounding infrastructure is likely to remain in the same locations. As Marigot is quite low-lying, the majority of the area is at high risk and therefore the risk map shows the risk when reconstructing damaged buildings here. Spatial

planning in the future should consider these risk areas.

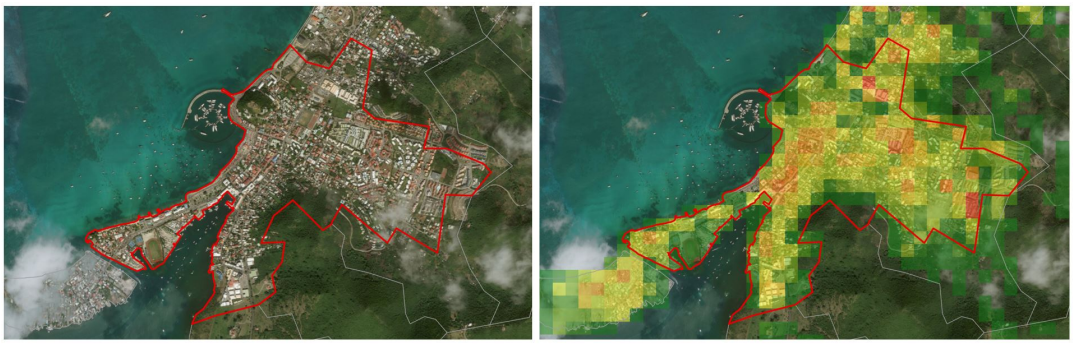

Figure 5.11: Aerial view of Marigot, Saint Martin (right) and the hurricane risk for the area (left).

Airports in Grand Case and Simpson Bay

The final areas that are highlighted are the two airports on the island, and the areas surrounding their runways. One airport is located on the French Half of the island and is known as Grand Case-Espérance Airport. An aerial view of the airport is shown in Figure 5.12 from a distance.

Figure 5.12: Aerial view of the Grand Case-Espérance Airport, Saint Martin (Wikimedia Commons, 2006).

From this aerial view we see how the runway is surrounded by water and separated by a strip of land from the ocean. The risk map for the airport is shown in Figure 5.13, and shows the high risk for the areas surrounding the airport. Building back stronger and faster are both applicable in this case as any damage hindering the airport will prevent an important transportation feature of the island. It is therefore important to restore functioning after a disaster event as quickly as possible. Having recovery plans for the airport is very important. This is also the case for the airport on the Dutch half of the island, Princess Juliana Airport, shown in Figure 5.14. Here it is also clear that the runway and airport facilities are close to the coastline and therefore at risk to both coastal flooding and wind damages. It is therefore equally important that if damages do occur, that reconstruction focuses on these and aims to improve where standards where possible, focusing on both wind and flood impact.

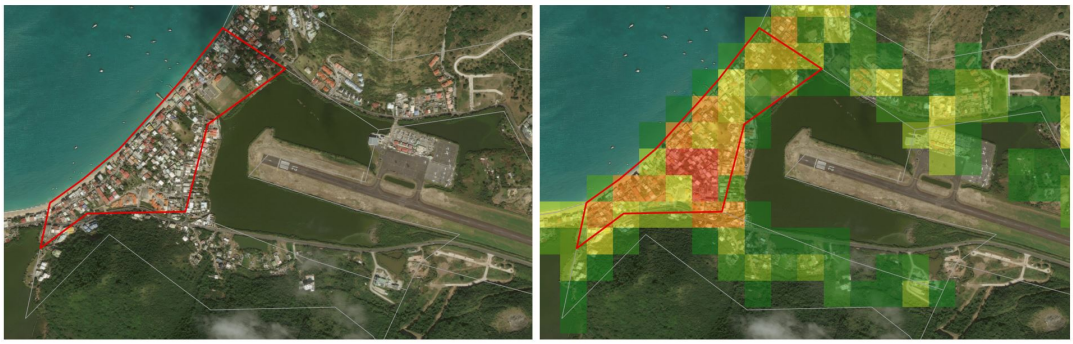

Figure 5.13: Aerial view of Grand Case, Saint Martin (right) and the hurricane risk for the area (left).

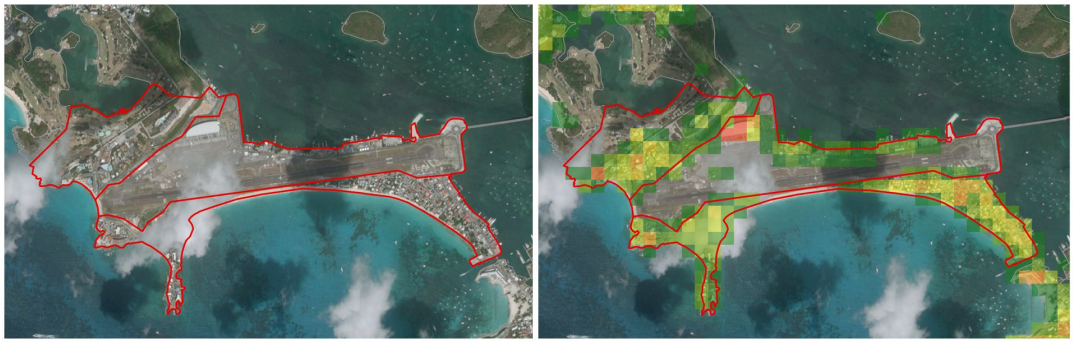

Figure 5.14: Aerial view of Simpson Bay, Sint Maarten (right) and the hurricane risk for the area (left).

Princess Juliana airport is shown in Figure 5.15 where the airport is shown shortly after Hurricane Irma hit, and an aerial view showing the runway and surrounding areas is also shown. The vulnerability of these airports are reflected in their respective risk maps, and therefore should be focal points when determining how to build back better. Infrastructure and buildings that are important for the connection of the island to the outside world are essential and plans should be put in place for if these places are hit hard.

Figure 5.15: Left: View of Princess Juliana Airport shortly after Hurricane Irma (Ferlise, 2017). Right: Aerial view of Princess Juliana Airport, Sint Maarten (Your Flight Reviews, 2016).

Besides the highlighted areas discussed above the rest of St. Martin is also at risk to hurricane activity. The extent of the risk differs around the island however it is clear that in order to prepare for the future hurricane seasons a building back better approach can be useful. This approach looks at putting measures into place to reduce vulnerability and risk in high risk areas. In terms of building back stronger this can be in the form of spatial planning and deciding not to rebuild in high risk areas if not essential. If building in high risk areas

is necessary, then plans can be put into place regarding evacuation and preparation when extreme events do occur. Another option is to improve the building standards to include flooding and wind damage norms (Hallegatte et al., 2018).

Building back faster can also be applied in St. Martin. Communication between the two sides of the island, and their international alliances is vital. Co-ordination of recovery and humanitarian aid can be discussed before hand to clarify which agencies are responsible for what. Furthermore, the regulations for the distribution of the financial aid should be discussed and set up in a way that funds become available immediately when needed. Building back more inclusively should be approached in the same way. Plans to help the more vulnerable communities should be put into place beforehand, as it should be expected that these will be hit hardest when extreme events occur. Setting up large and flexible registries that include beneficiaries and contingency plans is an example of how this could be done. Another example is providing affordable financial solutions or mobile money accounts for unbanked adults (Hallegatte et al., 2018).

The risks identified in this study are meant to ignite discussion around St. Martin and disaster resilience. Decision makers can look at the island and determine where focus should be applied based on their local knowledge, such as GDP distribution, which is not easily available to the public. Relocation of industry and residents if possible, and rebuilding stronger when relocation is not an option. All these aspects should be considered when aiming to improve disaster resilience in St. Martin.

6

Discussion

The following chapter is a discussion of the methodology and risk assessment that make up the results of this research. The first aspect of discussion in the flood model sensitivity in Section 6.1. Here the influence of uncertainty in wave setup estimation is explored along with aspects not included when applying a static approach to calculate overland flooding. The limitations of the flood model are also discussed. The second aspect covered is the wind interaction and how wind speeds were modelled for the risk assessment in Section 6.2. The discussion of open-ocean wind speeds versus over-land wind speeds in damages estimation is explored, and the limitations of the model used in this research are discussed. The third aspect to consider, is data scarcity and the role it plays in steering the choices for modelling and managing expectations. Section 6.3 looks specifically at the role data played and how to deal with situations where modelling numerous scenarios may not be possible. The example of fitting the modelled water level data is used. Finally, the application to risk in general is discussed in Section 6.4.

6.1. Flood model Sensitivity

When simulating hurricane-induced flooding, ideally all processes that contribute to flooding are modelled, namely; storm surge, tides, waves and rainfall. This means the inland flooding model would be forced with coastal water levels due these components, as well as a rainfall component that is correlated to the hurricane track. Modelling all of these processes however, requires a significant amount of computational effort and the accuracy of the results are only as reliable as the input of the model. This input is comprised of the topographic data of the island, a rainfall time-series and water level time-series during the hurricane event. In this research the coastal model was limited to simulating coastal flow dynamics, and did not include wave transformation and reef interaction. The inland flood model was limited to using coastal levels as a static inundation to determine flooding. No rainfall or interaction with inland waterways was included. The limitations of these two aspects are discussed here.

6.1.1. Hydrodynamics and Reef Interaction

The static "bathtub" approach was used to estimate flooding on St. Martin. Wave influence was therefore only included by estimating wave setup at the coastline. This was done by first using a parametric model relating hurricane wind speed to maximum offshore wave height (I. Young, 1988). The wave setup at the coastline was then estimated by assuming a percentage of the significant wave height at the breaker zone. In reality however, wave transformation and wave setup depend on many factors, such as local bathymetry and the spatially varying hurricane-induced wind speeds.

As St. Martin is a reef island, storm surge is mainly pressure induced and not predominantly wind-driven. Wind-driven surge is dependent on the shallowness and width of the continental shelf, therefore for large, shallow shelf's, with large fetches, the wind-driven storm surge to given space and time to develop. St. Martin on the other hand, is located on the Caribbean shelf where the slope is steep, and the shelf space does not allow for this wind-driven surge to develop fully. This therefore, limits the wind-driven surge. Furthermore, the coastline is not long and smooth, like the North American coastline for example, and wind driven surge has no room to pile up. Both these facts mean that storm surge is relevant but does not dominate coastal flooding and wind generated waves cannot be neglected. A coupled flow and wave model was set up in Delft3D to determine what contribution waves had when simulating water levels induced by Hurricane Irma. Figure 6.1 shows a time series comparing the water level at the coast calculated using a coupled model, versus a flow only model. Here we see that waves are significant compared to storm surge and therefore cannot be excluded for a flood assessment in St. Martin.

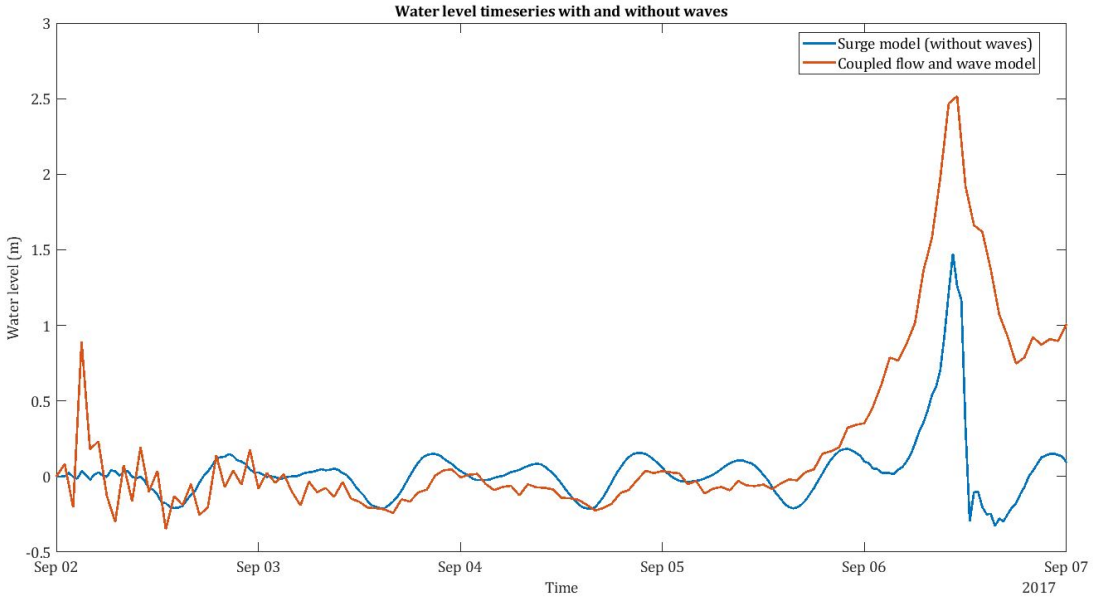

Figure 6.1: Water levels during the hurricane event of Hurricane Irma for a coastal model (Delft3D) including waves and a model only including flow.

When considering the influence of wave-induced flooding on St. Martin, the interaction with the surrounding reef system has to also be considered. The reef system around the island (see Section 3.1) shows that not only that reefs exist along the coast, but that waves will interact with the reefs differently, depending on where you are around the island. Along the Eastern coastline of St. Martin there is a system of shallow reef bars that will influence the wave climate and setup at the coastline. The beach slope at the coast also affects the wave setup at the shoreline, and therefore is an important factor when calculating inland flooding (Pearson, 2016). Furthermore, reef environments dissipate wave energy due to the friction provided by the coral, sand and grassy environment often present on the reef. This too influences the wave setup and therefore can be overestimated when using a parametric model like that of I. Young (1988) and assuming a percentage as setup.

As discussed, the wave setup is important for simulating coastal flooding on St. Martin. This is due to the fact that waves are not insignificant when compared to storm surge as the interaction between the waves and the bathymetry (reef system) induces significant water levels. A sensitivity analysis was done to determine the influence of the wave setup estimate made during this research. Furthermore, the influence of varying wave heights around the island was also done, as during the research wave setup was assumed to be constant around the island. As seen Figure 6.2 this is not the case. This figure is based on a study by Duvat et al. (2019) on Hurricane Irma in St. Martin. The figure shows the variation in wave height around the island of St. Martin, which makes it clear that waves, and wave setup around the island are not uniform.

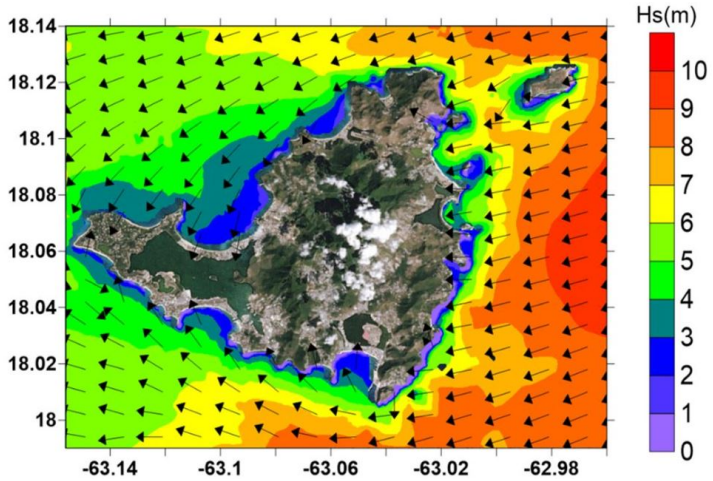

Figure 6.2: Significant wave heights around the island of St. Martin for Hurricane Irma (Duvat et al., 2019).

Four cases were considered in the sensitivity analysis for St. Martin. The first three cases considered different assumptions for the amount of wave setup at the coastline. In the modelling done for all the hurricane scenarios, wave setup was assumed to be 20% of the wave height in the surf zone. This is considered as the base case, with which all the sensitivity cases were compared. Cases assuming 5%, 10% and 30% were compared to the base case. The fourth case was to determine the influence of including varying wave heights around the island based on the results of the study by Duvat et al. (2019). In this case 20% setup was assumed and compared to the base case. Table 6.1 shows the results of the sensitivity analysis. Two indicators were used to compare the cases. The first was the number of flooded cells, and the second was the total damages as calculated by the impact model setup during the research.

Table 6.1: Sensitivity Analysis results for including different wave setup values in the static approach model for Hurricane Irma. Total number of cells in the flood model is 11,659.

Case	# Flooded Cells	Flood Damages (million $)
Base	608	54.5
5% setup	333	23.0
10% setup	402	28.5
30% setup	732	77.5
varied wave heights	514	36.8

The number of flooded cells was used as an indicator to determine how many cells were flooded compared to the base case. This is important because the flood vulnerability functions are concave down and therefore the first few meters of flooding are significant in the amount of damage. The second indicator was the amount of flood damage, as this was the end goal of the model setup. From the results it is clear that the estimation of wave-induced flooding plays a significant role is damage estimation. The difference between the base case and an estimation of half the wave setup produces a difference in flood damages of around 26 million dollars. This means compared to wind damages the percentage of flood damages is only 1% compared to the 2% of the base case. This is the same for the case of an increased estimate of wave setup of 30%. Here total damages reach over 77 million dollars and bring percentage of flood damage up to 3%. The influence of wave setup on flood damages is in the order of 10's of millions of dollars, however compared to total damages due to wind and flooding it only varies between 1% to 3%.

This is also confirmed when looking at varying wave heights around the island. Compared to the base case we see lower flood damages indicated possible overestimation when not modelled the wave transformation and reef interaction. In the case of varying wave heights, the number of flooded elements differs by less than 100 cells, however total damages differ with around 18 million dollars. This sensitivity analysis shows the influence of wave setup, and its significance in determining flood damages. It also shows however, that this change reflects as only a couple percent compared to total damages.

6.1.2. Rainfall

When simulating inland flooding due to hurricanes, an important factor to consider in the rainfall a hurricane brings with it. In this case a static "bathtub" approach was used to simulate inland flooding and therefore the influence of rainfall on flooding depths was not included. When modelling rainfall there are two factors that need to be considered. Firstly, the data regarding historical rainfall due to hurricanes for the location of interest, and secondly, the overland modelling of run off and inland waterways, and their interaction with the coastal flooding event.

When combining coastal-induced flooding and rainfall-induced flooding, the question of compound flooding arises, as these processes are both linked to the hurricane event in question. Compound flooding refers to the combination of high sea levels and extreme rainfall and inland flooding. If the two processes magnify one another, and induce flooding that previously may not have been a problem, compound flooding should be considered. Figure 6.3 shows the time series of rainfall versus storm surge for the case of Hurricane Irma, based on hind-cast modelling results of Irma (Leijnse, 2018). There is a time difference as to when each of these processes occur however, they overlap and therefore the effect of compound flooding has to be taken into account. This means that when modelling rainfall, it cannot simply be added to the model without further investigation into the dynamic processes involved. In this case, rainfall was therefore not included due to the simplified model choice and the data scarcity limiting the inland modelling possibilities.

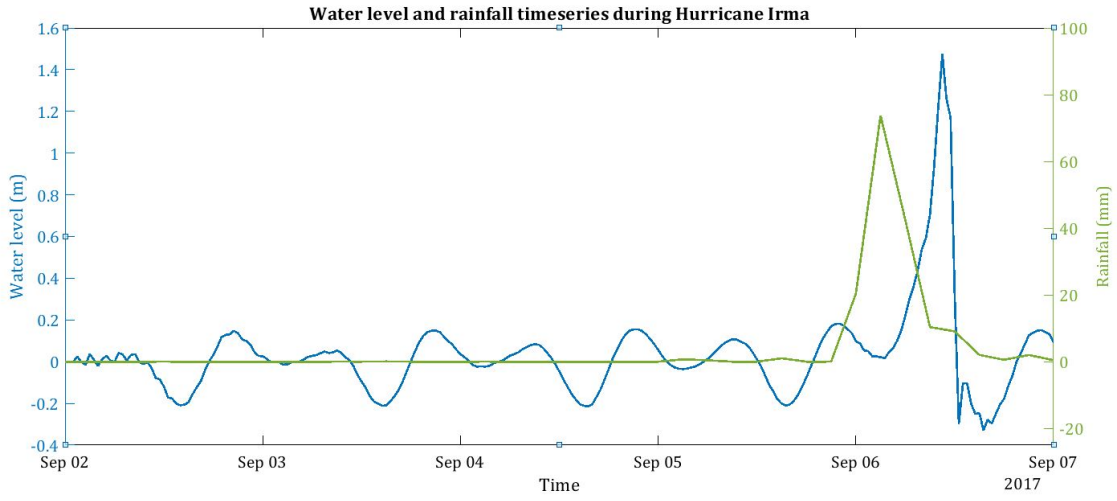

Figure 6.3: Rainfall and surge levels during the hurricane event of Hurricane Irma modelled in Delft3D.

The second problem with modelling synthetic hurricane tracks for St. Martin, is the lack of historical rainfall data due to hurricane events. Synthetic rainfall data is therefore also needed in order to model inland flooding due to rainfall. Parametric models exist that relate hurricane characteristics to rainfall quantities. One of these models is the parametric model by Snaiki and Wu (2017), which uses the hurricane maximum sustained wind speed, translation speed and central pressure of the hurricane to determine the expected rainfall rate. The outcome of the parametric model is a spatial rainfall for each time step of the hurricane, derived from the wind speed characteristics. This can be implemented into a more advanced hydrodynamic model to model rainfall runoff and infiltration for the location of interest by creating a rainfall time series based on the wind during a hurricane event. In this research the static approach was not able to model the physics involved when including rainfall. Using a more advanced model is able to simulate these processes however, information regarding runoff, infiltration and rivers on the island is also limited or not publicly available. Estimating rainfall flooding therefore also remains difficult to validate.

6.1.3. Limitations

The limitations of the flooding approach are summarised here. Firstly, the static "bathtub" approach used to determine *flood modelling*, is a simplification when it comes to the hydrodynamics involved in hurricane-induced flooding. It assumes that the coastal water level is static, and inundates land below the forcing level. Furthermore, the coastal water levels that provided boundary conditions to the bathtub model, were based on flow simulations and not coupled to wave processes. The wave setup was estimated using a parameter-sation, and was added to the storm surge levels. The static approach was conservative in estimating coastal flooding, as it does not take wave attenuation, velocities and complex processes into account. It was not conservative in estimating the influence of wind inland, as it does not model the physics of wind setup inland. It also excluded the dynamics of rainfall and compound flooding.

The second limitation is the application of the wave setup estimation. The *wave parametrisation* by I. Young (1988) is only appropriate for waves in the direction of the hurricane path and movement. The equivalent fetch is based on the difference between the hurricane translation speed and the group velocity of the waves and only applies to waves moving in the same direction as the hurricane. This means that when applying the parameterisation, the wave heights are only applicable to locations directly in the path of the hurricane, and therefore, waves and wave height at specific locations is vaguer. The parameterisation was therefore only used to estimate extreme maximum wave conditions offshore (Hoek, 2017), and is conservative in estimating wave heights, assuming waves travelling in the direction of the storm are the largest induced waves.

6.2. Wind interaction

The wind speeds used to determine the wind damages due to a hurricane, were the wind speeds over the open ocean. These are different to those experienced inland, due to the local topographic conditions, especially on islands like St. Martin, where elevations reach 415 m in the centre of the island where a mountain is situated. Figure 6.4 shows the modelled wind speeds based on the open ocean 10 m wind speeds, where the wind speed is taken as the maximum wind speed during the simulation. Here the wind speeds are calculated as if there is no height variation where the island is located compared to the open ocean. In the figure the wind speed map is fairly uniform with wind speeds ranging from 240 km/h to 270 km/h. This small variation is due to the fact the topography has not been included and therefore the interaction of the wind and the land form of St. Martin is not captured.

Figure 6.5 shows the variation in wind speed around the island when a physical model is used to calculate wind speeds. These are the results from a study done on St. Martin to simulate the actual wind speeds experienced during Hurricane Irma on land (Duvat et al., 2019). In the figure depressions and peaks of wind speeds can be seen. One of the most noticeable is the dark blue depression of a sheltered area on the French half of the island. The wind speeds are no longer uniforms with small variation. Here the differences in wind speeds around the island are in the order of tens to hundreds of km/h. The difference between included the topographic effects and the open ocean wind speeds show that the open ocean wind speeds overestimate wind speeds by up to 100 km/h (30 m/s) in sheltered areas. In order to determine how this variation translates to wind damage, and therefore risk, a sensitivity analysis was done. This is similar to the analysis done for wave setup.

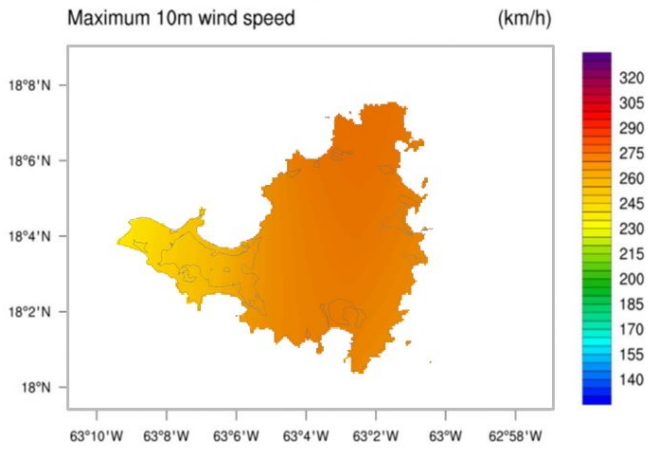

Figure 6.4: Wind speeds modelled using the open ocean 10 m elevation wind speed for the island of St. Martin for Hurricane Irma.

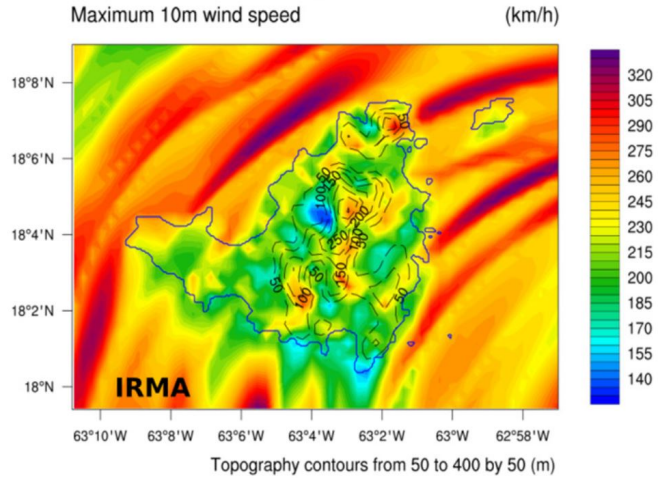

Figure 6.5: Wind speeds modelled using a physical wind model for the island of St. Martin for Hurricane Irma (Duvat et al., 2019).

The sensitivity analysis for the influence of error in wind estimation was done for a situation where the depressions, found in the study by Duvat et al. (2019), were included in the damage calculation. Table 6.2 shows the results compared to the base case. Two cases including depressions were calculated, firstly a more conservative calculation where depressions of 176 km/h were included, and secondly, a more realistic value of 200 km/h was included. In the base case wind damages totalled around 2.6 billion dollars, and wind speeds were based upon the open ocean 10 m elevation wind speeds. This shows the importance of wind estimation, and in turn damages based on these wind speeds. Including depressions shows a reduction in wind damages of 19 % in the case of the conservative calculation, and 13% in the more realistic calculation.

Table 6.2: Sensitivity Analysis results for including wind depressions according to the study by Duvat et al. (2019).

Case	Wind Damages (billion $)
Base	2.6
Depressions (176 km/h)	2.1
Depressions (200 km/h)	2.25

From the sensitivity analysis it is clear that the estimation of wind speeds has a far larger influence on total damages than the estimation in flooding levels. Here we see overestimation in damages between 13% and 19%.

6.2.1. Limitations

The wind modelling was based on the open ocean wind speeds at 10 m elevation, and therefore did not take into account the effect of topography over the island. Sheltered areas were therefore overestimated when it came to wind speeds inland, and therefore, also for damages. A sensitivity analysis shows that overestimation of damages are in the order of 10% to 20%. The overestimation in damages is especially amplified in very high wind speeds due to the shape of the vulnerability function. Only for wind speeds exceeding around 230 km/h (65 m/s) do these large overestimations occur. Generally, the exceedance probabilities of these wind speeds are much lower and therefore the overestimation in risk is lower than the overestimation in damages.

The influence of the physical wind processes are not therefore modelled in this approach. These models are too computationally expensive and depend on the detail of data available for the area of interest. Wind damages form a large part of the total damages due to Hurricane Irma, and consequently to the total risk on St. Martin. It is therefore important to note the overestimation involved in the wind modelling and what it means for the total risk outcome. These results are intended to identify risk prone areas and the exact monetary values associated with this are meant to be indications of the order of damages and risk involved.

6.3. Data Scarcity

Data scarcity played a central role to this research, and it is therefore important to identify how the research was influenced by it. The most important limitation of hazard and impact modelling is discussed in this section. Furthermore, investigation in how to deal with time constraints and a lack of data is explored by looking at fitted distributions for the exceedance probabilities of the coastal water levels. The investigation into these fitted distributions was twofold. Firstly, analysis of the coastal water levels around the island was done to determine if the empirical relationships of each flooding basin, for which probabilities were defined, were the same. In this way we determine whether the same distribution is applicable around the entire coastline of St. Martin. The second reason is to determine what distributions can be applied when modelling of coastal water levels is not possible. Future studies on the island can use the fitted distributions as a boundary condition when performing more detailed probability analyses.

6.3.1. Modelling Limitations

The data used in the risk assessment for St. Martin included various sources of bathymetry data, topographic data and exposure data for the island. Bathymetry data was improved to an acceptable level for modelling the complex hydrodynamics of the island however, the same could not be done for the topographic data. This, combined with the computational time constraints when performing a risk assessment, resulted in the choice of a static approach to model flooding in St. Martin. An improvement in topographic data could improve the estimation of flooding significantly, and outweighs the improvement that a detailed model, that resolves all processes, would provide. The computational effort needed to solve all the processes involved in hurricane-induced flooding was therefore not feasible if compared to the accuracy of the global elevation data.

Damages, and therefore risk, were determined by regarding physical damages only, or more specifically building damage. A complete risk assessment should include looking at indirect and intrinsic damages due to a hurricane as well. Examples of these include reputation damages, unemployment, injuries, and social disruption. These types of damages are very difficult to quantify. The exposure data available for the island only included information on building structures, their use and their construction material. Furthermore, the missing exposure data for buildings on the island was assumed to be the same as other known buildings on the island. Therefore the assumption was made that construction methods and buildings for the French half of the island and the Dutch half of the island were the same. Application of the vulnerability functions for wind speeds also were based on the assumption that the buildings built on St. Martin were built under the same standard as in Puerto Rico, another Caribbean island.

Building damages were further limited to include only wind damage and coastal flood damage. The hydrodynamic analysis done on St. Martin shows that waves and flow velocities play a major role during hurricane events. Relationships between waves and flow velocities to building damage were not investigated during this risk assessment however this does not mean they are not relevant. This means that the flood damages are conservative in terms of flood depth however, do not include the dynamic effects of wave damage.

6.3.2. Fitted distributions

The damage probabilities used in the risk assessment for the island of St. Martin were based on the empirical relationship found for the coastal water levels and their exceedance probabilities. The empirical distribution of these water levels are explored to determine which distribution best fits the modelled water levels, and whether the water levels around the island all follow the same distribution. The aim is to provide information of the coastal water levels for future studies on the island, and to comment on how the distributions vary for each flooding basin defined for St. Martin.

The water levels were fitted with nine distributions to determine which represented the data the best. The results of this analysis can be used when synthetic data is not available and a choice for a distribution should be made. The distributions chosen to evaluate were the Extreme Value, Gamma, Generalised Extreme Value, Kernel, Logistic, Normal, Rayleigh, Stable and t-location Stable (Jonkman et al., 2017). Figure 6.6 shows the modelled data and the tested distributions and how they fit compared to the modelled values. The figure shows the probability density functions according to each formulation, and these are explained in detail in Appendix B. Important to note is that the figures here represent one flood basin (basin 1 in Figure 4.14) for illustration purposes. The evaluation however was done for all flood basins.

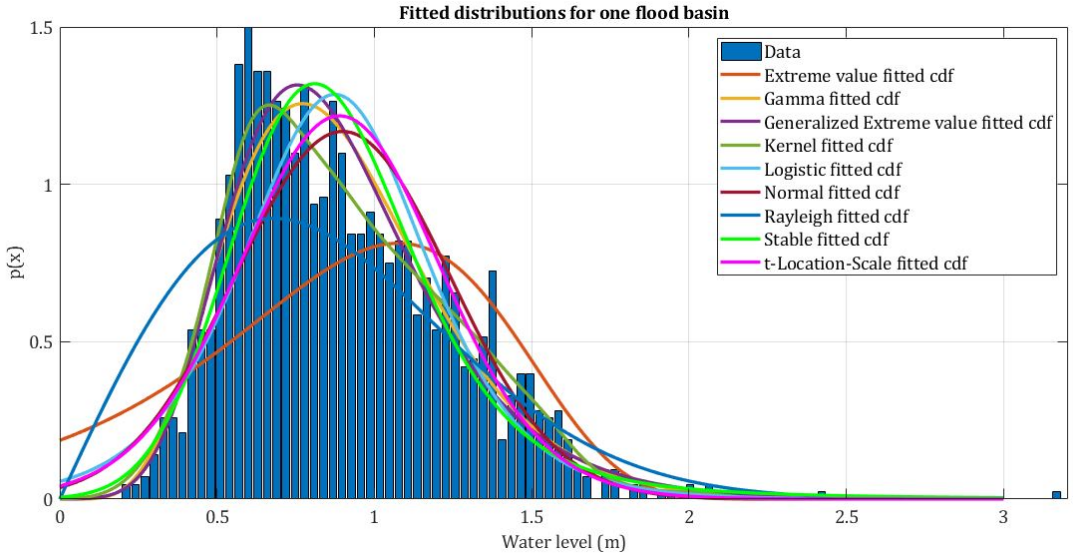

Figure 6.6: Fitted distributions for the probability density distributions for hurricane-induced water levels on the island of St. Martin.

In Figure 6.6 the shape of each distribution is shown compared to the modelled data. In all cases the peak of the modelled data is not reached, however some distributions seem to capture this more than others. When choosing a distribution as a representation it is important as to what part of the data should be represented most accurately. If the extreme values are important, as for performing a risk assessment, then representing the peak in the data is not as important as the higher water level (tail) values.

The cumulative distributions of the different formulations were fitted to the modelled data and are shown in Figure 6.7. This too is an example of one flood basin however the same processed was followed for each basin. From Figure 6.7 it is already clear that certain formulations perform better than others when representing the data. The extreme Value distribution for example does not seem to follow the data as closely, especially for the lower water levels.

These differences become even more apparent when the distributions are shown as probability of exceedance curves in Figure 6.8. In the figure the distributions follow the data quite well, however for the higher water levels, with lower exceedance probabilities, large differences occur. The best fit distribution is therefore highly influenced by the instances of high water levels. These are not as frequent as the lower water levels and therefore uncertainty exists.

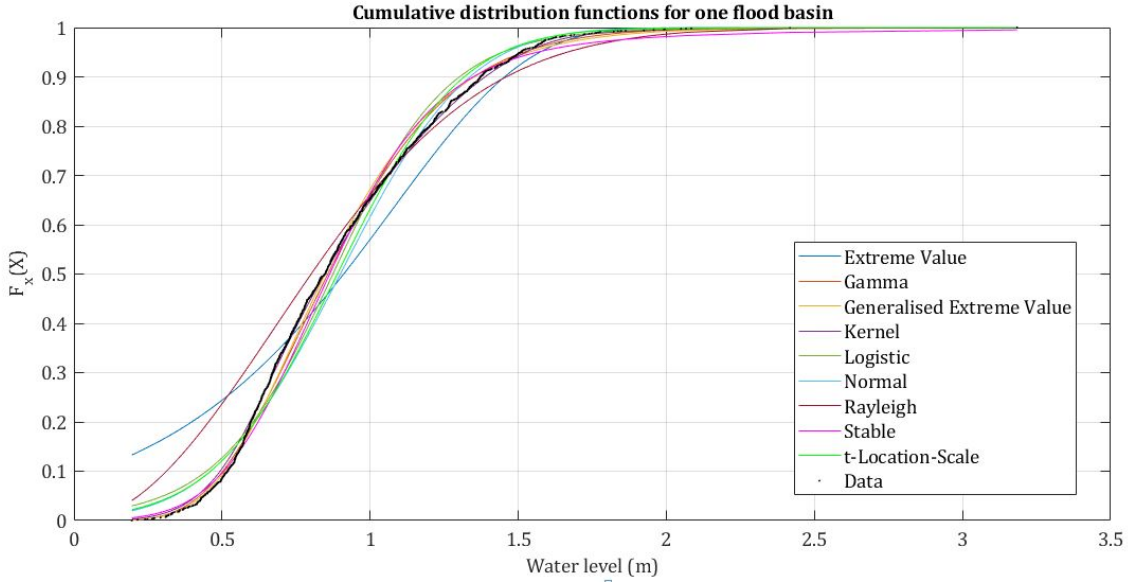

Figure 6.7: Fitted distributions for the cumulative density distribution for hurricane-induced water levels on the island of St. Martin for one of the flood basins.

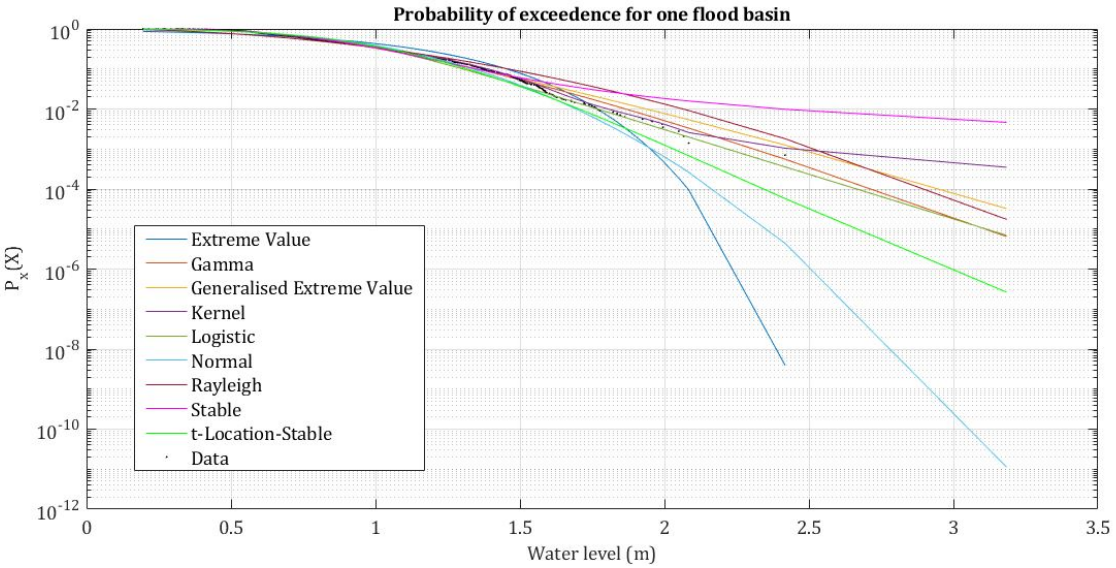

Figure 6.8: Fitted distributions for the probability of exceedance for hurricane-induced water levels on the island of St. Martin for one of the flood basins.

In order to determine which distribution best represents the data, various tests can be done. In this case the "goodness of fit"test was performed as well as the Quantile to Quantile plot. Based on the results for all the flooding basins a choice was made on the best representative distribution.

The first test was determining the "goodness of fit", where the normalised root mean square is determined for the difference between the modelled water levels and the predicted water levels of the distribution. Table 6.3 shows an example of the results for one of the flooding basins, where NMSE is the Normalised Mean Squared Error and NRMSE is the Normalised Root Mean Square Error. Values closer to 1 indicate a better fit overall however, it is also important, when considering a distribution, where these errors are, and which water levels are important to fit accurately. In this case the best fit is represented by the Kernel distribution, as was the case for all the other flood basins.

Table 6.3: Fitted distributions and their respective fit against the empirical distribution of the water levels.

Distribution	NRMSE	NMSE
Extreme value	0.62	0.845
Gamma	0.93	0.994
Generalised Extreme	0.93	0.995
Kernel	0.97	0.998
Logistic	0.87	0.983
Normal	0.84	0.977
Rayleigh	0.68	0.895
Stable	0.90	0.990
t-location	0.86	0.980

The reason the Quantile to Quantile test was also done was to determine which distributions fit which part of the data the best. The test determines how the distribution represents the data for the different quantiles (low, mean and high values), and shows how these are represented by each distribution.

Figure 6.9 shows the results of the Quantile to Quantile test of the fitted data versus the empirical data. A perfect fit would show the data to lie along the line where y is equal to x (indicated by the dashed line). Here we see that the extreme value, logistic, normal, and t-location distributions drift away from the ideal line for estimating the lower tail water levels, as well as for the higher tail water levels. The stable fit also does not estimate the higher tail water level values well. The Gamma, Generalised Extreme Value, Kernel and Rayleigh distributions perform much better when estimating the distribution for each quantile, especially for the higher tail end values. When performing a risk assessment this is important as the extreme conditions have to be represented well. From the analysis, the Kernel distribution performs the best in predicting the distributions for the extreme coastal water levels. This was the case for all flood basins.

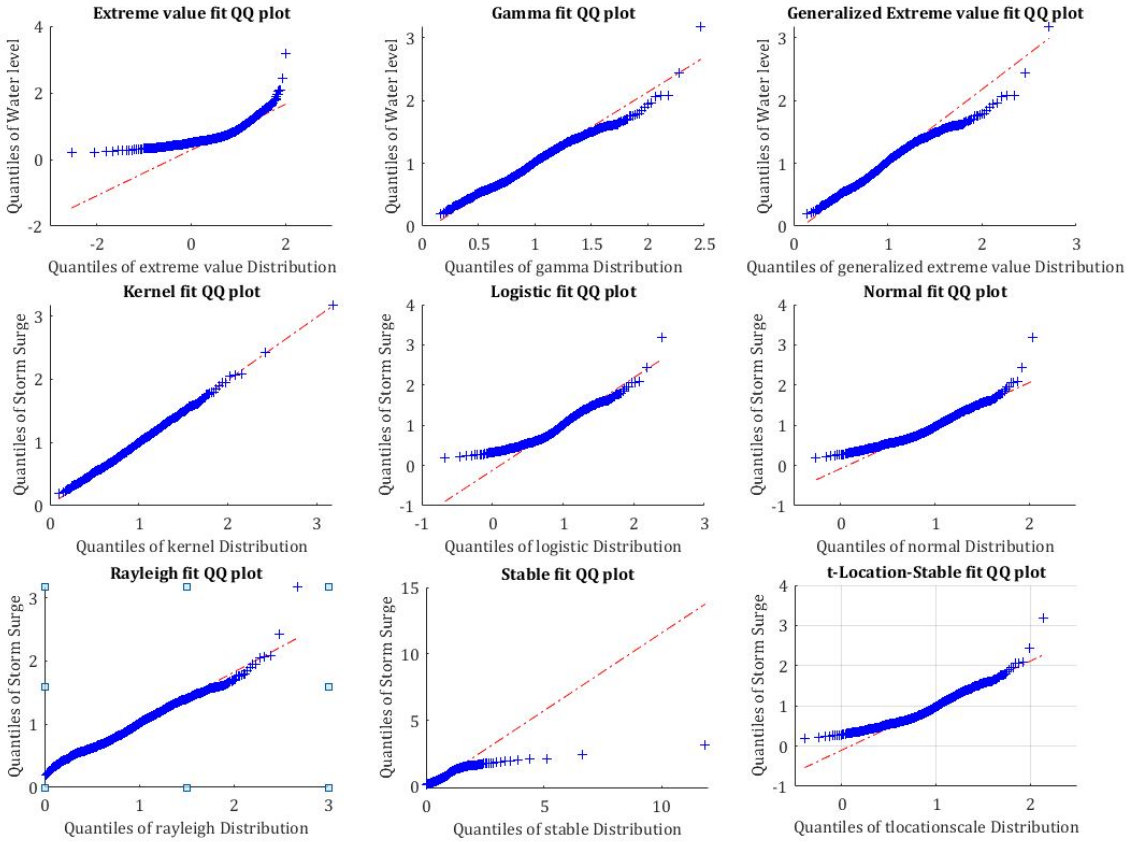

Figure 6.9: Quantile plots for the tested distributions for the hurricane-induced water levels.

6.4. Application to Risk

The intention of the proposed methodology is that it can be applied to a location of interest to determine the hurricane risk, and determine where to focus resources for recovery and measure to improve disaster resilience. The extension of the research is that the methodology was applied to a data scarce area, and therefore the proposed modelling and methods are also applicable in cases where extensive input and validation data is not available. In this way, the *Build Back Better* (Hallegatte et al., 2018) approach can be implemented based on the outcome of applying this methodology. For disaster risk management this means using the results to improve disaster resilience.

The general application of the risk map is identifying high risk areas, and based on these, determine the best strategy to improve disaster resilience. These results specifically highlight vulnerabilities due to building infrastructure, and therefore, this should be the main focus in improving resilience based on these results. This can be done by introducing measures to increase resilience of physical assets being reconstructed, for example by revisiting building regulations (GFDRR, 2017). For flood prone areas this can be done by including floor elevations and for wind prone areas, including roof strapping or resistant building materials. Spatial planning can be discussed for communities where changes can be made, and these cases high risk areas can be avoided for reconstruction. In cases where this is not possible, evacuation and disaster recovery plans can be drawn up for the vulnerable communities.

When applying the proposed methodology there are limitations which need to be considered, and these can be divided into two main aspects. The first is in terms of uncertainty due to the data input, and the second is due to the uncertainty in the methodology. Improvements in these uncertainties will improve the overall certainty of the outcome.

6.4.1. Limitations

Data scarcity was one of the main challenges for applying the methodology presented in this research. Uncertainties presented themselves in the topography and bathymetry during the hazard modelling, and in the exposure data and vulnerability relationships in the impact modelling. The overland topography resolution dictated the resolution of the flooding model and produced uncertainty in the flooding estimations for the island. Uncertainty in bathymetry data, due to the digitisation of navigational charts, influences the coastal storm surge levels modelled for St. Martin. These water levels are used as boundary conditions for flooding over the island and therefore, these uncertainties are carried over to flooding depths. The order of magnitude of the boundary conditions are however, satisfactory for flood risk assessment modelling. When modelling more detailed processes, an improvement of bathymetry and topography data is essential. Validation of the models were also limited due to the observational and historical data on the island. More validation data will mean that more complex models can be modelled when data is available to validate, for example rainfall and inland waterway flood modelling. Data scarcity in exposure data also produced uncertainty in the impact modelling, as assumptions had to be made about the distribution and structural integrity of buildings on the island. This data in turn dictated the vulnerability functions used in the impact model which could only be as detailed as the exposure data was. This meant that the magnitude of damages was of the right order, as validated by looking as damages assessments done for Hurricane Irma, however uncertainty exists in the exact damages, per household for example.

The uncertainty due to the proposed method exists in the hazard and impact modelling, as well as the probabilistic analysis and risk assessment. The hazard modelling was focused on two aspects, namely wind modelling and coastal flooding. The method to determine wind hazard on St. Martin was based on open-ocean wind speeds and therefore uncertainty exists in the overestimation of the wind speeds. In the same way, coastal flooding was determined using a wave parametrisation for the coastal water levels and a static approach for inland flooding. Both these contribute to the uncertainty for final flooding level which are also conservative. These approaches are simplified and therefore do not capture more dynamic processes, which means funnelling of wind speeds, sheltered areas, and wind-induced inland setup are among the processes not captured. Similarly, uncertainty in the damage estimation exists as the vulnerability relationships are assumed to be static. This means that damages do not change over time, and therefore this method of impact modelling does not capture variation or amplification in time. Lastly, the method used to estimate risk for hurricane activity was based on assumptions that too, bring uncertainty with them. The main assumption made, is that the wind and flooding impacts are linearly related and do not interact with each other in

terms of amplification. This means that the combination of the respective damages does not include any non-linearity's that may exist.

Both these aspects contribute to the total uncertainty presented in the results for the case study of St. Martin. The outcome of the proposed methodology is therefore a risk assessment of the island due to hurricane-induced winds and flooding. Uncertainties exist due to the data input as well as the methodology used which in some cases, was steered by the data availability. The outcome however, represents that ratio of wind and coastal flood damage well and highlight high risk areas in St. Martin. The application of this methodology should therefore be used to determine the order of magnitude of hurricane-induced hazard and damage, and the ratio of these to one another. Furthermore, the final result of the risk map should be used in igniting discussion around disaster risk management to improve disaster resilient of the area of interest.


Tropical
Tropical
HANJIN
APL
CMA CGM
MAERSK
Tropical

7

Conclusions

The following chapter summarises the conclusions of this research by relating them back to the main research questions, and describing where opportunities for future research lie. Section 7.1 looks specifically at the improvements and clarifications of the proposed methodology to determine hurricane risk. Findings for each step of the methodology are described. The application to the island of St. Martin is also summarised according to the findings regarding the boundary conditions to delineate hurricane risk. Section 7.2 describes recommendations for future work and improvements based on the discussion points of the methodology and application. The subjects highlighted included data set improvement, physical wind modelling, parametric wave studies, and synthetic rainfall modelling.

7.1. Key Findings

The key findings of the research are summarised in this section by referring back to the original research questions. Answering these two questions resulted in the main research objective which was:

"To set up a framework for determining multi-hazard risks due to hurricane activity, as a basis for triggering decision making on disaster resilience, using the island of St. Martin as a case study".

Research Question 1:

What improvements, and clarifications, can be made to the existing methodology for determining multi-hazard risk due to hurricane activity?

The existing methodology for determining multi-hazard risk was used to define six steps that represent the steps used to arrive at hurricane risk for the location of interest. Each of these steps are clarified below in terms of process and input, and improvements were determined by applying the steps to the data scarce region of St. Martin. The biggest improvement therefore is the clarification, and the applicability to regions where data availability is limited. The improvement in each step is described below and forms the final methodology for a multi-hazard risk assessment. The first three steps form the first phase of the assessment, and the last three steps form the second phase of the assessment.

1. **Hazard Model Setup and Validation**

   Based on the hazards of interest, the corresponding hazard models should be set up. When calculating wind and flood hazard in data scarce regions often a simplified model is useful as the computational requirements are low and it is not necessary to solve for complex processes while data input quality is low. Digitisation of public navigation and/or topographic maps can be used to improve public data sets of low resolution. The complexity of the model is dependent on the time constraints and the data input. Furthermore, the data availability, as well as the number of required simulations, steers the choices of model requirements. The innovation applied in this research for this step, was using unconventional sources to improve input data and validate the flooding model. Online sources, such as Twitter, we used to determine flooding depths experienced during the hurricane event, and were used to validate flooding estimations. This can be applied to simple models, such as those used in this research, but can also be used for more complex models, when validation data is scarce.

2. **Hazard Vulnerability**

   Vulnerability relationships are determined based on site-specific information such as exposure data. Existing relationships can be used that have been specifically developed for the location of interest. If these are not available, relationships based on surrounding areas with similar exposure can be used. When selecting vulnerability relationships, often the type of exposure data that is available, will steer which ones should be used. When exposure data is limited, assumptions can be made based on surrounding regions or pockets of data available for the area of interest.

3. **Impact Modelling and Validation**

   The impact models use the hazard maps, exposure data and vulnerability relationships as input, and therefore, are only as accurate as the data used as input. Furthermore, maximum damages for each exposure class are needed for the final calculation. In general, impact is calculated based on each hazard separately. The validation of these models was also done using unconventional means, by comparing online published maps and articles to the modelled results. Important for data scarce areas, is that all sources of information are utilised in any way possible. The results of the analysis provide insight into the ratio of the various hazards being considered, and therefore insight into how measure should be structured, and where the focus should lie.

   The hazard and impact models that have been set up and validated should then be applied to the range of probabilistic scenarios to perform the final risk assessment.

4. **Synthetic Data Generation and Scenario Selection**

   To assess the risk, various scenarios have to be developed for the area of interest. For remote locations or areas where historical data is limited, synthetic scenarios based on historical data can be generated. In the case of hurricane risk, this data generation involves synthetic hurricane tracks, and filtering these for the specific location of interest. These scenarios can then be used to determine the hazard extent and damages in each case.

5. **Exceedance Probabilities**

   Exceedance probabilities for induced damages should be related to the exceedance probabilities of the hazards being considered. For the case of hurricane risk, the exceedance probabilities are based on the empirical distribution of the extreme water levels. The total damages should include damages due to all hazards being considered, and should introduce a threshold as to prevent damages exceeding 100%. The combination of the total damages, means each total damage corresponds to one exceedance probability.

6. **Final Risk Assessment**

   The risk integral is calculated for the relationship between damages and their exceedance probabilities. This forms the distribution of Expected Annual Damages (EAD) for the region of interest. The resulting risk map should be used to identify high risk locations (where EAD are highest). Based on these findings, discussions regarding resilience and spatial planning can be triggered and target areas for funding can be identified. This can be done after a disaster to help distribute funds to the most vulnerable locations but also in general decision making on spatial planning.

Research Question 2:

What are the boundary conditions to delineate hurricane risk in St. Martin based on the application of the proposed methodology?

The proposed methodology was applied to the case study of St. Martin to determine the boundary conditions for delineating hurricane risk on the island. The outcome of the of the application was a risk map indicating Expected Annual Damages (EAD) on the island with a resolution of ninety meters. The conclusions for each step of the applied methodology are described here for this research question.

The choice of hazard models was based on the availability of data, and the computational effort required to simulate 5000 years' worth of hurricane track scenarios. The models used to model wind and coastal flooding included, WES to simulate wind, Delft 3D to simulate coastal surge levels and a static approach to determine coastal inland flooding. Hazard modelling of Hurricane Irma was used to validate the wind and coastal flooding models used for St. Martin. Wind speeds reached 240 km/h to 270 km/h, and, based on the hydrodynamic model, storm surge levels around the island varied between 1.1 m and 1.6 m. Offshore maximum wave heights reached up to 20 m, inducing wave setup at the coastline in the order of 0.9 m. Coastal flooding on St. Martin was mostly limited to the coastal zone, and was used to identify 15 flood prone areas. The wind speed distribution was fairly uniformly distributed as these were modelled without taking elevation data into account.

The hazard extents were used to determine the impact due to each hazard for Hurricane Irma and resulted in damage estimations of around $2.6 billion in wind damages, and around $54.5 million in flood damages. This showed that on St. Martin, wind damages accounted for up to 98% of damages due to hurricane Irma, and only 2% due to coastal flooding. This does not mean that coastal flooding is insignificant, however in order to improve disaster resilience, a focus on wind impact could result in larger improvements.

The final risk assessment for St. Martin included modelling the same hazard and impact models for 1431 out of the 10,000 hurricane tracks of the Northern Atlantic Ocean basin. The exceedance probabilities for the coastal water levels were used to assign probabilities to the total damages for each scenario. From this the annual exceedance probability of Hurricane Irma was estimated to be 1 in 500. The water levels around the island also all seemed to follow similar extreme distributions, with little variation in their behaviour. For St.

Martin, the coastal water levels can be best described by the Kernel distribution.

The integration of risk over the island of St. Martin resulted in a risk map showing areas with high and low risk of hurricane activity. This map provides the boundary conditions necessary to delineate hurricane risk on the island, by indicating levels of high risk using the measure of Expected Annual Damages. High EAD represents high risk. Decisions of how to Build Back Better in St. Martin should take these results into consideration. On a local scale, individuals can determine whether they are located in high risk areas, and make decisions based on that. This could involve relocation or housing reinforcement. On a country, and island wide, scale, governance of building regulations, spatial planning, disaster risk management and preparation of future events should include this information as part of their analysis and decision making.

7.2. Recommendations

The following recommendations are made based on the key findings and limitations of this research. These are opportunities for future research and improvement of current methodologies.

1. **Data set improvement**

   Location specific data remains the biggest challenge for hazard modelling in these areas. Additional data collection is therefore vital for future work. Improvement in data sets for bathymetry and topography means better estimation of the actual impact the hazards have. This specifically means measuring elevations and water depths for the location of interest at resolutions better than those publicly available. Measurements of bathymetry and topography data will help to reduce uncertainty in hazard modelling. In the same way, data collection regarding exposure and vulnerability, will reduce uncertainty in impact modelling. Measurements of housing types, materials and uses can improve damage estimations.

   Along with data set improvement for modelling, data set improvement for model validation is equally important. After extreme hurricane events, recording changes and damages is crucial. Information of coastline changes, high water level marks, and structural damages help in deriving site-specific vulnerability relationships, as well as validation of hazard modelling. Improvement of validation data is necessary before more complex processes can be simulated. Currently the means are available however, there is no way to determine if the models reflect reality if no recorded data is made publicly available.

2. **Physical wind modelling**

   The damage estimation for wind damage in the proposed methodology does not account for variation in elevation. Variations in topography, especially for mountainous islands, influences the flow and interaction of wind and the infrastructure. Investigating the influence of a more complex wind model to determine the influence of topography is therefore recommended. In this way a comparison can be done to determine the overestimation of a more simple model and determine the order of overestimation. This is especially important when specific details as to wind damage costs are required, or when building regulations and standards need to be adjusted.

3. **Parametric wave study for St. Martin**

   Site specific investigation into the transformation of wave heights from offshore to near-shore can be used to develop a parametric wave model for St. Martin. This can be used to estimate the wave-induced setup at the coastline for different locations on the island and improved flooding estimations. This can then be compared to more general relationships and the overestimation of coastal flooding can be determined.

   Furthermore, the coastline and bathymetry of St. Martin is complex, and includes a reef system along the Eastern coastline. Interaction between the reef system and the waves could influence the setup at the coastline. This could be due to wave dissipation over the reef, or increased setup due to the influence of long waves. Many of these more complex and detailed processes have not been included, as solving these processes involves detailed modelling. Investigation into parametric relationships for wave setup and induced flooding over a reef could help better estimate coastal flooding in risk assessments.

4. **Synthetic Rainfall Modelling**

   The inland modelling of St. Martin was simplified to only include coastal flooding. An important factor to also consider, is inland flooding due to rainfall and compound flooding. For data scarce areas this can be included by generating synthetic rainfall data and basing the spatial distribution on the hurricane characteristics (Snaiki & Wu, 2017). In order to include this however, overland detailed DEM data is needed, and lack thereof is one of the reasons it was not included. Data regarding rainfall runoff, infiltration and inland waterway capacity is also important when simulating rainfall-induced flooding. If a synthetic relationship can be determined to translate rainfall distributions of hurricane events into flooding depths, this could be more easily included in this type of risk assessment.

   Compound flooding should also be investigated to determine empirical relationships that could be used when using synthetic events in data sparse areas. The relationship between inland flooding due to rainfall and coastal flooding is important, and therefore including this is the risk assessment will improve estimations (Torres Duenas, 2018).

Overall the work regarding hurricane induced hazards in data scarce regions is far from done. This research and improved methodology hope to provide a basis for triggering resilience discussions and decision making in a place like St. Martin. The results of applying the methodology give insight into areas of the community that need the help the most, and to determine what measures will improve the local disaster resilience the most.

References

510 Red Cross. (2017). Damage Percentage per Sub-Area of St . Maarten. (September), 2017. Retrieved from https://reliefweb.int/country/sxm

BBC News. (2017). *Hurricane Irma causes devastation in the Caribbean - BBC News*. Retrieved 2019-06-29, from https://www.bbc.com/news/world-latin-america-41182991

BCQS. (2016). *Mark Trend Report 2016 - Latin American and Caribbean Construction* (Tech. Rep.). Retrieved from www.bcqs.comI1

Beccario, C. (2019). *earth: a global map of wind, weather, and ocean conditions*. Retrieved 2019-07-07, from https://earth.nullschool.net/about.html

Bertinelli, L., & Strobl, E. (2008). Quantifying the Economic Damage due to Hurricane Strikes. *Animal Genetics*, *39*, 561–563.

Bloemendaal, N., Muis, S., Haarsma, R. J., Verlaan, M., Irazoqui Apecechea, M., De Moel, H., ... Aerts, J. C. J. H. (2018). Global modeling of tropical cyclone storm surges using high-resolution forecasts. *Climate Dynamics*.

Boon, J. D., & Green, M. O. (1988). Caribbean beach-face slopes and beach equilibrium profiles abstract. *Coastal Engineering Proceedings*, *1*(21), 1618–1630.

Bosboom, J., & Stive, M. J. F. (2013). *Coastal Dynamics I: Lecture notes CIE4305* (4th ed.). Delft: VVSD.

Bouwer, L. M., & Botzen, W. J. (2011). How Sensitive are US Hurricane Damages to Climate? Comment on a Paper by W. D. Nordhaus. *Climate Change Economics*.

British Oceanographic Data Centre. (2018). *Gridded Bathymetry Data*. Retrieved 2019-04-24, from https://www.gebco.net/data{_}and{_}products/gridded{_}bathymetry{_}data/

Cangialosi, J. P., Latto, A. S., & Berg, R. (2017). Tropical Cyclone Report - Hurricane Irma. *Journal of Trauma and Acute Care Surgery*.

CDCC. (2018). Irma and Maria by Numbers. *FOCUS*.

Cerema, & DEAL Guadeloupe. (2017). *Inundation Hazard Map of Saint Martin after Hurricane Irma*. Retrieved 2019-04-24, from http://www.com-saint-martin.fr/ressources/annexe2{_}carte{_}alea{_}PPR{_}submersion{_}IRMA{_}Saint-Martin.pdf

Charnock, H. (1955). Wind stress on a water surface. *Quarterly Journal of the Royal Meteorological Society*, *81*, 639–640.

Copernicus. (2017). *Hurricane Irma in Sint Maarten*. Retrieved 2019-02-10, from https://emergency.copernicus.eu/mapping/ems/hurricane-irma-sint-maarten

de Hamer, J. (2018). *Dutch Quarter, Sint Maarten [photography]*. Philipsburg, SXM.

Deltares. (2014). *Delft3D WES* (Tech. Rep.). Retrieved from https://oss.deltares.nl/documents/183920/185723/Delft3D-WES{_}User{_}Manual.pdf/686377dc-a405-4c44-9604-2dbdd322dda2?version=1.0

Deltares. (2019). *User Manual D-Flow Flexible Mesh* (Tech. Rep.).

de Moel, H., Jongman, B., Kreibich, H., Merz, B., Penning-Rowsell, E., & Ward, P. J. (2015). Flood risk assessments at different spatial scales. *Mitigation and Adaptation Strategies for Global Change*, *20*.

Didier, D., Baudry, J., Bernatchez, P., Dumont, D., Sadegh, M., Bismuth, E., ... Sévigny, C. (2018). Multihazard simulation for coastal flood mapping: Bathtub versus numerical modelling in an open estuary, Eastern Canada. *Journal of Flood Risk Management*.

Donev, J. (2016). *Energy Education: Storm surge*. Retrieved 2019-06-27, from https://energyeducation.ca/encyclopedia/Storm{_}surge{#}cite{_}note-6

Doocy, S., Daniels, A., Murray, S., & Kirsch, T. (2013). The Human Impact: a Historical Review of Events 1980-2009 and Systematic Literature Review. *PLOS Currents: Disaster*.

Duvat, V., Pillet, V., Volto, N., Krien, Y., Cécé, R., & Bernard, D. (2019). High human influence on beach response to tropical cyclones in small islands: Saint-Martin Island, Lesser Antilles. *Geomorphology*, *325*.

Easy Voyage. (2019). *St Martin-Nettle Bay, Saint-Martin*. Retrieved 2019-04-03, from https://www.easyvoyage.co.uk/hotels/st-martin-nettle-bay/le-flamboyant-1045

Emanuel, K. (2005). Increasing destructiveness of tropical cyclones over the past 30 years. *Nature, 436*, 686–688.

Emanuel, K., Desautels, C., Holloway, C., & Korty, R. (2004). *Environmental Control of Tropical Cyclone Intensity* (Tech. Rep.).

Emanuel, K., Ravela, S., Vivant, E., & Risi, C. (2006). A statistical deterministic approach to hurricane risk assessment. *Bulletin of the American Meteorological Society*.

Emanuel, K., Ravela, S., Vivant, E., & Risi, C. (2011). Application of stochastic and deterministic modelling to Hurricane wind risk assessment.

Ferlise, J. (2017). *Initial Assessment of Damage at Princess Juliana International Airport Revealed.* Retrieved 2019-07-03, from https://www.sxmstrong.com/2017/09/28/initial-assessment-damage-princess-juliana-international-airport-revealed/

Gallina, V., Torresan, S., Critto, A., Sperotto, A., Glade, T., & Marcomini, A. (2016). A review of multi-risk methodologies for natural hazards: Consequences and challenges for a climate change impact assessment.

GFDRR. (2017). Building Back Better in Post-Disaster Recovery.

Giardino, A., Nederhoff, K., & Vousdoukas, M. (2018). Coastal hazard risk assessment for small islands: assessing the impact of climate change and disaster reduction measures on Ebeye (Marshall Islands). *Regional Environmental Change, 18*.

Gomes, M. P., Pinho, J. L., Antunes do Carmo, J. S., & Santos, L. (2015). Hazard assessment of storm events for The Battery, New York. *Ocean and Coastal Management, 118*, 22–31.

Google Earth V 7.3.2.5776. (2005). *Saint Martin, 18° 03' 39.99"N, 63° 04' 19.92"W, Eye alt 22.11km.* Retrieved 2019-04-03, from http://www.earth.google.com

Hall, T., & Jewson, S. (2007). Statistical modelling of North Atlantic tropical cyclone tracks. *The Authors Journal compilation C*.

Hallegatte, S. (2007). The Use of Synthetic Hurricane Tracks in Risk Analysis and Climate Change Damage Assessment.

Hallegatte, S., Rentschler, J., & Walsh, B. (2018). *Achieving resilience through stronger, faster, and more inclusive post-disaster reconstruction* (Tech. Rep.).

Hatari Labs. (2018). *How to calculate the Root Mean Square Error (RMSE) of an interpolated pH raster?* Retrieved 2019-06-19, from https://www.hatarilabs.com/ih-en/how-to-calculate-the-root-mean-square-error-rmse-of-an-interpolated-ph-raster

Hatzikyriakou, A., & Lin, N. (2017). Simulating storm surge waves for structural vulnerability estimation and flood hazard mapping.

Hawker, L., Rougier, J., Neal, J., Bates, P., Archer, L., & Yamazaki, D. (2018). Implications of Simulating Global Digital Elevation Models for Flood Inundation Studies. *Water Resources Research, 54*, 7910–7928.

Hoek, J. (2017). *Tropical Cyclone Wind Statistical Estimation* (Tech. Rep.). Delft: TU Delft.

Holland, G. J. (1980). An Analytical Model of the Wind and Pressure Profiles in Hurricanes.

Holland, G. J., Belanger, J. I., & Fritz, A. (2010). A Revised Model for Radial Profiles of Hurricane Winds.

Holthuijsen, L. H. (2007). *Waves in Oceanic and Coastal Waters* (Tech. Rep.).

Hottot, A. (2017). *Photograph of Geneve Bay, St. Martin by Adele Hottot.* Retrieved 2019-04-03, from https://www.instagram.com/p/BUnVvZDAALG/?utm{_}source=ig{_}embed{%}0A

Huizinga, J., De Moel, H., & Szewczyk, W. (2017). *Global flood depth-damage functions - Methodology and the database with guidelines* (Tech. Rep.). JRC.

Hwang, P. A. (2005). Drag coefficient, dynamic roughness and reference wind speed. *Journal of Oceanography, 61*(3), 399–413.

Inman, D. L. (1994, jan). Chapter 6: Types of Coastal Zones: Similarities and Differences. In *Environmental science in the coastal zone: Issues for further research.* Washington, D.C.: National Academies Press. Retrieved from http://www.nap.edu/catalog/2249 doi: 10.17226/2249

James, M. K., & Mason, L. B. (2005). Synthetic Tropical Cyclone Database.

Jiang, H., Halverson, J. B., & Simpson, J. (2006). Difference of Rainfall Distribution for Tropical Cyclones Over Land and Ocean and Rainfall Potential Derived From Satellite Observations and Its Implication on Hurricane.

Jonkman, S. N., Steenbergen, R. D. J. M., Morales-Nápoles, O., Vrouwenvelder, A. C. W. M., & Vrijling, J. K. (2017). *Probabilistic Design: Risk and Reliability Analysis in Civil Engineering Lecture notes CIE4130* (Tech. Rep.).

Jonkman, S. N., Van Gelder, P. H., & Vrijling, J. K. (2003). An overview of quantitative risk measures for loss of life and economic damage. *Journal of Hazardous Materials, 99*, 1–30.

Kaplan, S., & Garrick, J. B. (1981). *On The Quantitative Definition of Risk* (Tech. Rep.).

Kernkamp, H. W. J., Van Dam, A., Stelling, G. S., & de Goede, E. D. (2011). Efficient scheme for the shallow water equations on unstructured grids with application to the Continental Shelf. *Ocean Dynamics, 61*.

Khanduri, A. C., & Morrow, G. C. (2003). *Vulnerability of buildings to windstorms and insurance loss estimation* (Tech. Rep.).

Knipselkrant Curacao. (2017). *Een kwart van de inwoners van Sint Maarten is vertrokken | Knipselkrant Curacao*. Retrieved 2019-07-03, from https://www.knipselkrant-curacao.com/dolfijnfm-een-kwart-van-de-inwoners-van-sint-maarten-is-vertrokken/

Knowlton, C. (2015). *Hurricanes: Science and Society*. Retrieved 2019-04-18, from http://www.hurricanescience.org/science/science/primarycirculation/

Komi, K., Neal, J., Trigg, M. A., & Diekkrüger, B. (2017, apr). Modelling of flood hazard extent in data sparse areas: a case study of the Oti River basin, West Africa. *Journal of Hydrology: Regional Studies, 10*, 122–132. Retrieved from https://linkinghub.elsevier.com/retrieve/pii/S2214581817300757 doi: 10.1016/j.ejrh.2017.03.001

Kron, W. (2005). *Flood Risk = Hazard • Values • Vulnerability* (Vol. 30; Tech. Rep.). International Water Resources Association.

Langousis, A., & Veneziano, D. (2009). Theoretical model of rainfall in tropical cyclones for the assessment of long-term risk. *Journal of geophysical research, 114*.

Leijnse, T. (2018). Computationally Efficient Modelling of Compound Flooding due to Tropical Cyclones with the Explicit Inclusion of Wave-Driven Processes Research into the required processes and the Computationally Efficient Modelling of Compound Flooding due to Tropical Cy. , 145.

Lesser, G., Roelvink, J., van Kester, J., & Stelling, G. (2004). Development and validation of a three-dimensional morphological mode. *Coastal Engineering, 51*.

Liu, B., Ling Siu, Y., & Mitchell, G. (2016). Hazard interaction analysis for multi-hazard risk assessment: a systematic classification based on hazard-forming environment. *Natural Hazards and Earth System Sciences, 16*, 629–642.

Lu, P., Lin, N., Emanuel, K., Chavas, D., & Smith, J. (2018). Assessing Hurricane Rainfall Mechanisms Using a Physics-Based Model: Hurricanes Isabel (2003) and Irene (2011). *Journal of the Atmospheric Sciences*.

Makin, V. K. (2005). A Note on the Drag of the Sea Surface at Hurricane Winds. *Boundary-Layer Meteorology, 115*, 169–176.

Matyas, C. J. (2000). Relating Tropical Cyclone Rainfall Patterns To Storm Size.

Muis, S., Verlaan, M., Winsemius, H. C., Aerts, J. C. J. H., & Ward, P. J. (2016). A global reanalysis of storm surges and extreme sea levels. *Nature Communications*.

Multiverse. (2019). *Marigot French Saint Martin*. Retrieved 2019-07-03, from https://www.shutterstock.com/video/clip-14896741-marigot-french-saint-martin-aerial-view

Murnane, R. J., & Elsner, J. B. (2012). Maximum wind speeds and US hurricane losses. *Geophysical Research Letters*.

NAPSG Foundation. (2017). *Hurricane Irma Photo Map*. Retrieved 2019-05-01, from https://www.arcgis.com/apps/StoryMapCrowdsource/index.html?appid=65f0dde429504c3cb07f0cae0f2c4be6

NASA. (2014). *Shuttle Radar Topography Mission*. Retrieved 2019-04-24, from https://www2.jpl.nasa.gov/srtm/index.html

National Hurricane Center. (2018a). *NHC Data Archive*. Retrieved 2019-04-24, from https://www.nhc.noaa.gov/data/

National Hurricane Center. (2018b). *Storm Surge Overview*. Retrieved 2019-01-29, from https://www.nhc.noaa.gov/surge/

National Oceanic and Atmospheric Administration. (2018). *Best Track Data (HURDAT2)*. Retrieved 2019-05-09, from https://www.nhc.noaa.gov/data/{#}hurdat

Navionics. (2019). *Navionics Chart Viewer*. Retrieved 2019-03-25, from https://webapp.navionics.com

Nederhoff, K., Giardino, A., Van Ormondt, M., & Vatvani, D. (2019). Estimates of tropical cyclone geometry parameters based on best track data. *Natural Hazards and Earth System Sciences*.

@NNweather. (2017). *Images from before & after show the damage & flooding caused by #HurricaneIrma in Marigot on the Caribbean island of Saint Martin*. Retrieved 2019-05-02, from https://twitter.com/NNweather/status/905413126706929665

NOAA. (2018). *Hurricane Irma: Water Level and Meteorological Data Report* (Tech. Rep.).

NOAA SciLinks. (2018). *How does a hurricane form.* Retrieved 2019-02-06, from https://scijinks.gov/hurricane/

Nolan, J. P. (2018). *Univariate stable distributions.* Math/Stat Department, American University.

Nordhaus, W. D. (2010). The Economics of Hurricanes and Implications of Global Warming. *Climate Change Economics, 1*, 1–20.

NOS. (2018a). *Rekenkamer: wederopbouw Sint-Maarten verloopt traag.* Retrieved 2019-01-04, from https://nos.nl/artikel/2263348-rekenkamer-wederopbouw-sint-maarten-verloopt-traag.html

NOS. (2018b). *Sint-Maarten heeft geen tijd om te herdenken, een jaar na Irma.* Retrieved 2019-01-04, from https://nos.nl/artikel/2249304-sint-maarten-heeft-geen-tijd-om-te-herdenken-een-jaar-na-irma.html

NOS. (2019). *Pauw: 'De zwakkeren zijn nooit klaar, dat is op Sint-Maarten ook zo'.* Retrieved 2019-02-13, from https://nos.nl/artikel/2271520-pauw-de-zwakkeren-zijn-nooit-klaar-dat-is-op-sint-maarten-ook-zo.html

NPR. (2017). *Before And After: Satellite Images Show Irma's Caribbean Destruction : The Two-Way : NPR.* Retrieved 2019-03-05, from https://www.npr.org/sections/thetwo-way/2017/09/12/550424499/before-and-after-satellite-images-show-irmas-caribbean-destruction?t=1550762989830

NU. (2018). *Slechts klein deel van Nederlands hulpgeld voor Sint-Maarten besteed.* Retrieved 2019-01-04, from https://www.nu.nl/buitenland/5628185/slechts-klein-deel-van-nederlands-hulpgeld-sint-maarten-besteed.html

OnParOu. (2019). *Saint Martin.* Retrieved 2019-04-03, from http://www.onparou.com/Hotels-Saint-Martin/Anse-Marcel/4-etoiles/Hotel-Saint-Martin-fiche-descriptif{_}325.php

OpenStreetMap. (2019). *OpenStreetMap.* Retrieved 2019-04-24, from openstreetmap.org

Pacific Disaster Center. (2017). *Hurricane Irma - Estimated wind impacts based on actual track: Saint Martin & Sint Maarten.* Retrieved 2019-04-24, from https://reliefweb.int/map/sint-maarten-netherlands/hurricane-irma-estimated-wind-impacts-based-actual-track-saint-martin

PCRAFI. (2013). Better Risk Information for Smarter Investments: Catastrophe Risk Assessment Methodology.

Pearson, S. G. (2016). Predicting Wave-Induced Flooding on Low-Lying Tropical Islands. , 232.

Phadke, A. C., Martino, C. D., Cheung, K. F., Houston, S. H., & Cheung, K. F. (2003). Modeling of tropical cyclone winds and waves for emergency management. *Ocean Engineering*.

Poulter, B., & Halpin, P. N. (2008). Raster modelling of coastal flooding from sea-level rise. *International Journal of Geographical Information Science, 22*.

Powell, M., Cocke, S., Soukup, G., Gulati, S., Morisseau-Leroy, N., Landsea, C., … Axe, L. (2005). *State of Florida Hurricane Loss Projection Model: Atmospheric Science Component* (Tech. Rep.). NOAA Hurricane Research Division.

Powell, M. D., Houston, S. H., & Ares, I. (1995). Real-time Damage Assessment in Hurricanes. *Preprints of the 21st Conference on Hurricanes and Tropical Meteorology*.

Powell, M. D., Vickery, P. J., & Reinhold, T. A. (2003). Reduced drag coefficient for high wind speeds in tropical cyclones. *Nature, 422*.

Powers, J. G., KlemP, J. B., SKamaroCK, w. C., Davis, C., Dudhia, J., Gill, D., … Duda, m. G. (2017). The Weather Research and Forcasting model. *American Meteorological Society*. doi: 10.1175/BAMS-D-15-00308.1

Prahl, B. F., Rybski, D., Burghoff, O., & Kropp, J. P. (2015). Comparison of storm damage functions and their performance. *Natural Hazards and Earth System Sciences*.

Red Cross. (2017a). *Damage Assessment St. Martin.* Retrieved 2019-04-24, from https://reliefweb.int/country/sxm

Red Cross. (2017b). *Exposure data for Sint Maarten defined by roof material.*

Reef Base. (2019). *Reef Base: A Global Information System for Coral Reefs.* Retrieved 2019-04-24, from http://reefgis.reefbase.org/

Romali, N. S., & Sulaiman, M. S. A. K. (2015). Flood Damage Assessment: A Review of Flood Stage–Damage Function Curve. (January). Retrieved from http://link.springer.com/10.1007/978-981-287-365-1 doi: 10.1007/978-981-287-365-1

Schloemer, R. W. (1954). *Analysis and synthesis of hurricane wind patterns over lake Okeechobee, Florida* (Tech. Rep.). Washington, D C: U.S. Department of Army Corps of Engineers.

Schneider, B., Hoffmann, G., & Reicherter, K. (2016, apr). Scenario-based tsunami risk assessment using a static flooding approach and high-resolution digital elevation data: An example from Muscat in Oman. *Global and Planetary Change, 139*.

SHOM. (2018). *MNT bathymétrique de façade de Saint-Martin et Saint-Barthélemy.* Retrieved 2019-04-24, from https://diffusion.shom.fr/pro/mnt-facade-antn.html

Sill, B., & Kozlowsk, R. (1997). Analysis of storm-damage factors for low-rise structures. *Journal of Performance of Constructed Facilities, 11*, 168–177.

Slager, K., Burzel, A., Bos, E., de Bruijn, K., Wagenaar, D., Winsemius, H., ... van der Doef, M. (2016). *User Manual Delft-FIAT version 1.* Retrieved 2019-01-18, from https://publicwiki.deltares.nl/display/DFIAT/Delft-FIAT+Home

Smith, S. D., & Banke, E. G. (1975). Variation of the sea surface drag coefficient with wind speed. *Quarterly Journal of the Royal Meteorological Society*.

Snaiki, R., & Wu, T. (2017). A theoretical model for rapid estimates of rainfall during tropical cyclones. *Americas Conference on Wind Engineering*(April).

St. Martin Tourist Office. (2019). *St-Martin, an island with 37 beaches.* Retrieved 2019-04-03, from http://www.stmartinisland.org/st-martin-st-maarten-activities/st-martin-st-maarten-beaches.html

Taylor, A. (2018). *Photos of the Devastation Across Saint Martin Left by Hurricane Irma.* Retrieved 2018-12-10, from https://www.theatlantic.com/photo/2017/09/photos-from-saint-martin-after-hurricane-irma/539103/

The Crazy Tourist. (2019). *14 Best Beaches in St Maarten.* Retrieved 2019-04-03, from https://www.thecrazytourist.com/14-best-beaches-in-st-maarten/

The Guardian. (2017). *Before and after Hurricane Irma: images of Caribbean destruction.* Retrieved 2019-01-04, from https://www.theguardian.com/world/2017/sep/08/before-and-after-hurricane-irma-images-of-caribbean-destruction

The MathWorks Inc. (2018). *MATLAB and Statistics Toolbox Release 2018a.* Massachusetts, United States: Natick.

The Moorings. (2019). *St. Martin Cruising Conditions.* Retrieved 2019-04-03, from https://www.moorings.com/destinations/caribbean/st-martin-yacht-charters/cruising-conditions

Tomiczek, T., Asce, M., Kennedy, A., Zhang, Y., Owensby, M., Hope, M. E., ... Flory, A. (2017). Hurricane Damage Classification Methodology and Fragility Functions Derived from Hurricane Sandy's Effects in Coastal New Jersey. *American Society ofCivil Engineers*.

Torres Duenas, L. (2018). Flood risk assessment of the clear creek watershed, considering compound events.

University of Tokyo. (2018). *Multi-Error-Removed Improved-Terrain DEM.* Retrieved 2019-04-24, from http://hydro.iis.u-tokyo.ac.jp/{~}yamadai/MERIT{_}DEM/

US Army Corps of Engineers. (1992). *Catalog of residential depth-damage funcitons* (Tech. Rep.).

Valamanesh, V., Myers, A. T., Arwade, S. R., Hajjar, J. F., Hines, E., & Pang, W. (2016). Wind-wave prediction equations for probabilistic offshore hurricane hazard analysis. *Natural Hazards, 83*, 541–562.

van Rijn, L. (1990). *Principles of fluid flow and surface waves in rivers, estuaries, seas, and oceans.* Amsterdam: Amsterdam : Aqua.

van Rijn, L., Giardino, A., Quataert, E., Warren, A., Jeuken, A., Nederhoff, K., & Desramaut, N. (2017). SimpleCoast: Simple Assessments of Coastal Problems and Solutions. In *Proceedings of the medcoast 17 conference* (pp. 137–148). Malta.

Vatvani, D., Zweers, N. C., Van Ormondt, M., Smale, A. J., De Vries, H., & Makin, V. K. (2012). Storm surge and wave simulations in the Gulf of Mexico using a consistent drag relation for atmospheric and storm surge models. *Natural Hazards and Earth System Sciences*.

Vermeulen, M. (2013). *Philipsburg boulevard.* Retrieved 2019-07-03, from https://martijnver13.reislogger.nl/foto/philipsburg/philipsburg-boulevard.939060

Vickers, D., Mahrt, L., & Andreas, E. L. (2013). Estimates of the 10-m Neutral Sea Surface Drag Coefficient from Aircraft Eddy-Covariance Measurements. *Journal of Physical Oceanography*.

Vickery, P. J., Skerlj, P. F., Steckley, A. C., & Twisdale, L. A. (2000). Hurricane Wind Field Model for Use in Hurricane Simulations. *Article in Journal of Structural Engineering*.

Vickery, P. J., Wadhera, D., Twisdale, L. A., & Lavelle, F. M. (2009). U.S. Hurricane Wind Speed Risk and Uncertainty. *Journal of Structural Engineering, 135*, 301–320.

Vlaams Instituut voor de Zee. (2019). *Sea Level Station Monitoring Facility.* Retrieved 2019-05-02, from http://www.ioc-sealevelmonitoring.org/station.php?code=stmt

Vojinovic, Z., Ediriweera, J. C. W., & Fikri, A. K. (2008). *An approach to the model-based spatial assessment of damages caused by urban floods* (Tech. Rep.).

Vousdoukas, M. I., Bouziotas, D., Giardino, A., Bouwer, L. M., Mentaschi, L., Voukouvalas, E., & Feyen, L. (2018). Understanding epistemic uncertainty in large-scale coastal flood risk assessment for present and future climates. *Natural Hazards and Earth System Sciences*, *18*.

Vousdoukas, M. I., Voukouvalas, E., Mentaschi, L., Dottori, F., Giardino, A., Bouziotas, D., ... Feyen, L. (2016). Developments in large-scale coastal flood hazard mapping. *Natural Hazards and Earth System Sciences*, *16*.

Wikimedia Commons. (2006). *St. Martin - Grand Case (Esperance)*. Retrieved 2019-07-03, from https://commons.wikimedia.org/wiki/File:St.{_}Martin{_}-{_}Grand{_}Case{_}(Esperance){_}(CCE{_}-{_}SFG{_}-{_}TFFG){_}AN1026870.jpg

Wild Adventures. (2019). *Orient Bay, best beach in the Caribbean.* Retrieved 2019-04-03, from http://www.wind-adventures.com/orientbay.htm

WindAlert. (2019). *Wind Stations on St. Martin.* Retrieved 2019-05-02, from https://www.windalert.com/map{#}18.069,-63.008,12,1

World Bank Group. (2018). *The recovery of St. Maarten: Opportunities for Dutch companies.* Retrieved 2019-06-26, from https://nl4worldbank.org/2018/12/13/the-recovery-of-st-maarten-opportunities-for-dutch-companies/

World Meteorological Organization. (2011). *Guide to Storm Surge Forecasting* (Tech. Rep.). Retrieved from www.wmo.int

Wu, G., Shi, F., Kirby, J. T., Liang, B., & Shi, J. (2018). Modeling wave effects on storm surge and coastal inundation. *Coastal Engineering*, *140*.

Young, A. (2012). *Photograph of Little and Great Bay, St. Martin by Alistair Young.* Retrieved 2019-04-03, from https://www.flickr.com/photos/15192926@N00/8011931432

Young, I. (1988). Parametric hurricane wave prediction model.

Your Flight Reviews. (2016). *Princess Juliana International Airport Reviews | Your Flight Reviews.* Retrieved 2019-07-03, from http://yourflightreviews.com/princess-juliana-international-airport-reviews/

Zijlema, M. (2018). *Lecture Notes CIE4340: Computational modelling of flow and transport.* Delft: Delft University of Technology.

A

Vulnerability functions

The vulnerability functions used to calculate impact for St. Martin were based on two studies. A study by Khanduri and Morrow (2003) for wind damages in Puerto Rico and a study by Vojinovic et al. (2008) for flood damage in St. Martin.

A.1. Wind Speed Vulnerability Functions

The functions regarding wind damage were based on a study by Khanduri and Morrow (2003) where vulnerability functions were developed based on wind speed and damage fraction for the island of Puerto Rico. The vulnerability functions used for St. Martin for wind speed damage are shown in Figure A.1 for generic structure types, and Figure A.2 for concrete structure types. These are chosen for the island based on the exposure data made available for the impact assessment. This consisted of the buildings of St. Martin classified by their roof material. These classifications were for concrete, roof tiles and masonry. The only classification matching the study by Khanduri and Morrow (2003) was for a concrete structure and therefore the other classifications were considered as generic structures and the corresponding vulnerability function was used.

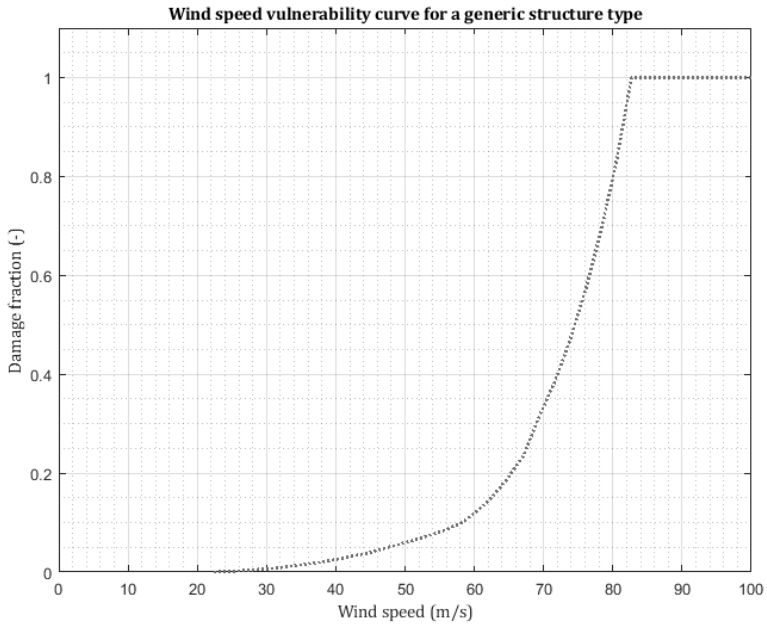

Figure A.1: Wind-damage vulnerability function for generic structures.

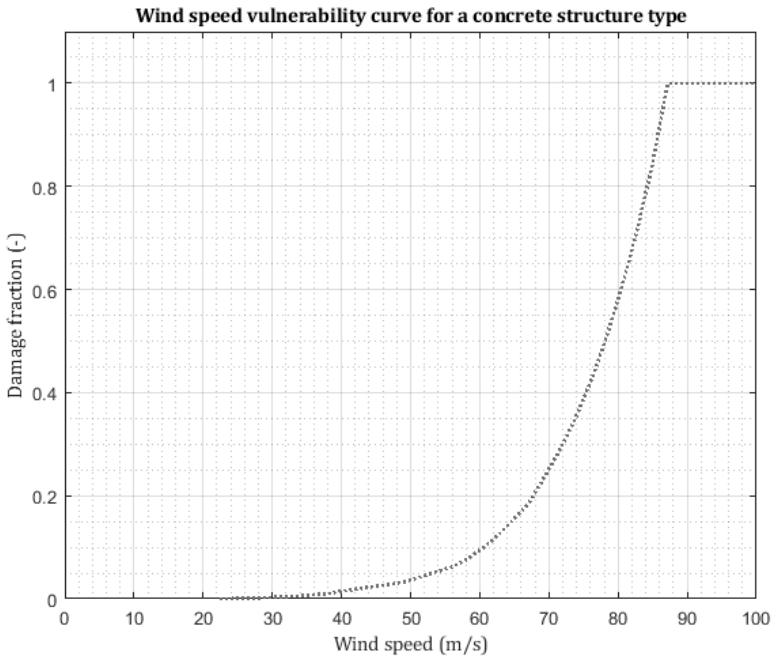

Figure A.2: Wind-damage vulnerability function for concrete structures.

A.2. Flood depth Vulnerability Functions

The functions regarding flood damage were based on a study by Vojinovic et al. (2008) where damages were related to flood depths during extreme rainfall events. These functions were developed for a classification of building by the use of the building. The three categories defined were residential use, commercial use and industrial use. These classifications of exposure data were also available for St. Martin from OpenStreetMap (2019). The classifications were further defined by their size. Residential buildings were defined by the area smaller and larger than 50 m^2 and the corresponding vulnerability functions are shown in Figure A.3 and A.4.

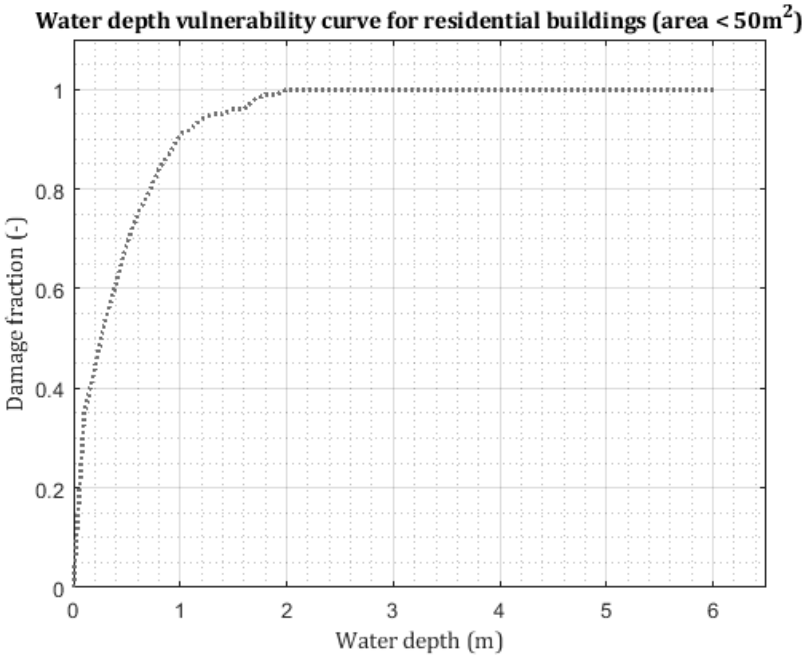

Figure A.3: Flood-damage vulnerability function for small residential buildings.

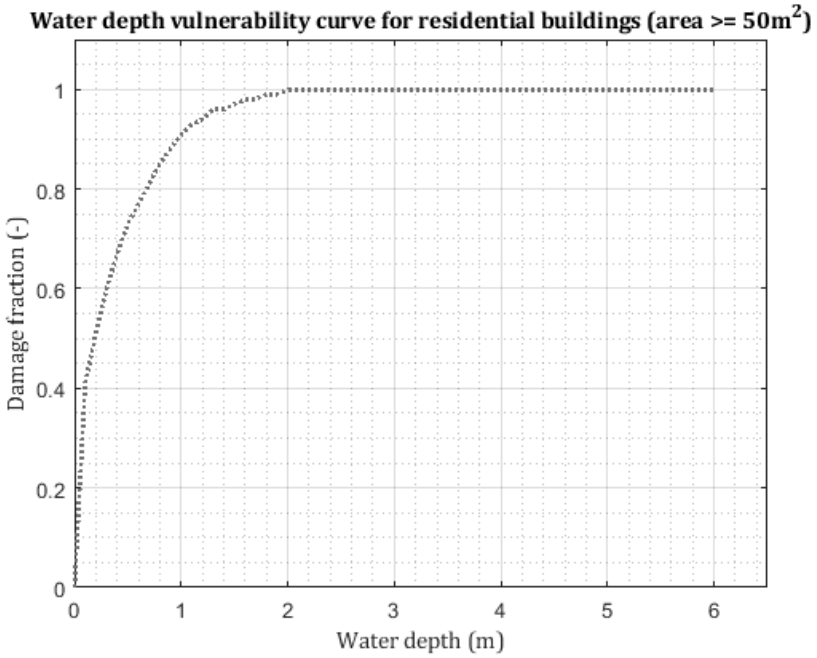

Figure A.4: Flood-damage vulnerability function for large residential buildings.

Commercial buildings were defined by areas less than 100 m^2, between 100 m^2 and 1000 m^2, and greater than 1000 m^2, and are shown in Figures A.5, A.6 and A.7 respectively.

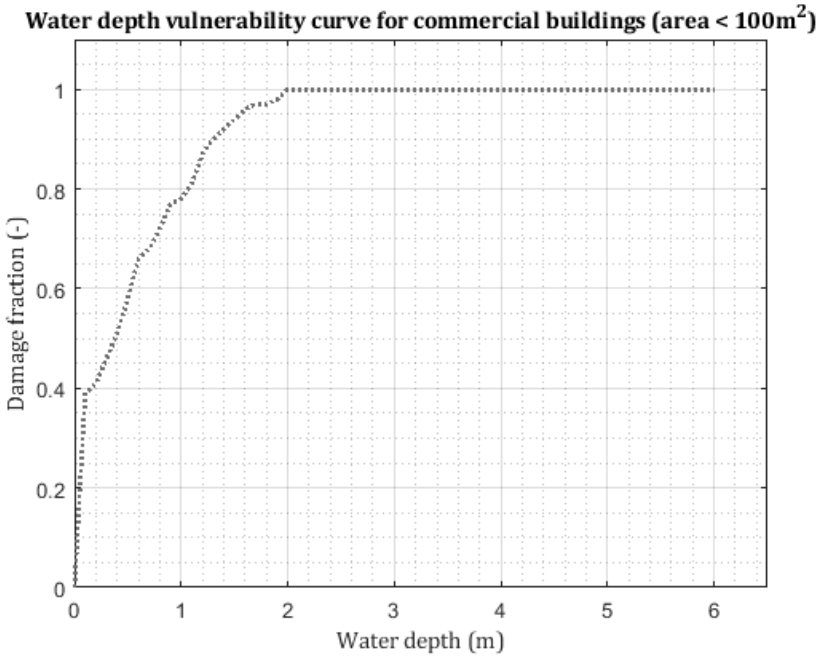

Figure A.5: Flood-damage vulnerability function for small commercial buildings.

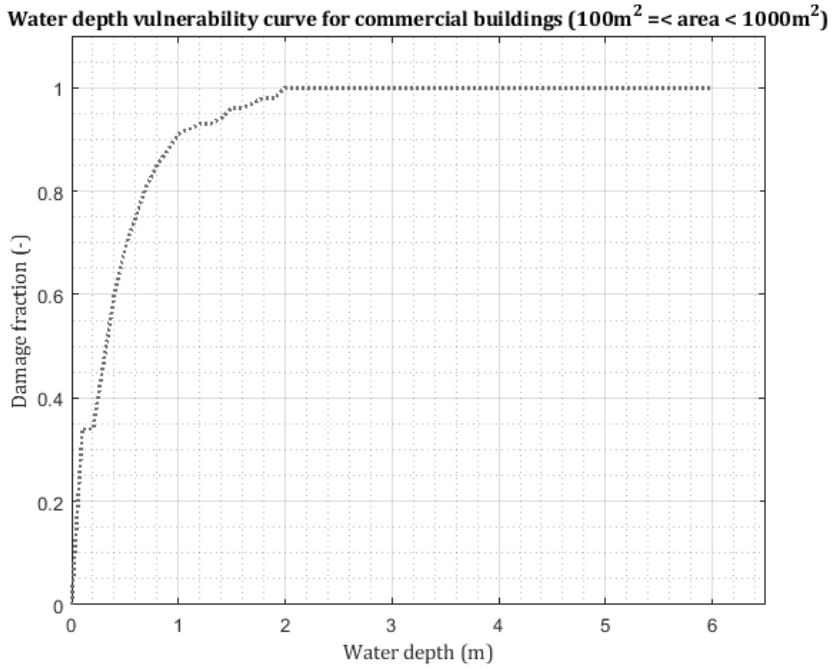

Figure A.6: Flood-damage vulnerability function for medium commercial buildings.

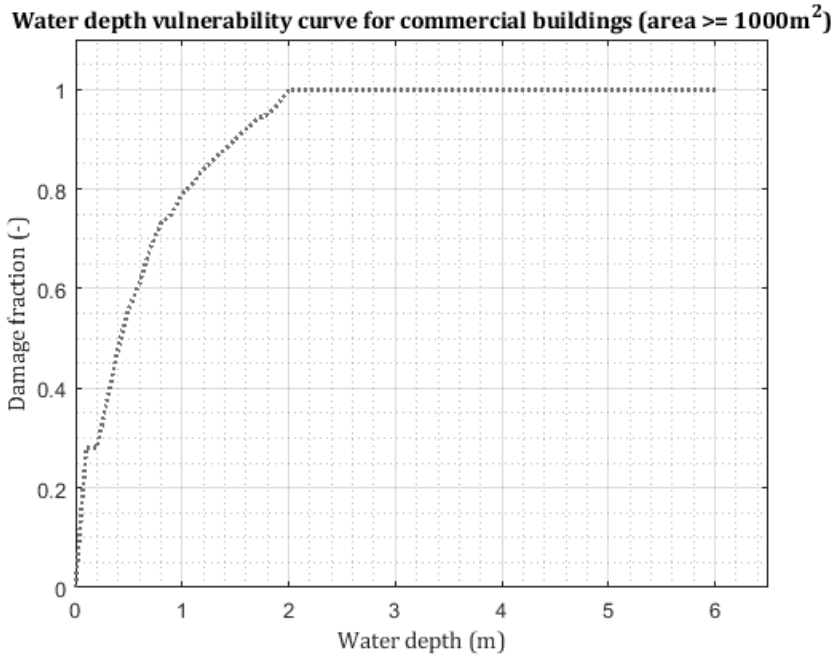

Figure A.7: Flood-damage vulnerability function for large commercial buildings.

Industrial buildings were defined by areas less than and greater than 100 m^2 shown in Figure A.8 and A.9.

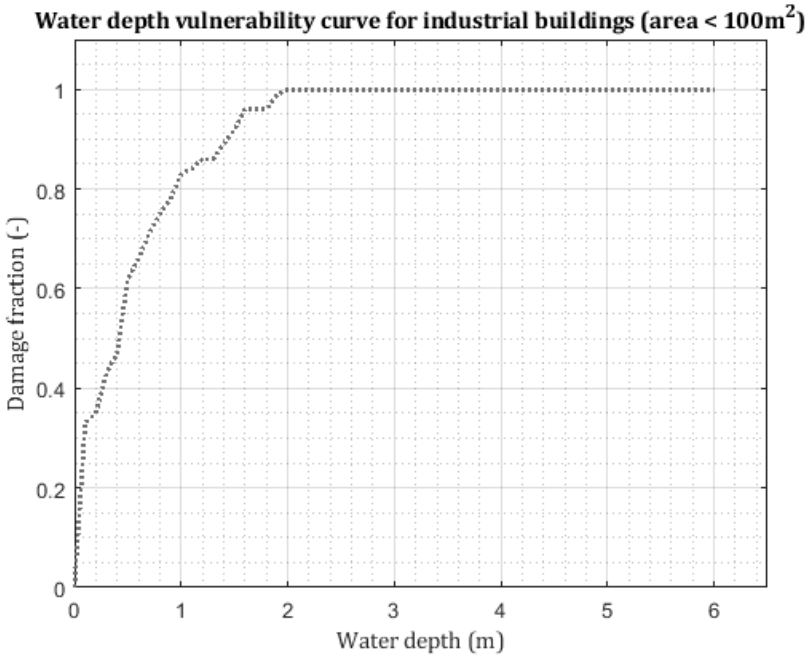

Figure A.8: Flood-damage vulnerability function for small industrial buildings.

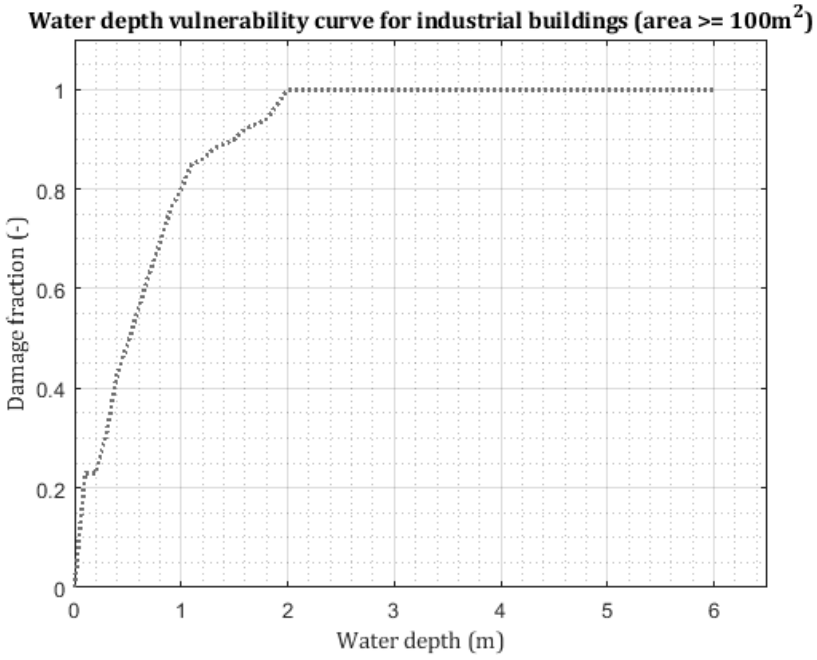

Figure A.9: Flood-damage vulnerability function for large industrial buildings.

B

Probability Distributions

Probabilistic analysis was done for the water levels and wind speeds of the synthetically generated hurricane tracks used to determine risk for St. Martin. The generated data is shown in Figure B.1 and B.2 which shows the data modelled for each of the flood basins of St. Martin. These water levels represent the maximum water level of each hurricane track scenario, therefore in all 1431 maximum water levels have been plotted.

The results of fitting various distributions are shown for one of the flooding basins for illustration purposes. The fitting and goodness tests however were done for all flooding basins and the final results are shown in Table B.1.

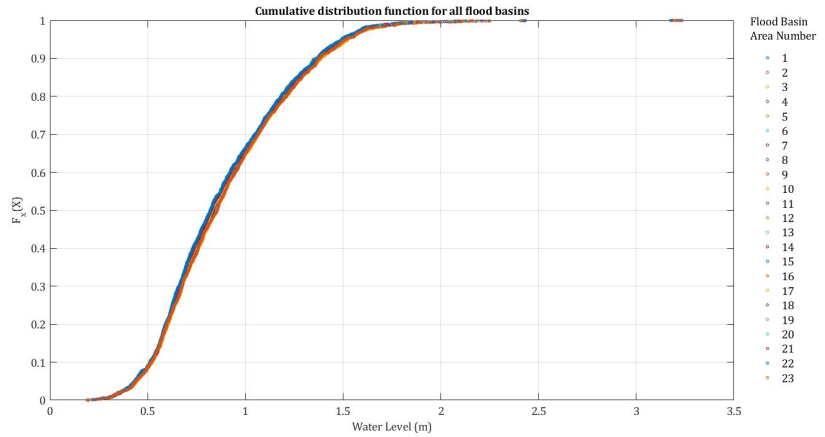

Figure B.1: Cumulative density distribution for hurricane-induced water levels on the island of St. Martin. These are defined for the 23 identified flooding basins on the island, numbered here from 1 to 23.

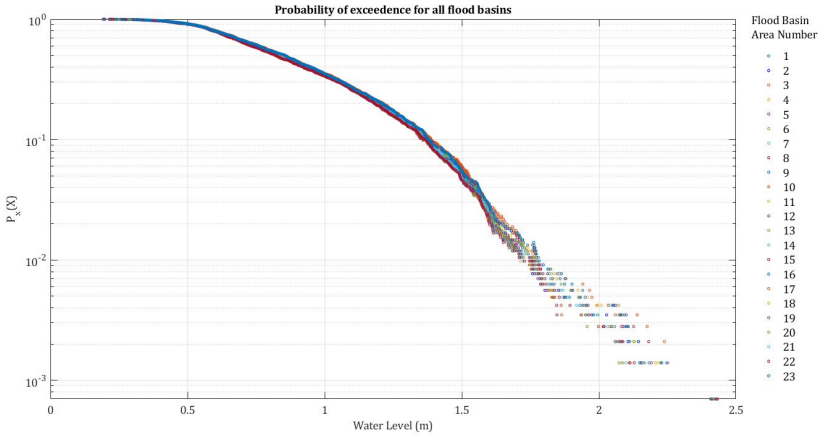

Figure B.2: Probability of exceedance for hurricane-induced water levels on the island of St. Martin. These are defined for the 23 identified flooding basins on the island, numbered here from 1 to 23.

B.1. Fitted Distributions

The extreme water levels modelled for various hurricanes relevant to St. Martin were used to determine the best fit distribution for the results. The considered distributions were the Normal, Extreme Value, Generalised Extreme Value, Gamma, Logistic, Kernel, Rayleigh, Stable and t-location Scale distributions. Here each distribution is explained along with the general form of the distribution and the fit to the modelled data.

B.1.1. Normal Distribution

This is the most commonly used distribution with Equation B.1 showing the formulation of the probability density function (Jonkman et al., 2017). σ represents the standard deviation of the distribution and μ represents the mean. For the modelled data points the mean is 0.89 m and the standard deviation is 0.33 m.

$$p_x(x) = \frac{1}{\sigma\sqrt{2\pi}} e^{\left(\frac{(x-\mu)^2}{2\sigma^2}\right)} \tag{B.1}$$

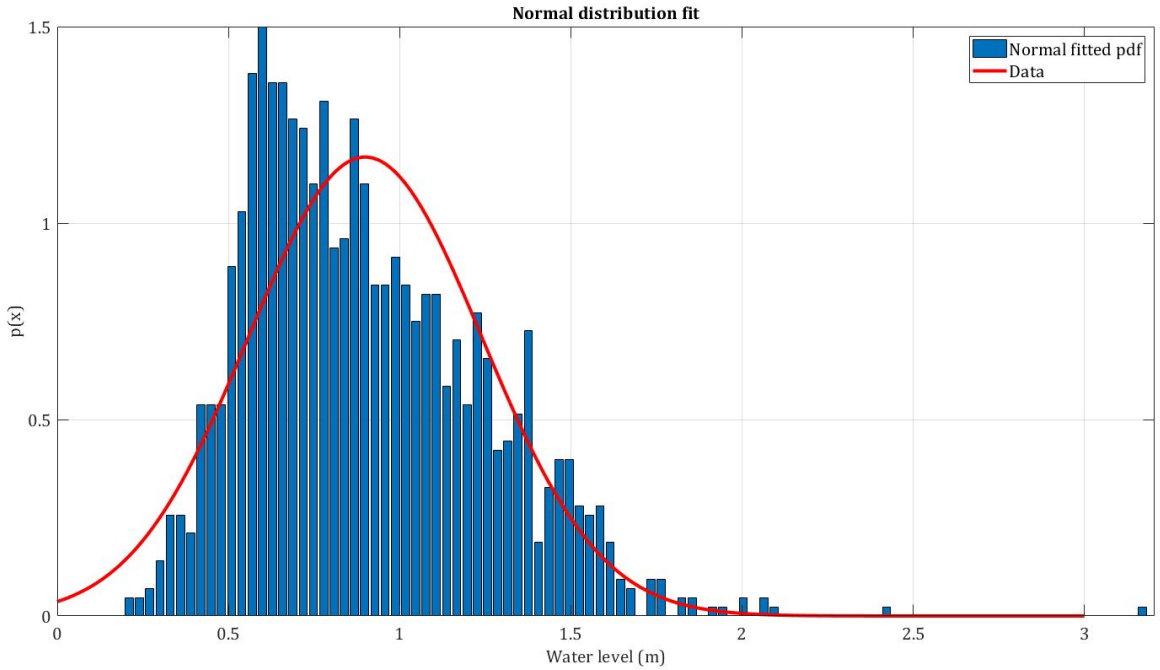

Figure B.3: Water level probability density function of modelled data and the Normal distribution.

B.1.2. Extreme Value Distributions

When it comes to extreme value distributions there are three types as shown in Equation B.2, B.3 and B.4 respectively. An Extreme Value distribution (type I) was fitted to the modelled data as well as the Generalised Extreme Value (GEV) distribution, which is a combination of type I, II and III. These distributions are described using μ, σ and k, which is a shape parameter of the distribution. A GEV distribution is defined for different values of k. When k approaches 0, it is defined by type I, when k < 0, type II and when k > 0, type III (Jonkman et al., 2017). Here for the GEV distribution k is 0.03, the mean is 0.73 m and the standard deviation is 0.27 m, shown in Figure B.4. For the Extreme Value distribution (type I) the mean is 1.06 m and the standard deviation is 0.45 m, shown in Figure B.5.

$$p_x(x) = \alpha \exp\left\{-\alpha(x-u) - e^{-\alpha(x-u)}\right\} \tag{B.2}$$

$$p_x(x) = \left(\frac{k}{\alpha}\right)\left(\frac{x-u}{\alpha}\right)^{-k-1} \exp\left\{\left(\frac{-(x-u)}{\alpha}\right)^{-k}\right\} \tag{B.3}$$

$$p_x(x) = -\left(\frac{k}{\alpha}\right)\left(\frac{x-u}{\alpha}\right)^{k+1} \exp\left\{\left(\frac{-(x-u)}{\alpha}\right)^{k}\right\} \tag{B.4}$$

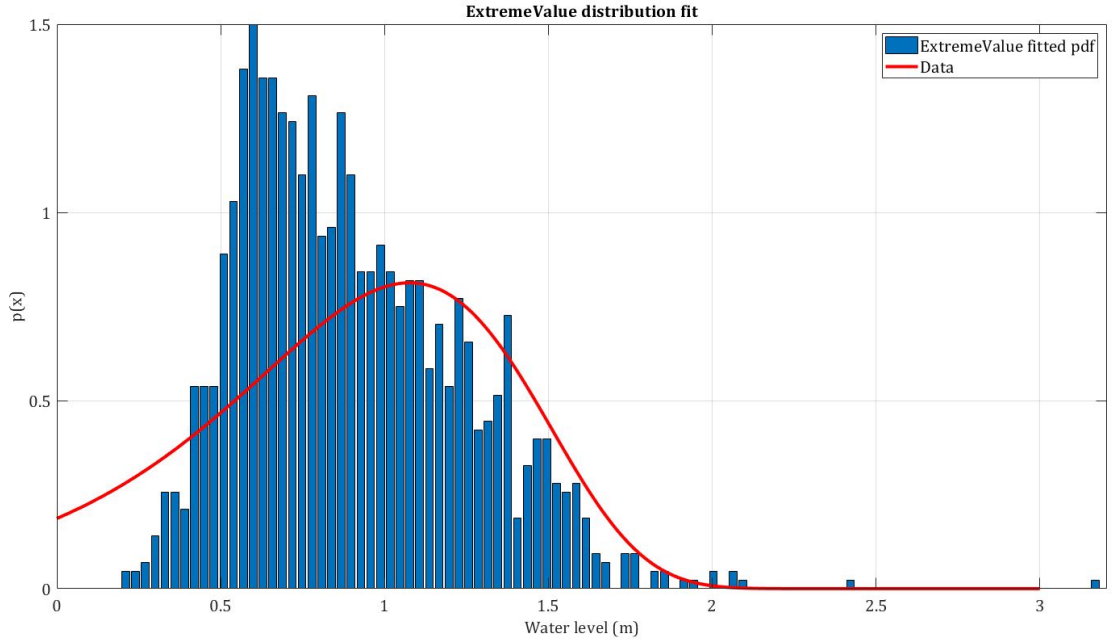

Figure B.4: Water level probability density function of modelled data and the Extreme Value distribution.

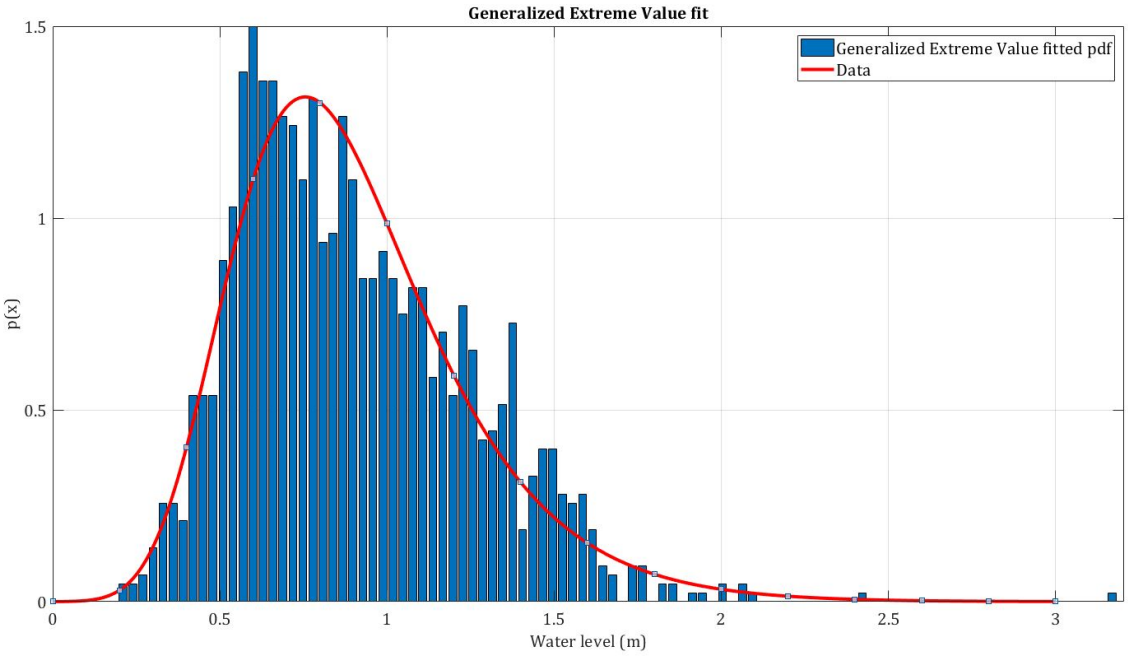

Figure B.5: Water level probability density function of modelled data and the Generalised Extreme Value distribution.

B.1.3. Gamma Distribution

The Gamma distribution is a continuous probability distribution and is commonly applied in mathematics. The distribution is described by shape parameters k and a and represented by the formulation of B.5. This distribution is often applied to economics and well represents waiting times. Special cases of this distribution include the Exponential, Erlang and Chi-Squared distributions (Jonkman et al., 2017). The modelled data was fitted with this distribution with a equal to 7.04 and k equal to 0.13 with the shape shown in Figure B.6.

$$p_x(x) = \frac{1}{a\Gamma(k)}\left(\frac{x}{a}\right)^{k-1} e^{\left(-\frac{x}{a}\right)} \tag{B.5}$$

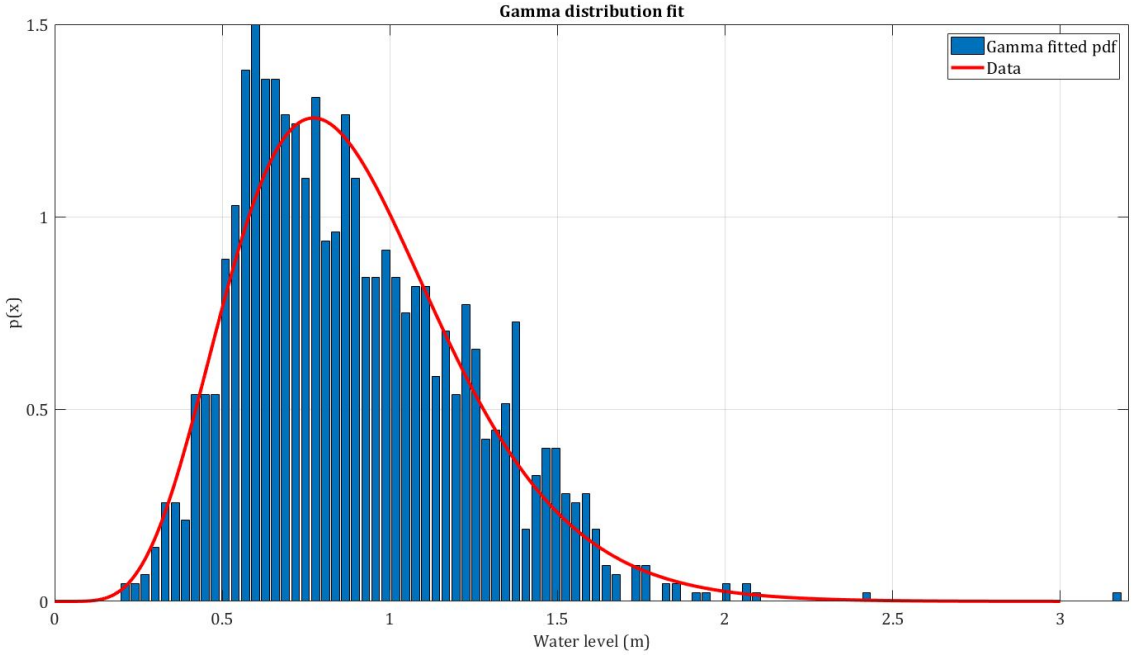

Figure B.6: Water level probability density function of modelled data and the Gamma distribution.

B.1.4. Logistic Distribution

This distribution is similar to the normal distribution in the sense that it is symmetrical (The MathWorks Inc., 2018). The distribution is represented by Equation B.6. This distribution is often used because of its ease to solve. The distribution was fitted to the modelled data and is shown in Figure B.7. Here the mean was 0.86 m and the standard deviation was 0.19 m.

$$p_x(x) = \frac{1}{\sigma\left(1+e^{-\frac{(x-\mu)}{\sigma}}\right)^2} e^{-\frac{(x-\mu)}{\sigma}} \tag{B.6}$$

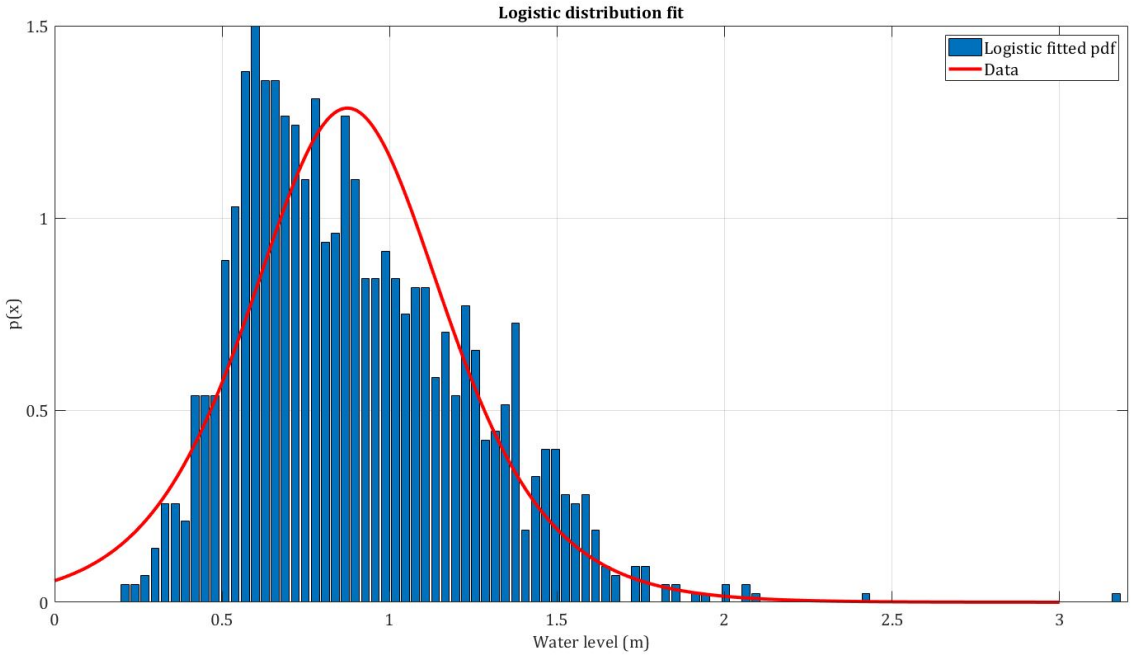

Figure B.7: Water level probability density function of modelled data and the Logistic distribution.

B.1.5. Kernel Distribution

The Kernel distribution is non-parametric meaning that the distribution is based directly on the input data and is shown in Equation B.7. The distribution is derived from the input data for specified intervals using a smoothing parameter known as the kernel (The MathWorks Inc., 2018). The distribution fitted to the modelled data is shown in Figure B.8 where k was 0.08 and N was the total number of water level data points.

$$p_x(x) = \sum_{i=1}^{N} K((y - x_i)/h) \tag{B.7}$$

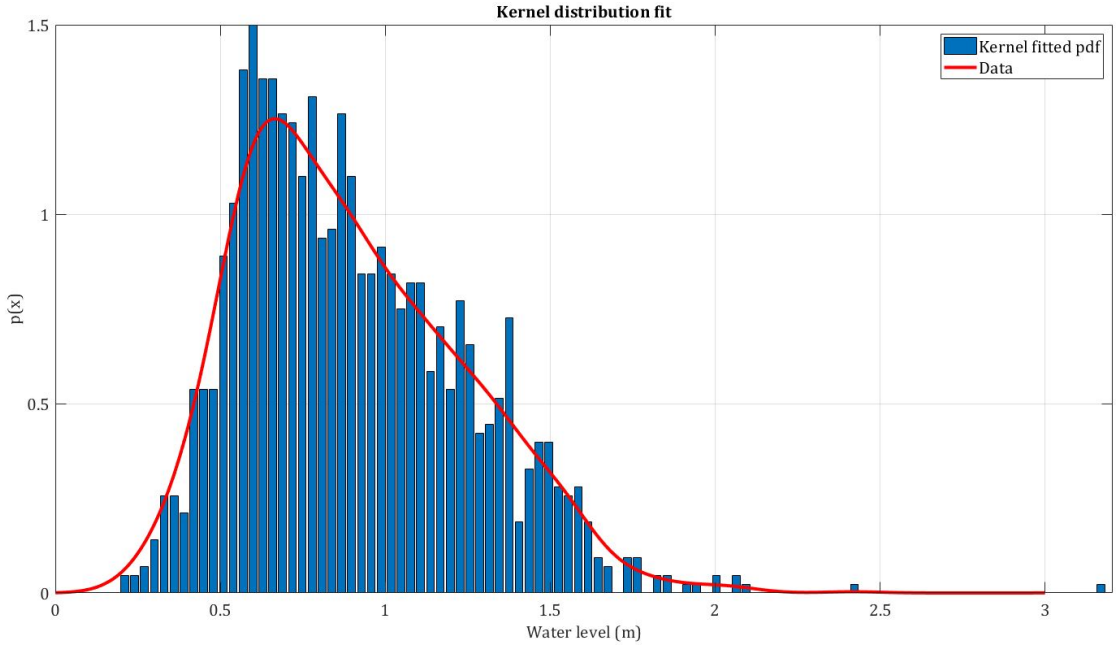

Figure B.8: Water level probability density function of modelled data and the Kernel distribution.

B.1.6. Stable Distribution

This distribution is typically applied to data with heavy tail ends and skewed to the left or right. This distribution applies the theory that the limit of normalised sums of independent identically distributed variables is stable (The MathWorks Inc., 2018). The fit is shown in Figure B.9 where the parameterisation according to (Nolan, 2018) is used with alpha, beta, gamma and delta equal to 1.68, 1, 0.21 and 0.81 respectively.

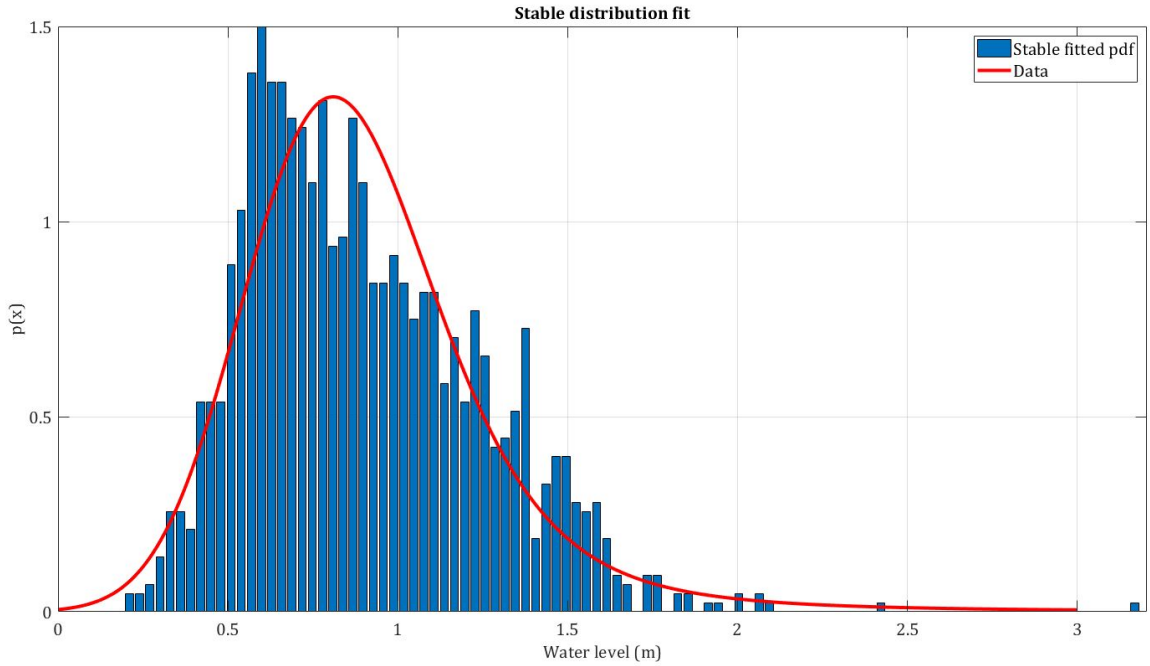

Figure B.9: Water level probability density function of modelled data and the Stable distribution.

B.1.7. Rayleigh Distribution

The Rayleigh distribution is a distribution with two degrees of freedom able to describe a random variable with more than one component. The distribution is described by Equation B.8 and the application to the modelled data is shown in Figure B.10. In this case the parameter b is equal to 0.67.

$$p_x(x) = \frac{x}{b^2} e^{-\frac{x^2}{\left(2b^2\right)}} \tag{B.8}$$

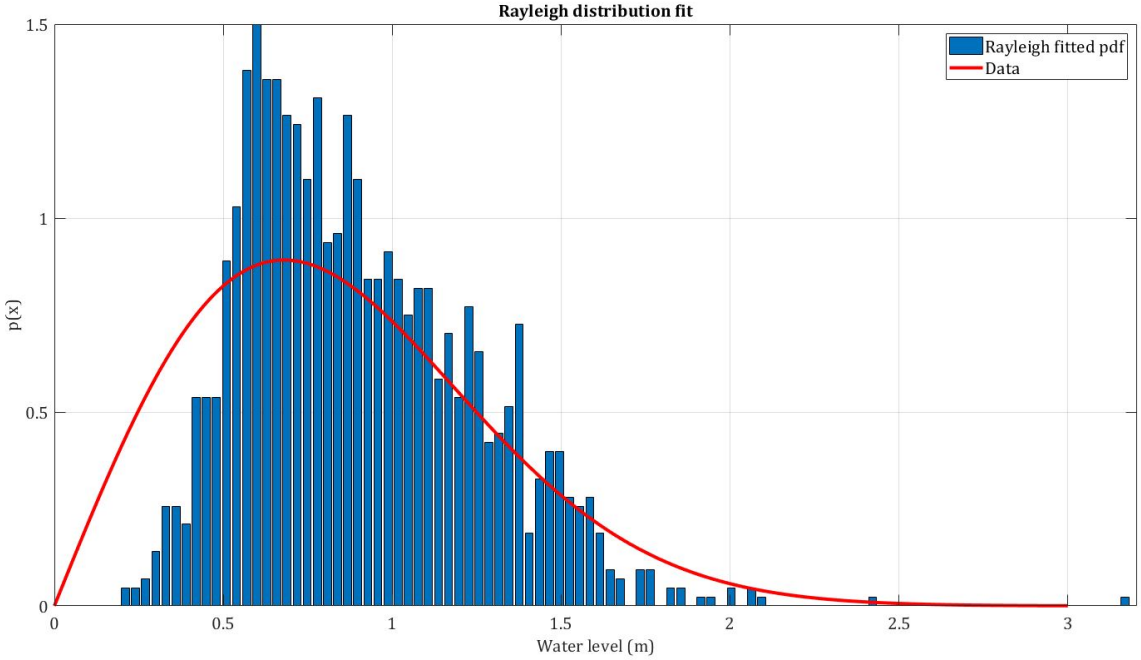

Figure B.10: Water level probability density function of modelled data and the Rayleigh distribution.

B.1.8. t-location Scale Distribution

The final considered distribution is the t-location Scale distribution which, like the stable distribution is generally applied to data with heavy tails and prone to outliers (The MathWorks Inc., 2018). Equation B.9 describes the distribution where smaller values of ν related to heavy tailed data. Figure B.11 shows the application to the modelled data where the mean is 0.88 m, the standard deviation is 0.32 m and ν is 21.7.

$$p_x(x) = \frac{\Gamma\left(\frac{\nu+1}{2}\right)}{\sqrt{\nu\pi}\Gamma\left(\frac{\nu}{2}\right)}\left(1+\frac{x^2}{\nu}\right)^{-\frac{\nu+1}{2}} \tag{B.9}$$

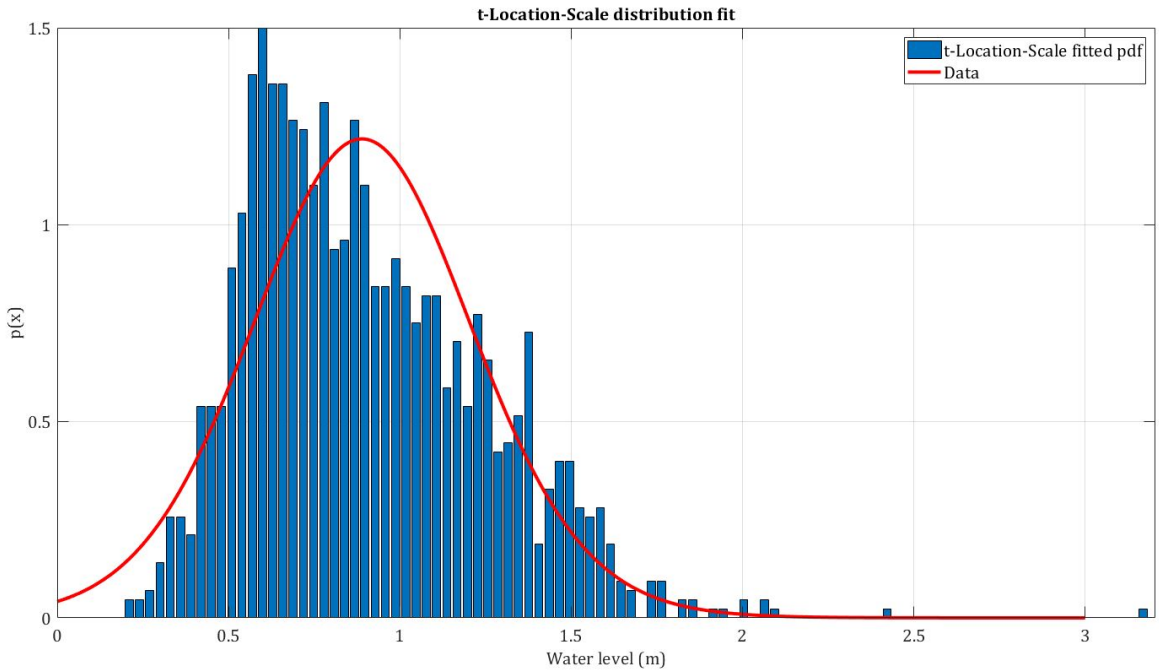

Figure B.11: Water level probability density function of modelled data and the t-location Scale distribution.

B.2. Application

Each fitted distribution was tested to determine the goodness of fit for each flood basin. The two indicators used to look at goodness of fit were the NMSE (Normalized Mean Squared Error) and NRMSE (Normalized Root Mean Square Error). The NMSE is calculated using Equation B.10 and the NRMSE is calculated according to Equation B.11. The concept of calculating the error is shown in Figure B.12 which shows the principle of determining the difference between the modelled data and the fitted distribution. Values closer to 1 indicate a better fit.

$$NMSE = \frac{1}{N}\sum_{i=1}^{N}(x_i - \hat{x}_i)^2 \tag{B.10}$$

$$NRMSE = \sqrt{\frac{1}{N}\sum_{i=1}^{N}(x_i - \hat{x}_i)^2} \tag{B.11}$$

Where N is the total number of data points, i is a count variable, x_i is the modelled data point, and $\hat{x}$ is the corresponding fitted point.

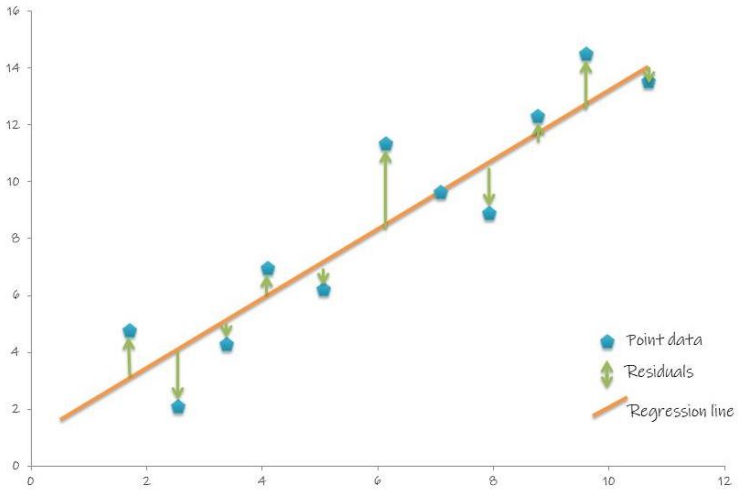

Figure B.12: Concept of determining the error between fitted data and the modelled data points (Hatari Labs, 2018).

The results for both tests for each flood area is shown are Table B.1 where for each flood area the best fit is the case of NMSE and NRMSE the best fit is the Kernel Distribution. The Extreme Value (EV), Gamma (GAM), Generalised Extreme Value (GEV), Logistic (LOG), Normal (NORM), Kernel (KERN), Rayleigh (RAY), Stable (STABLE) and t-location Scale (t-loc) distribution were tested.

Table B.1: Fitted distributions and their respective NMSE and NRMSE compared to the modelled water levels.

Area	Error	EV	GAM	GEV	KERN	LOG	NORM	RAY	STABLE	t-loc
1	NSME	0.854	0.994	0.995	0.999	0.984	0.977	0.895	0.991	0.981
	NRMSE	0.618	0.925	0.930	0.967	0.873	0.848	0.676	0.903	0.861
2	NSME	0.853	0.995	0.996	0.999	0.985	0.978	0.895	0.991	0.982
	NRMSE	0.616	0.930	0.934	0.969	0.877	0.851	0.675	0.906	0.865
3	NSME	0.852	0.996	0.996	0.999	0.986	0.978	0.893	0.992	0.983
	NRMSE	0.615	0.933	0.938	0.970	0.880	0.852	0.673	0.910	0.868
4	NSME	0.853	0.996	0.996	0.999	0.986	0.979	0.890	0.991	0.983
	NRMSE	0.617	0.935	0.937	0.970	0.881	0.856	0.668	0.908	0.870
5	NSME	0.855	0.996	0.997	0.999	0.987	0.981	0.888	0.992	0.985
	NRMSE	0.619	0.940	0.941	0.971	0.886	0.862	0.666	0.910	0.876
6	NSME	0.854	0.997	0.997	0.999	0.987	0.981	0.889	0.992	0.985
	NRMSE	0.618	0.942	0.941	0.971	0.887	0.864	0.667	0.911	0.877
7	NSME	0.853	0.997	0.997	0.999	0.987	0.981	0.892	0.992	0.985
	NRMSE	0.617	0.941	0.941	0.971	0.887	0.863	0.671	0.911	0.877
8	NSME	0.857	0.996	0.996	0.999	0.987	0.981	0.897	0.992	0.985
	NRMSE	0.621	0.941	0.941	0.970	0.886	0.862	0.679	0.911	0.876
9	NSME	0.860	0.997	0.997	0.999	0.987	0.981	0.896	0.992	0.985
	NRMSE	0.626	0.941	0.941	0.970	0.887	0.862	0.678	0.912	0.877
10	NSME	0.865	0.996	0.997	0.999	0.987	0.981	0.892	0.992	0.985
	NRMSE	0.632	0.941	0.941	0.971	0.886	0.862	0.672	0.911	0.876
11	NSME	0.862	0.996	0.996	0.999	0.986	0.980	0.893	0.992	0.984
	NRMSE	0.628	0.937	0.939	0.970	0.884	0.859	0.673	0.909	0.872
12	NSME	0.860	0.996	0.996	0.999	0.986	0.980	0.892	0.992	0.983
	NRMSE	0.626	0.935	0.937	0.970	0.882	0.857	0.671	0.908	0.871
13	NSME	0.860	0.996	0.996	0.999	0.986	0.980	0.891	0.991	0.983
	NRMSE	0.626	0.935	0.937	0.969	0.881	0.857	0.670	0.908	0.870
14	NSME	0.859	0.995	0.996	0.999	0.986	0.979	0.889	0.991	0.983
	NRMSE	0.625	0.933	0.935	0.969	0.880	0.855	0.668	0.906	0.869
15	NSME	0.858	0.995	0.996	0.999	0.985	0.979	0.887	0.991	0.982
	NRMSE	0.623	0.931	0.934	0.969	0.879	0.855	0.664	0.905	0.867
16	NSME	0.852	0.995	0.996	0.999	0.985	0.978	0.887	0.991	0.982
	NRMSE	0.615	0.929	0.933	0.968	0.876	0.852	0.664	0.904	0.865
17	NSME	0.856	0.995	0.995	0.999	0.985	0.979	0.885	0.991	0.982
	NRMSE	0.620	0.929	0.933	0.968	0.877	0.854	0.661	0.904	0.866
18	NSME	0.853	0.995	0.995	0.999	0.984	0.978	0.888	0.991	0.981
	NRMSE	0.617	0.927	0.931	0.967	0.875	0.851	0.666	0.903	0.863
19	NSME	0.853	0.995	0.995	0.999	0.984	0.977	0.890	0.990	0.981
	NRMSE	0.617	0.926	0.931	0.967	0.874	0.850	0.668	0.902	0.863
20	NSME	0.853	0.994	0.995	0.999	0.984	0.977	0.892	0.990	0.981
	NRMSE	0.617	0.925	0.930	0.967	0.873	0.848	0.671	0.902	0.861
21	NSME	0.854	0.994	0.995	0.999	0.984	0.977	0.893	0.990	0.981
	NRMSE	0.618	0.925	0.930	0.967	0.872	0.847	0.674	0.902	0.860
22	NSME	0.854	0.994	0.995	0.999	0.984	0.977	0.896	0.990	0.980
	NRMSE	0.618	0.925	0.930	0.967	0.872	0.847	0.677	0.902	0.860
23	NSME	0.863	0.997	0.997	0.999	0.987	0.981	0.896	0.992	0.985
	NRMSE	0.630	0.941	0.941	0.970	0.887	0.862	0.678	0.912	0.877